# Water Oxidation by Organic-Inorganic Supramolecular "Quantasomes"

Maurizio Prato
University of Trieste, Italy
AXA Chair, CIC Biomagune, San Sebastián, Spain


**National Geographic**

http://ngm.nationalgeographic.com/ngm/0406/feature5/index.html

# Hydrogen, clean fuel

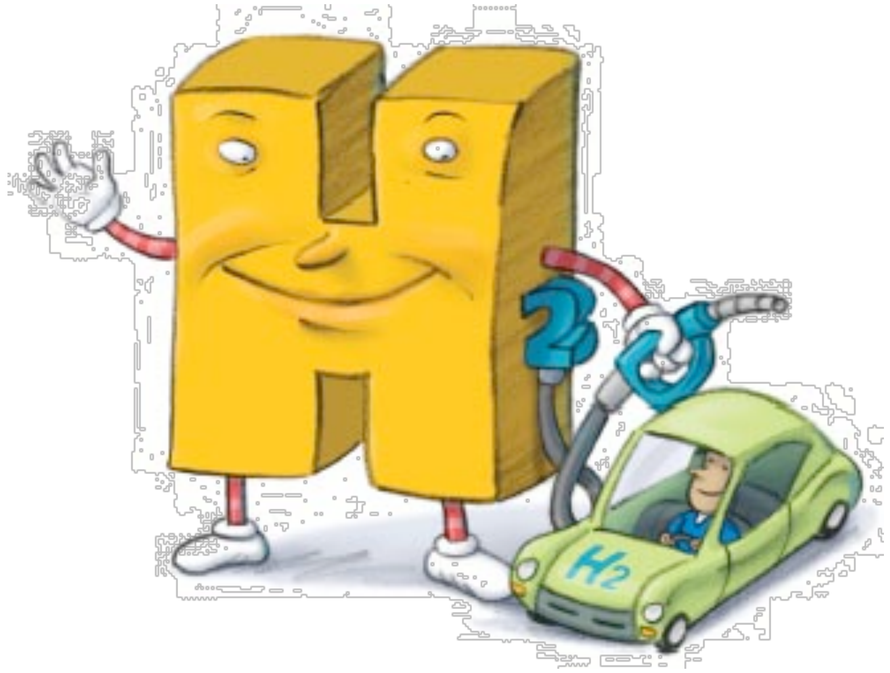


energy carrier

First element of the periodic table, hydrogen has the highest energy content per mass unit

# Steam reforming (700-1000 °C)

$$CH_4 + H_2O \rightarrow CO + 3\,H_2$$
$$CO + H_2O \rightarrow CO_2 + H_2$$


https://hydrogeneurope.eu/bmw-says-goodbye-to-electric-cars-it-has-now-solved-the-problem-of-hydrogen-engines-mes/#:~:text=31%20January%202024-,BMW%20says%20Goodbye%20to%20Electric%20Cars%3B%20it%20has%20now%20Solved,have%20been%20in%20the%20shadows.

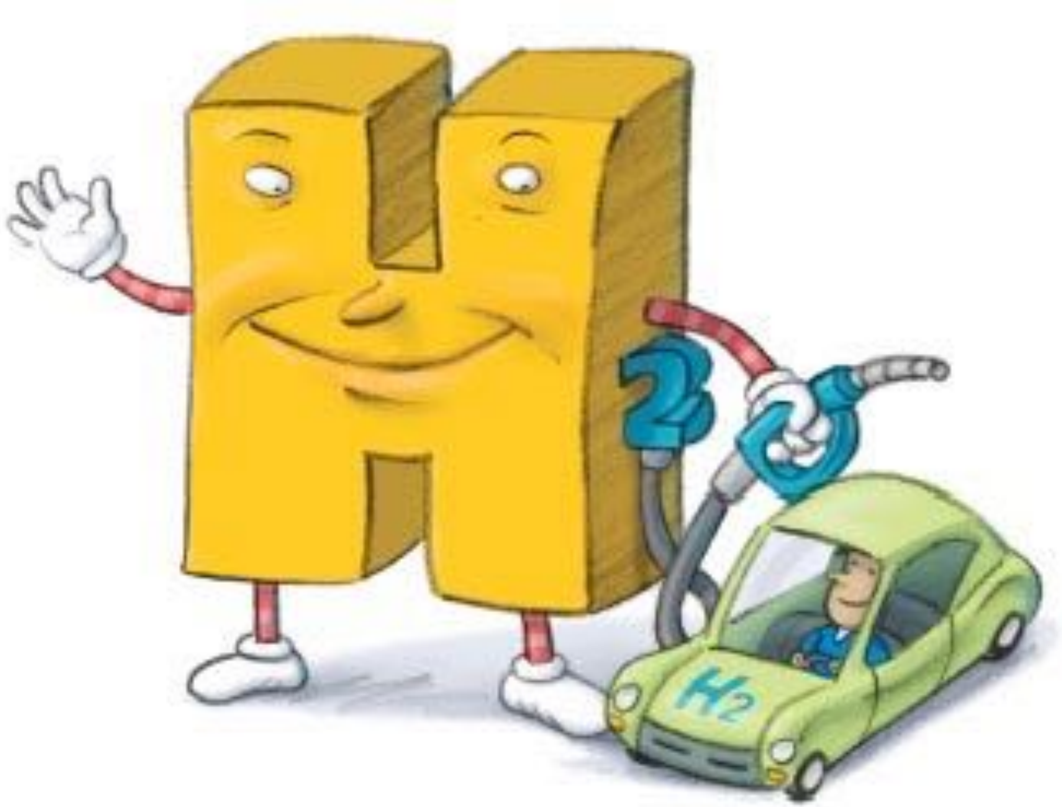


$2\ H_2O \longrightarrow 2\ H_2 + O_2$

$2\ H_2 + O_2 \longrightarrow 2\ H_2O$

# **Splitting** of water into **Hydrogen** and **Oxygen**

a high-energy process

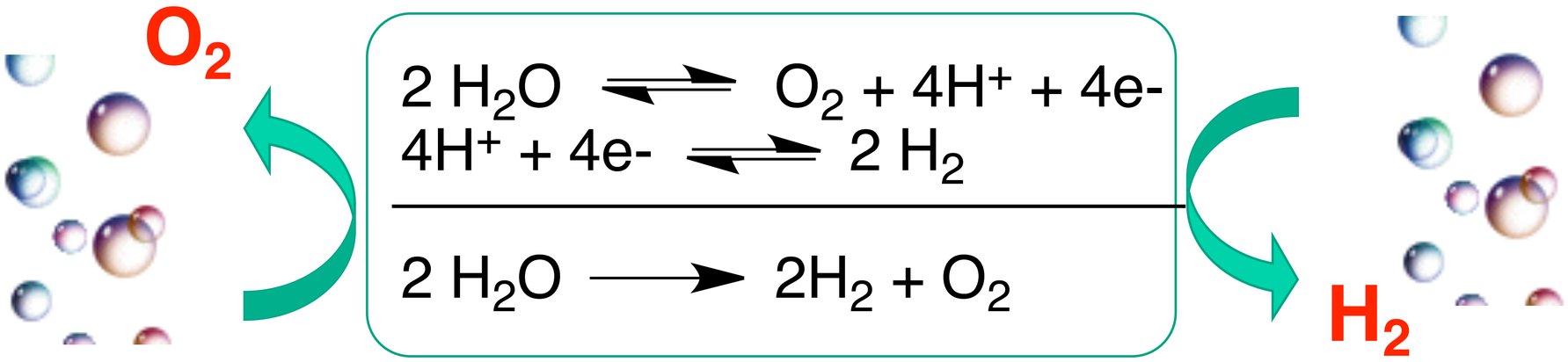


- Thermal splitting of water requires temperatures above 2500°C

-Electrochemical splitting of water is costly E= –1.23 V

## the $2H_2O/O_2$ half reaction is considerably complex

✓the removal of 4-electrons from 2 $H_2O$ molecules

✓the removal of 4 protons

✓the formation of a new oxygen-oxygen bond

# Tuning Electrocatalytic Interfaces with Carbon Nanostructures (CNS) in water

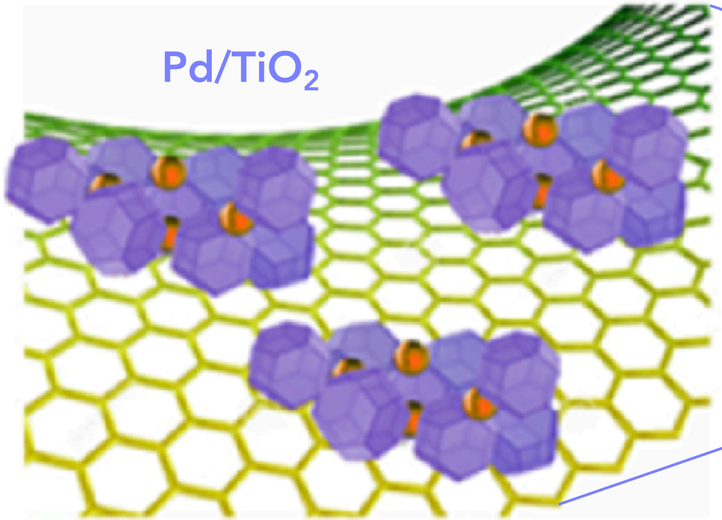


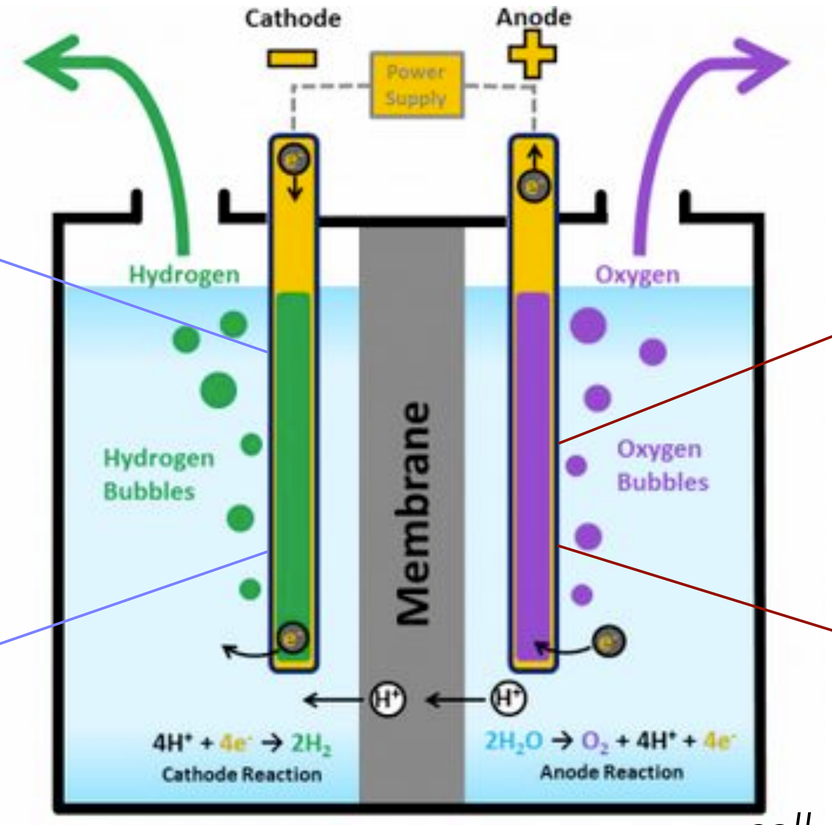


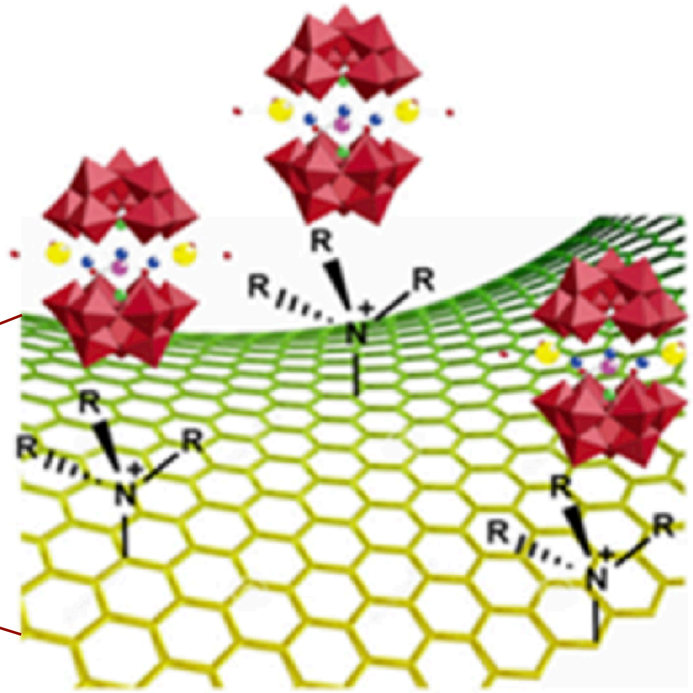


*coll. with prof. Paolo Fornasiero (U Trieste) and prof. Marcella Bonchio (U Padova)*

*Nat. Commun. 7 (2016) 13549*
*Energy Environ. Sci. 11 (2018) 1571–1580.*
*Energy Environ. Sci. 14 (2021) 5816–5833*

*coll. with prof. Marcella Bonchio (U Padova)*

*Nat. Chem. 2 (2010) 826–831*
*ACS Nano. 7 (2013) 811–817*
*Nat. Chem. 11 (2019) 146–153*
*J. Am. Chem. Soc. 144 (2022) 14021–14025*

TiO2 photoanode

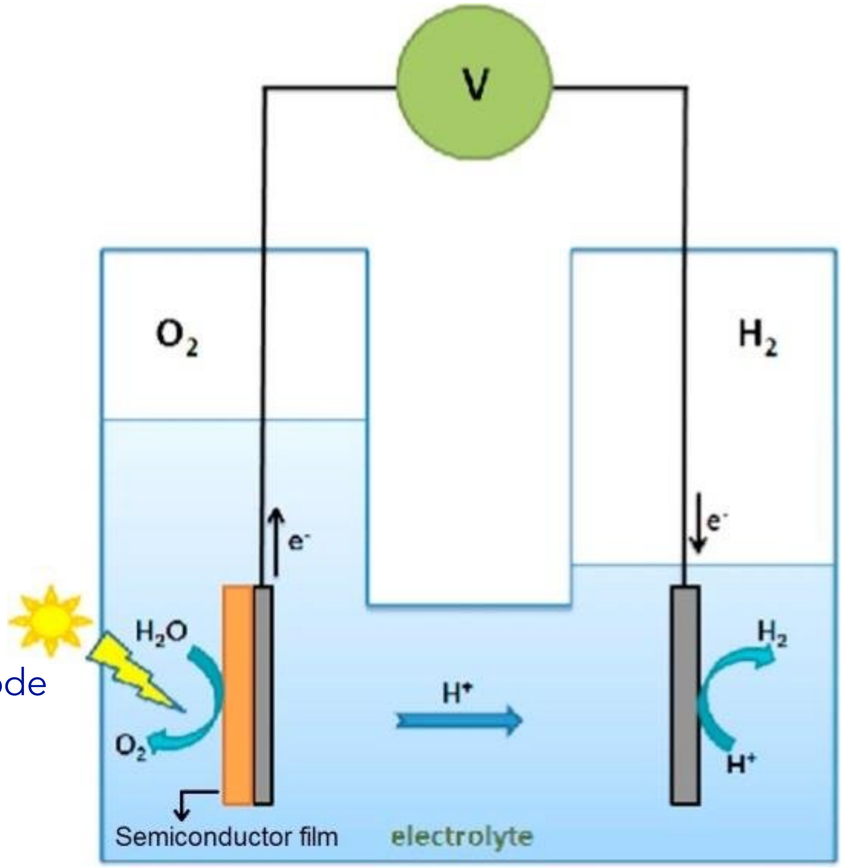


platinum black cathode

The first experimental demonstration of light-driven water splitting was reported in 1972 by Honda and Fujishima. The photoelectrochemical cell (PEC) was composed of TiO2 photoanode and platinum black cathode. By illumination of the photoanode (λ>400 nm), O2 and H2 were generated at the photoanode and cathode, respectively. The same group reported later a photocatalytic CO2 reduction with aqueous suspension of various semiconductor particles.

A. Fujishima, K. Honda, Nature 1972, 238, 37.
F. Akira, H. Kenichi, Bull. Chem. Soc. Jpn. 1971, 44, 1148.
T. Inoue, A. Fujishima, S. Konishi, K. Honda, Nature 1979, 277, 637.

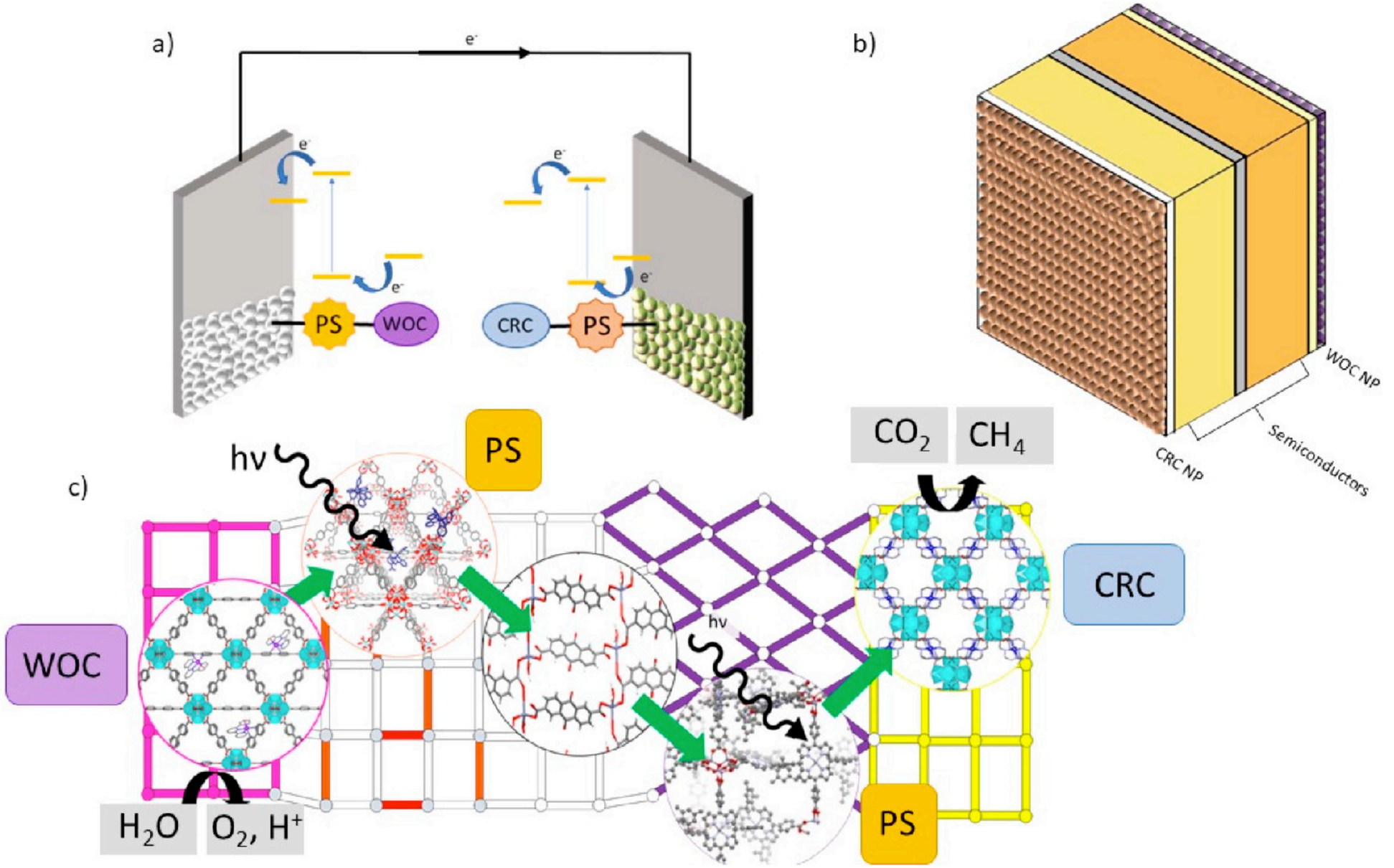


Schematics for artificial photosynthetic assemblies showing DSPECs featuring a photosensitizer (PS), water oxidation catalyst (WOC), and CO2 reduction catalyst (CRC), multijunction semiconductors with catalytic nanoparticles (NP), and a proposed all-MOF artificial photosynthetic assembly. J. Am. Chem. Soc. 2022, 144, 39, 17723–17736.

# Photosynthesis: let's learn from plants

$$6\,H_2O + 6\,CO_2 + 48\,h\nu \longrightarrow C_6H_{12}O_6 + O_2$$

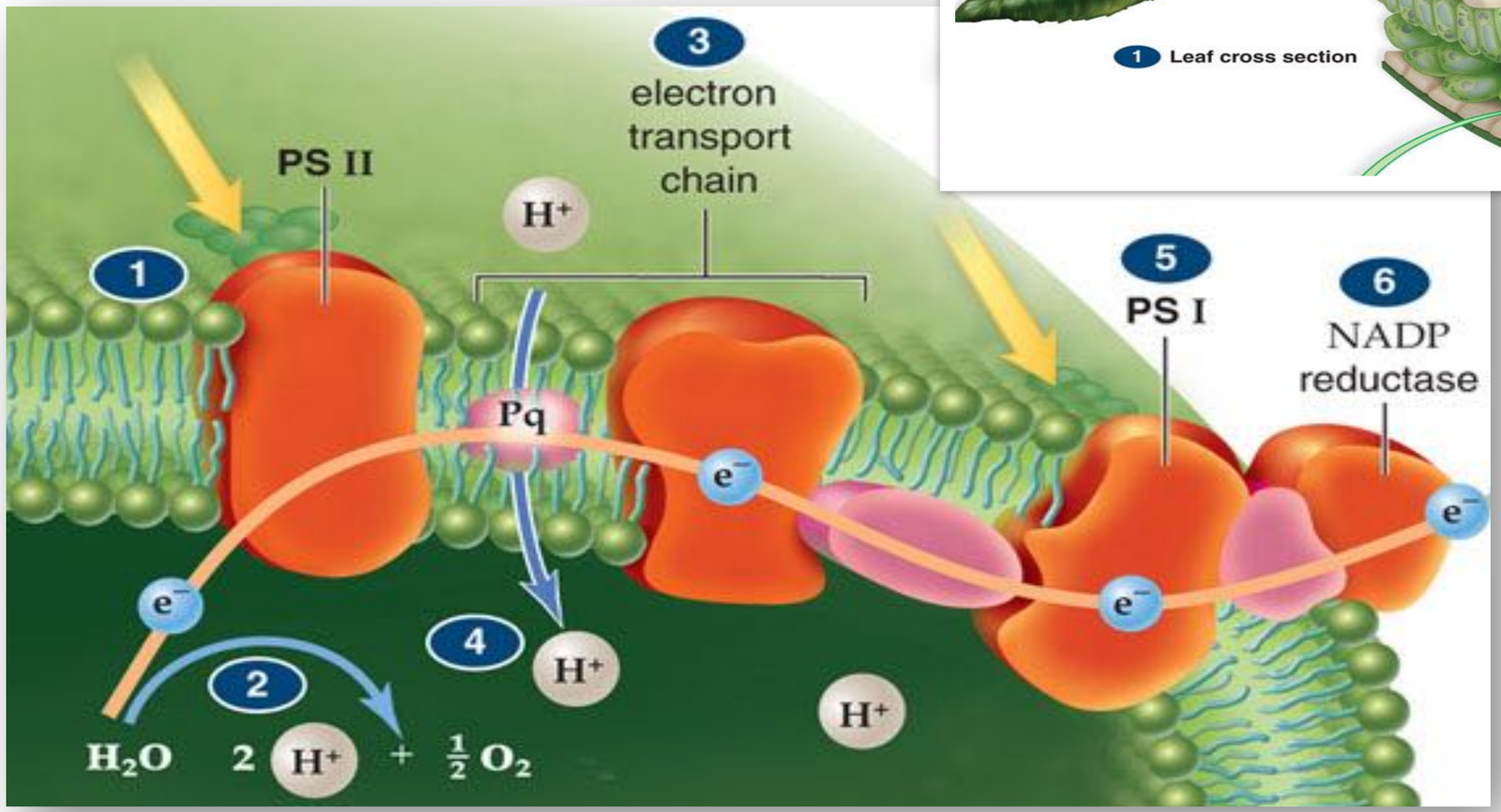


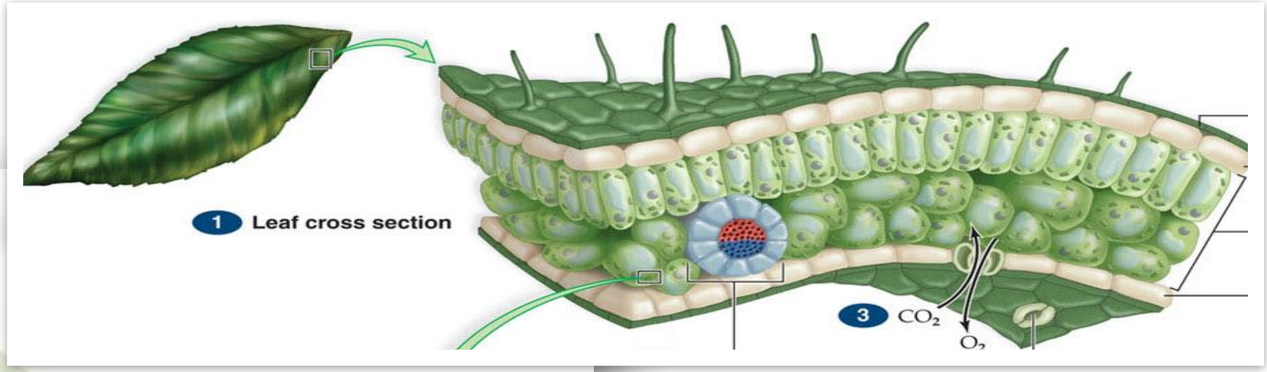


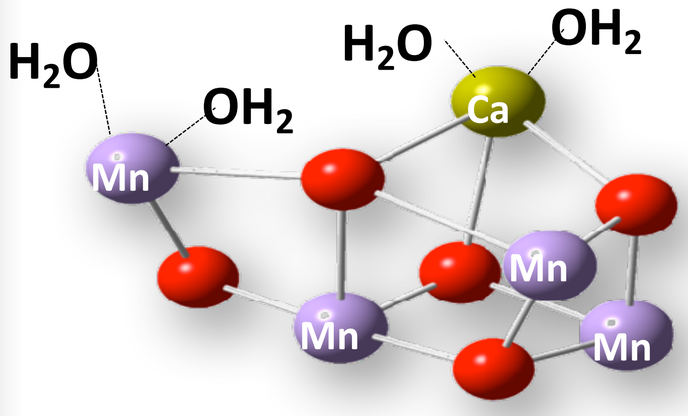

# Lesson from Nature: PSII Light Harvesting

PSII native assembly architecture (a) scanning electron micrograph of the thylakoid membrane showing fluid-to-paracrystalline PSII domains left (b) AFM of hexagonally packed LH complexes (dashed box), Inset: PSII core-complex showing the RC completely surrounded by an elliptical LH1 assembly, scale 20 Å

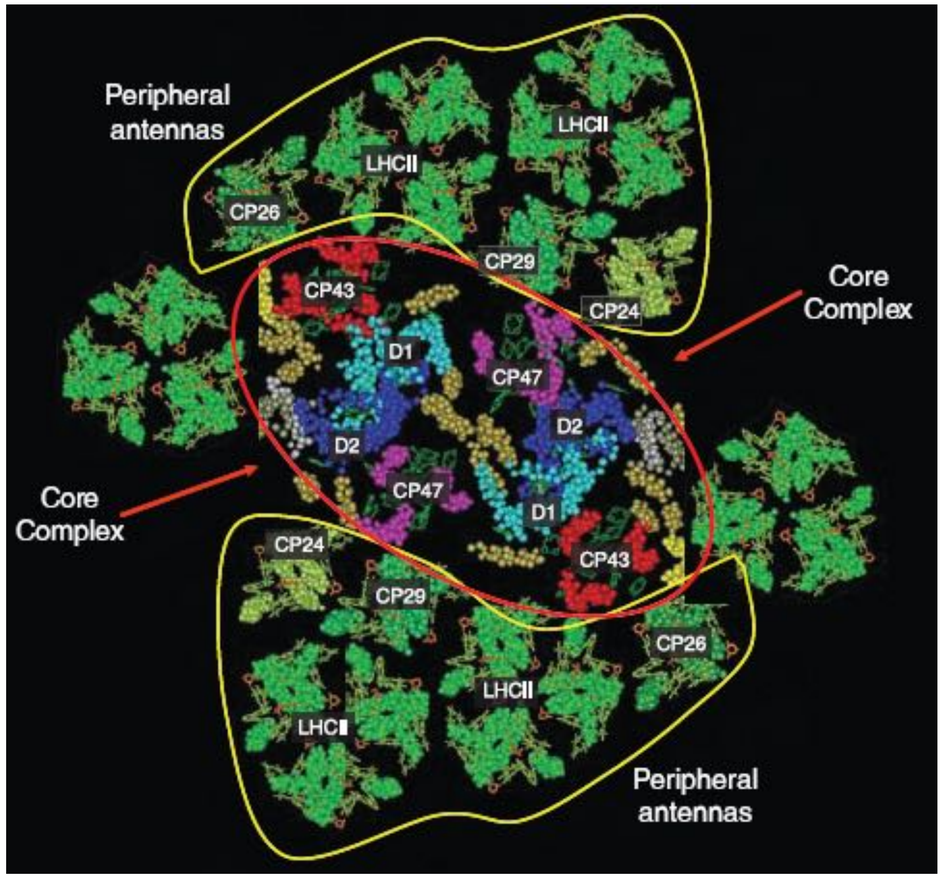


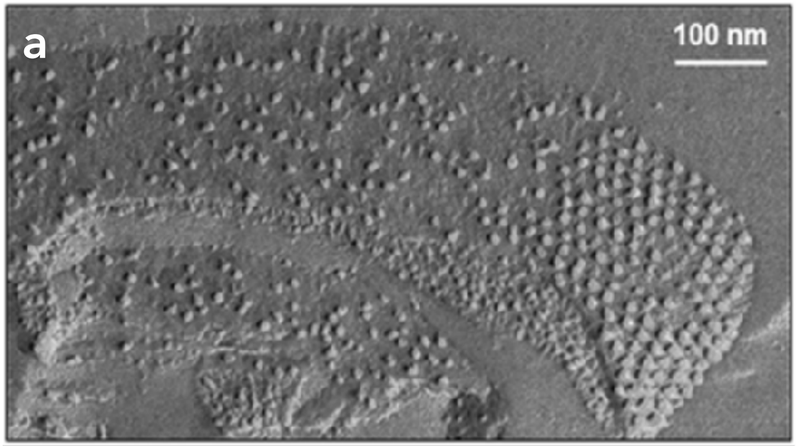


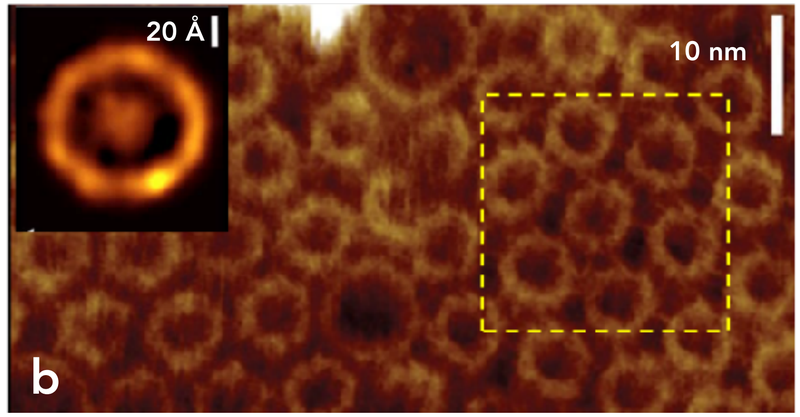


R. Bassi, G. R. Fleming et al. *Science* **2008**, *320*, pp. 794-797. J. Barber et al. *Inorganic Chemistry*, **2008**, 47, 1700-1710
S. Scheuring and J. N. Sturgis, *Science*, **2005**, *309*, 484-487

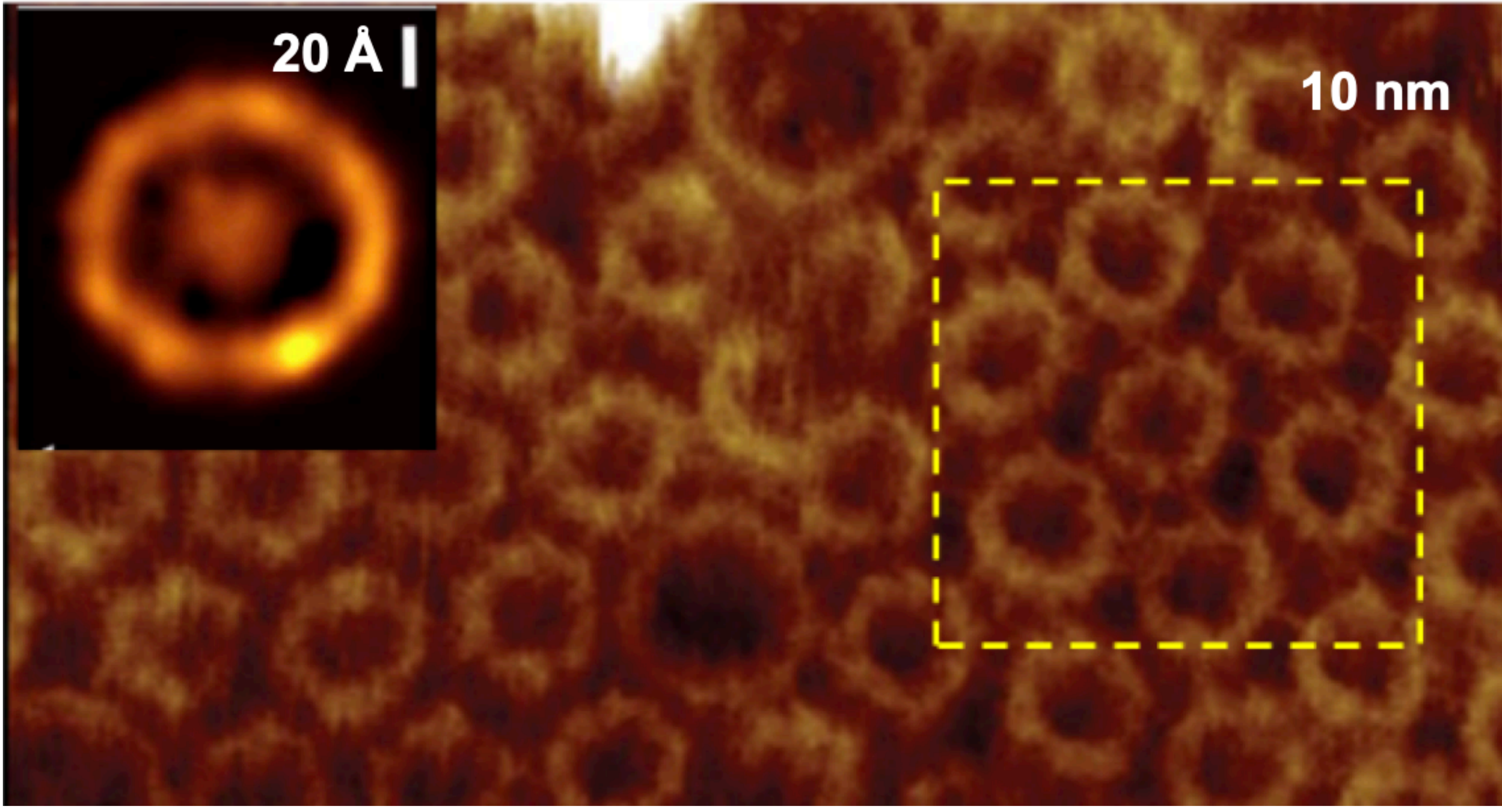
20 Å
10 nm

# *The quantasome concept*

R. B. Park, J. Biggins, Quantasome: Size and Composition (1964) Science 144, 1009

√ **identifies the minimal photosynthetic unit responsible for the "quantum" solar energy conversion,** taking place within the chloroplast membrane. In its essentials: the integration of a light-harvesting (LH) antenna in combination with catalytic co-factors.

√ **goes beyond a simple photocatalytic dyad** based on a 1:1 conjugation of a light absorber with the catalyst. The quantasome model calls for a significantly different approach: **the LH components, of selected type and number, together with their spatial organization need to be specifically optimized according to the CATALYST requirements, with the final aim to leverage its multi-ET mechanism.**

# *The catalytic system (artificial quantasome)*

The catalyst

?

The antenna
(photosensitizer)

?

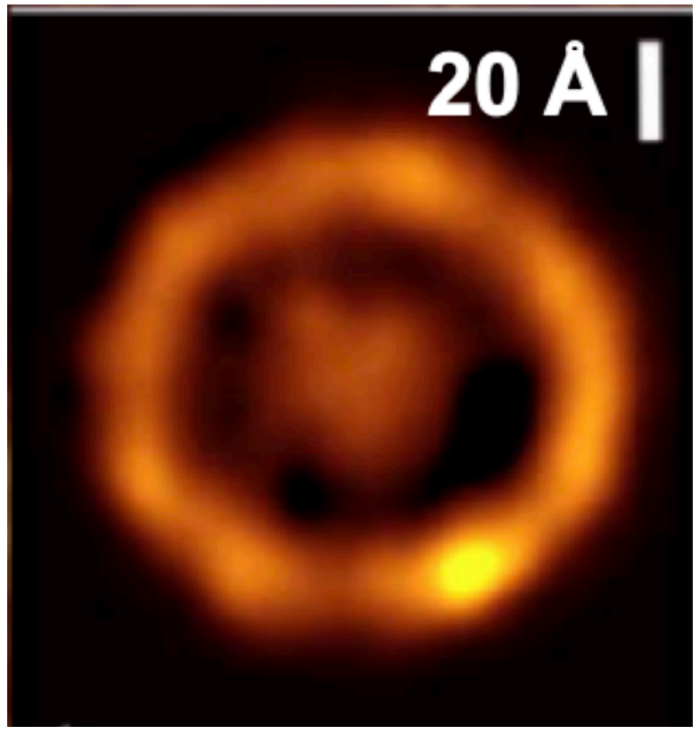

# synthesis of $[Ru_4(\mu\text{-}O)_4(\mu\text{-}OH)_2(H_2O)_4\gamma\text{-}(SiW_{10}O_{36})_2]^{10-}$

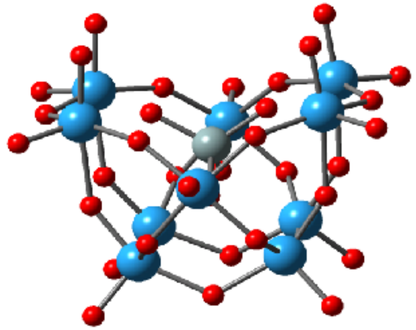

$K_8\gamma\text{-}[(SiO_4)W_{10}O_{36}]$

+

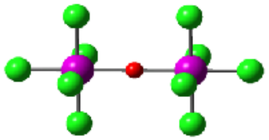

$K_4(\mu\text{-}O)Ru_2Cl_{10}$

1. $H_2O$, 70°C, 1 h

2. CsCl

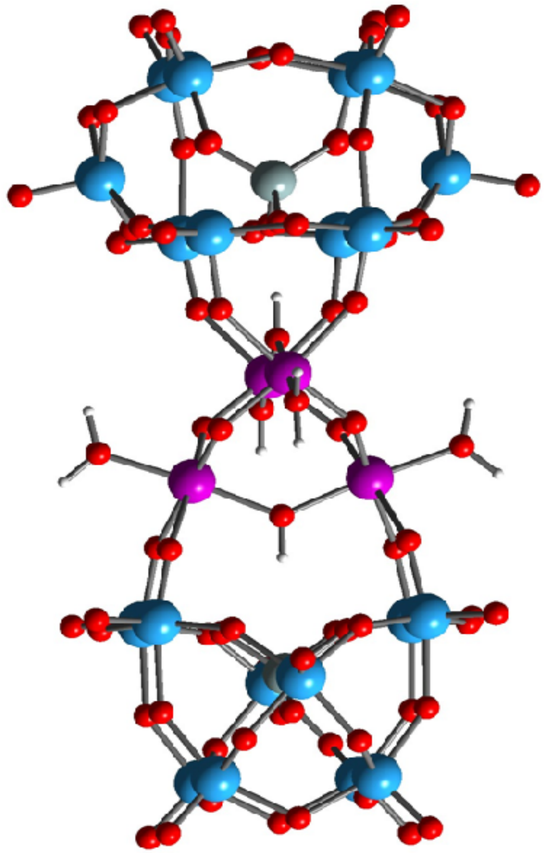

**$Ru_4$POM**

M. Bonchio and coll. *J. Am. Chem. Soc.* **2008**, *130*, 5006; *J. Am. Chem. Soc.* **2009**, *131*, 16051.

# ➢ POM embedding a tetra-Ruthenium(IV) core

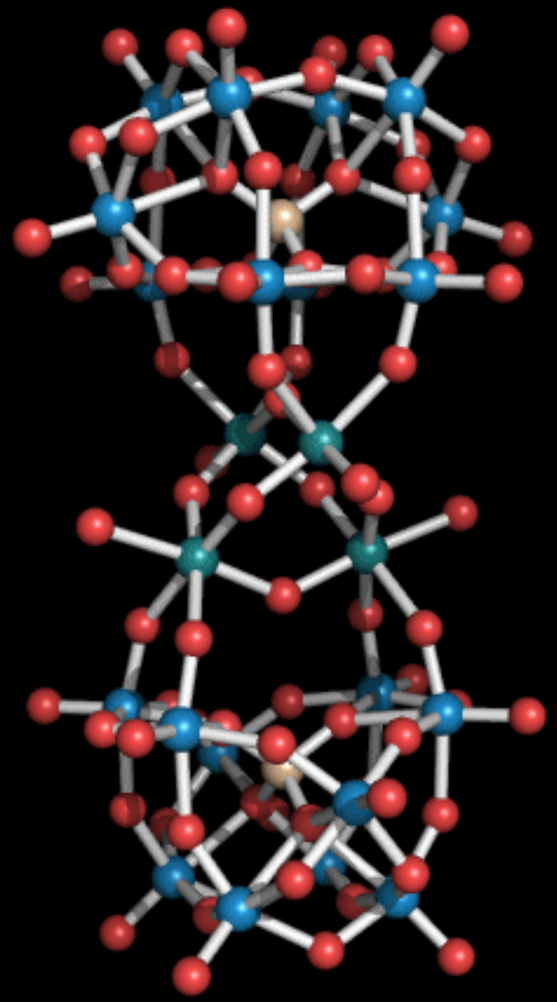

# the adamantane-like tetra-ruthenium(IV)-oxo-core

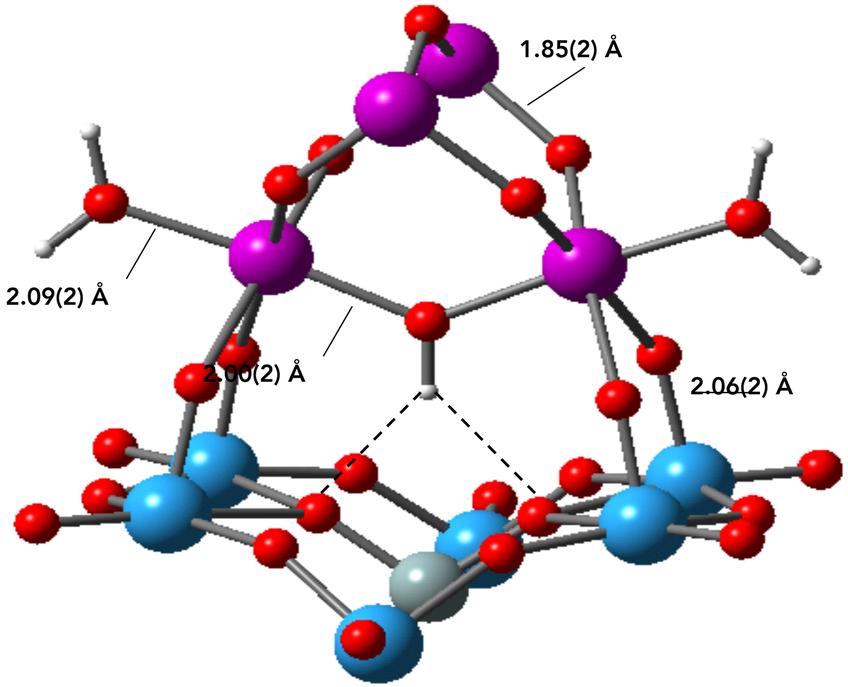


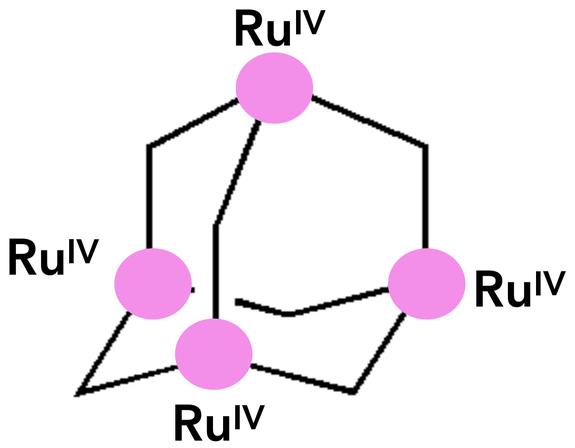


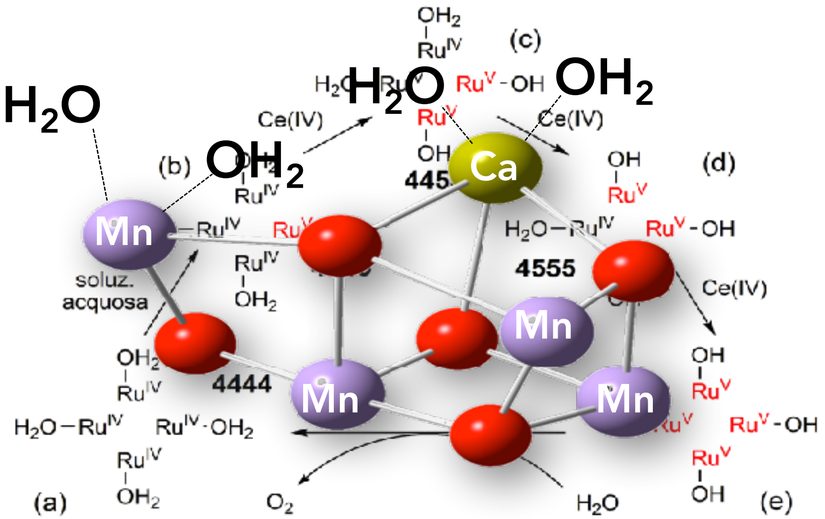


- water soluble
- presence of 4 redox active Ru centers
- presence of 4 water ligands involved in proton transfers
- POM framework stabilize high valent metal-oxo intermediates

M. Bonchio and coll. *J. Am. Chem. Soc.* **2008**, *130*, 5006; *J. Am. Chem. Soc.* **2009**, *131*, 16051

# Oxygen Evolving Catalysis in water

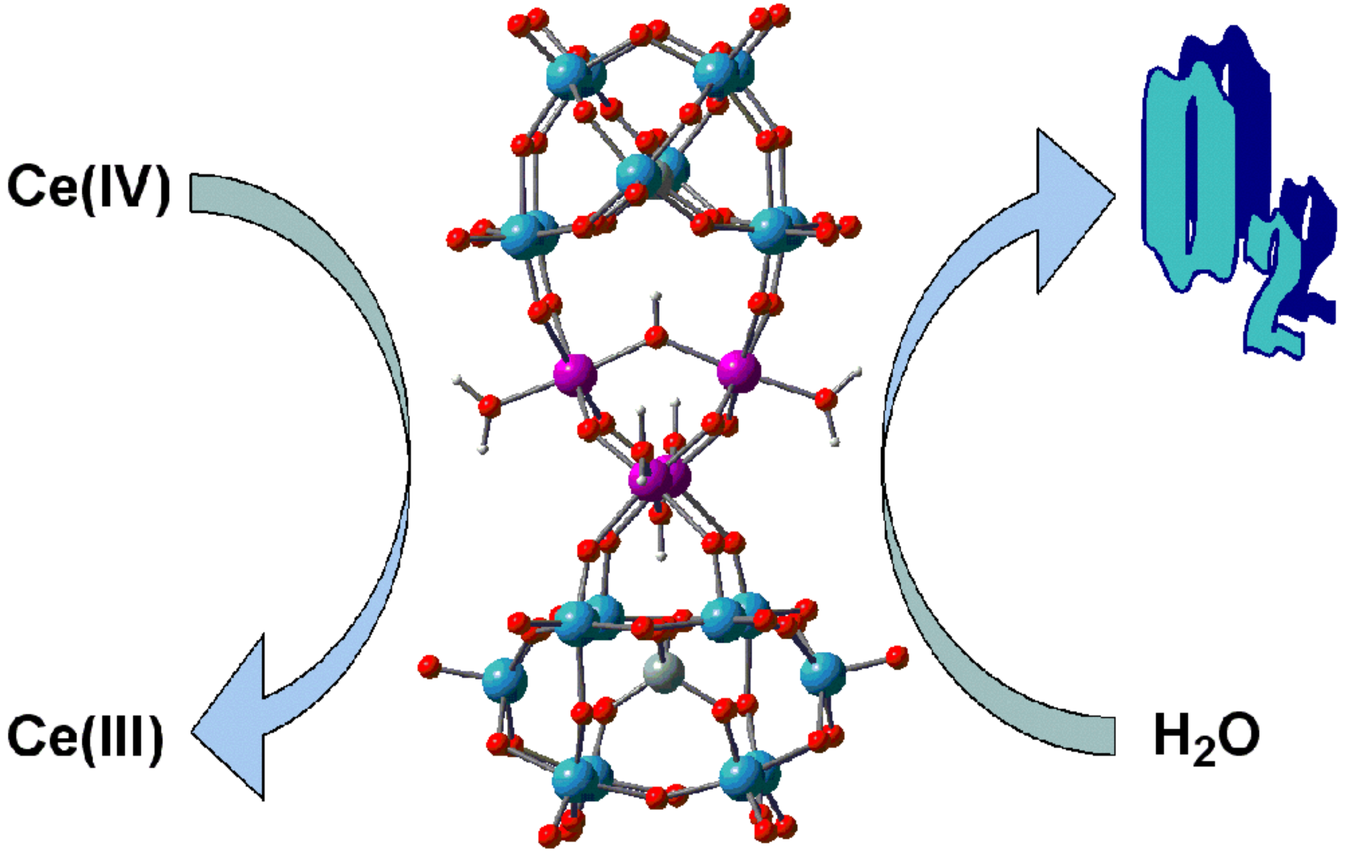


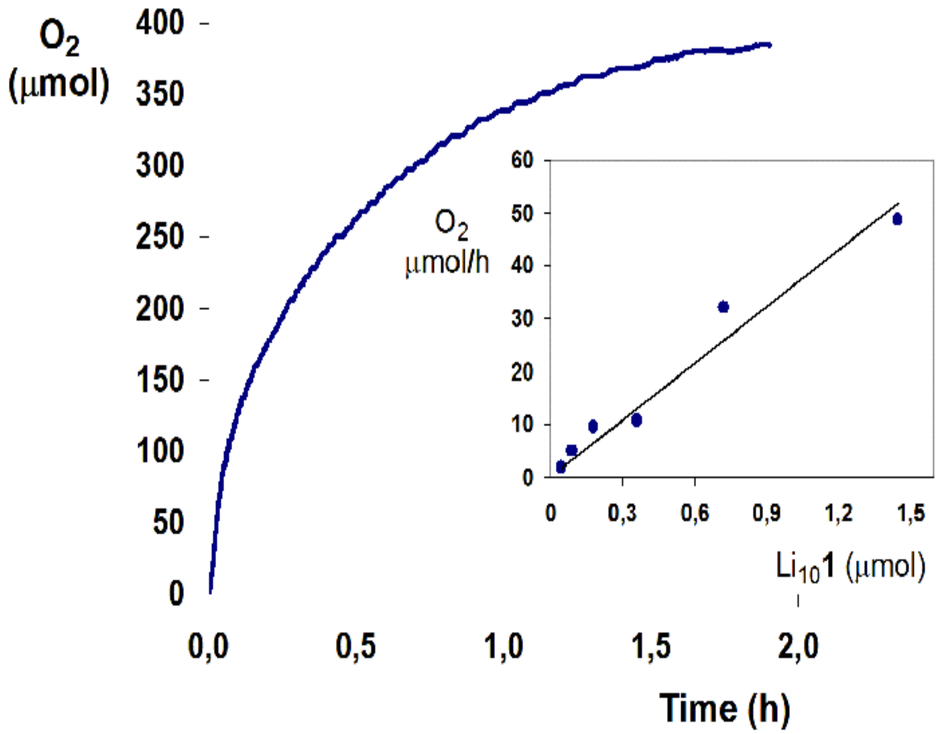


**500 TON; TOF= 450 $h^{-1}$**

Kinetics of $O_2$ evolution catalyzed by $Li_{10}$**1**, (4.3 µmol) with $Ce^{IV}$ (1720 µmol), in $H_2O$ (pH=0.6), at 20 °C; 90%yield

M. Bonchio and coll. *J. Am. Chem. Soc.* **2008**, *130*, 5006; *J. Am. Chem. Soc.* **2009**, *131*, 16051

# *The catalytic system (artificial quantasome)*

The catalyst

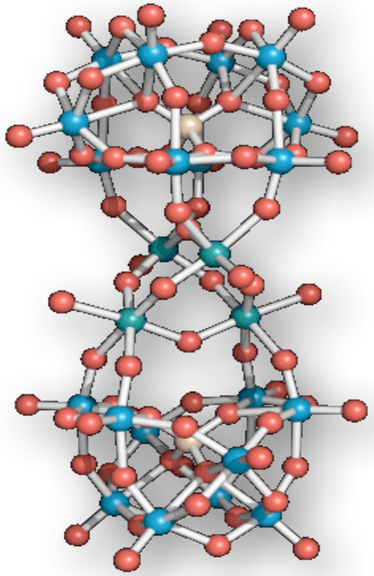

The antenna
(photosensitizer)

?

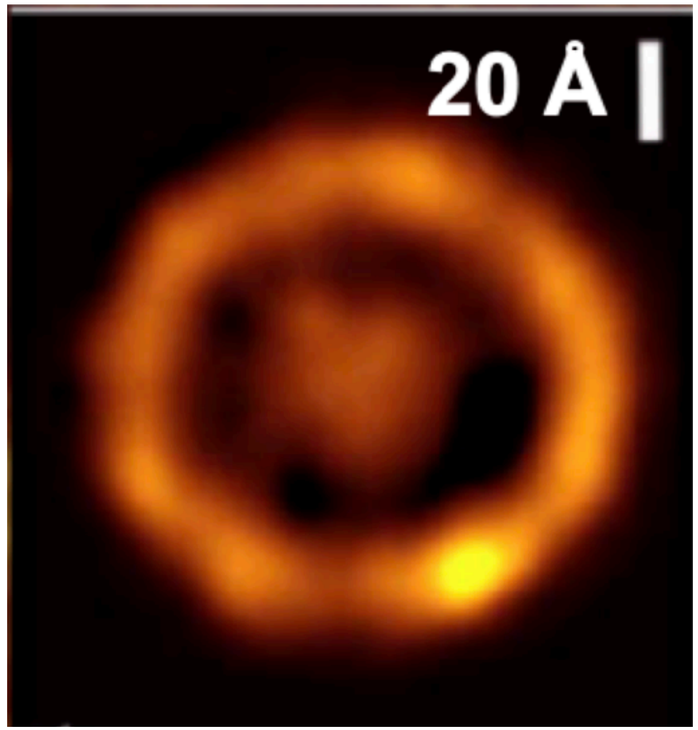

# Perylene bisimides

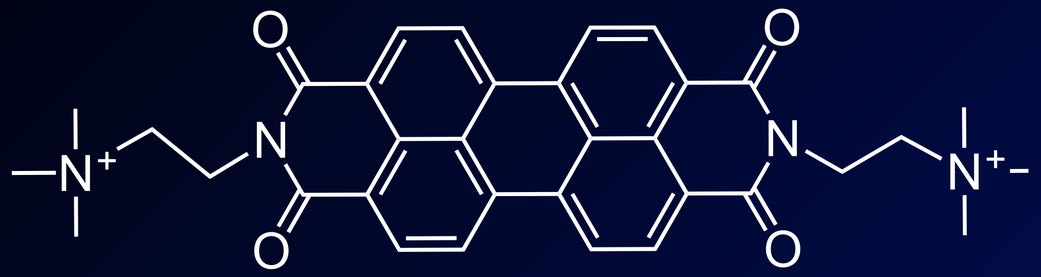

- wide absorption range
- Fluorescent
- HOMO-LUMO energies
- strong and robust photo-generated oxidant upon visible light ($\lambda$ > 500 nm, E(**PBI**$^{*/-}$) **=** 2.20 V vs NHE (Phys. Chem. Chem. Phys. 2013, **15,** 2539)
-

# *Water oxidation*

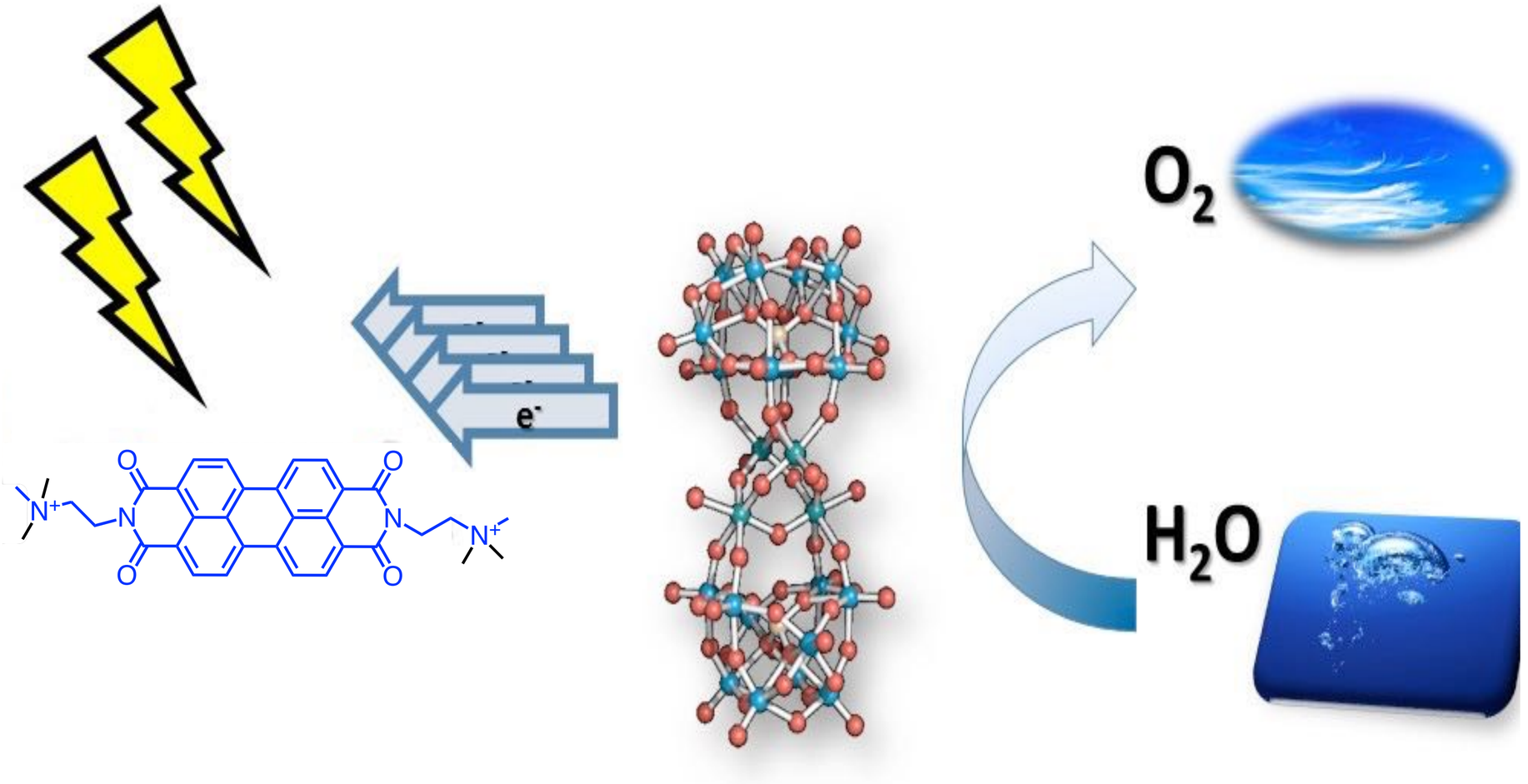

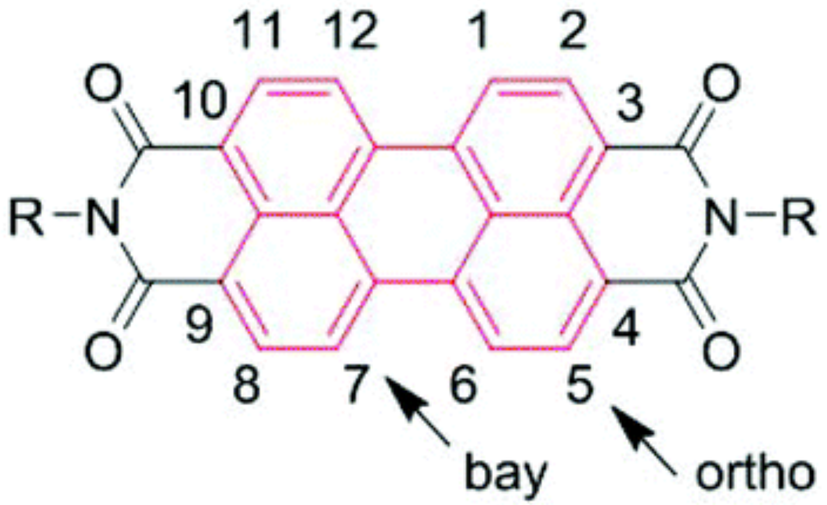


- intense absorption
- fluorescence $\Phi_f$ = 100 %
- (photo-)stability
- good electron acceptor & stable radical anions

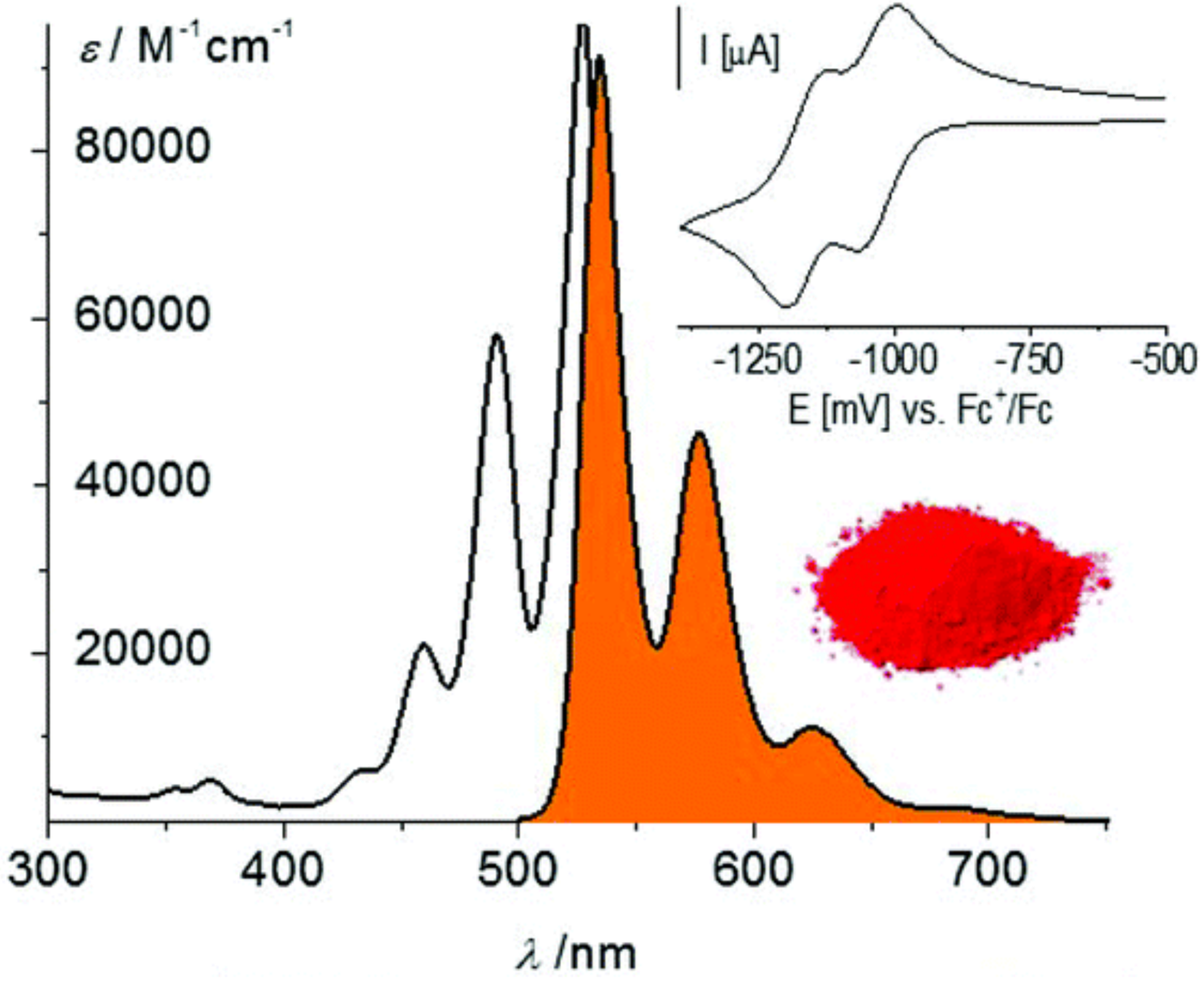

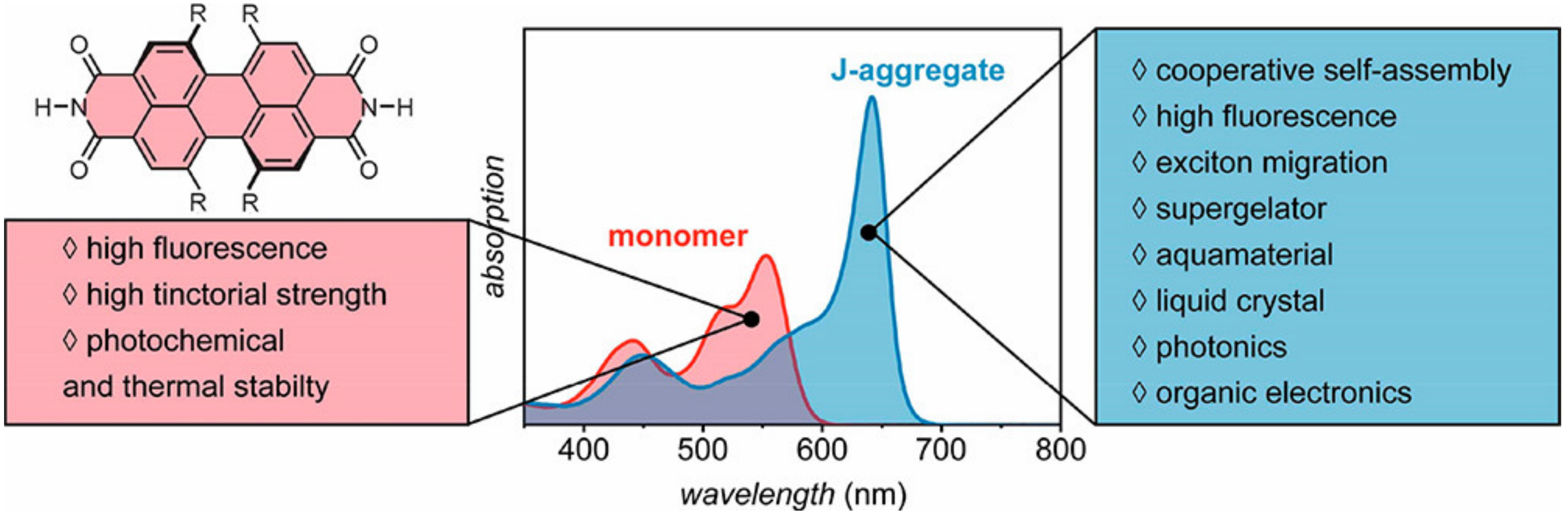
R
R
O
O
H–N
N–H
O
O
R
R
◊ high fluorescence
◊ high tinctorial strength
◊ photochemical
and thermal stabilty
absorption
monomer
J-aggregate
400
500
600
700
800
wavelength (nm)
◊ cooperative self-assembly
◊ high fluorescence
◊ exciton migration
◊ supergelator
◊ aquamaterial
◊ liquid crystal
◊ photonics
◊ organic electronics

# Absorption and Emission Spectra of Monomeric PDI

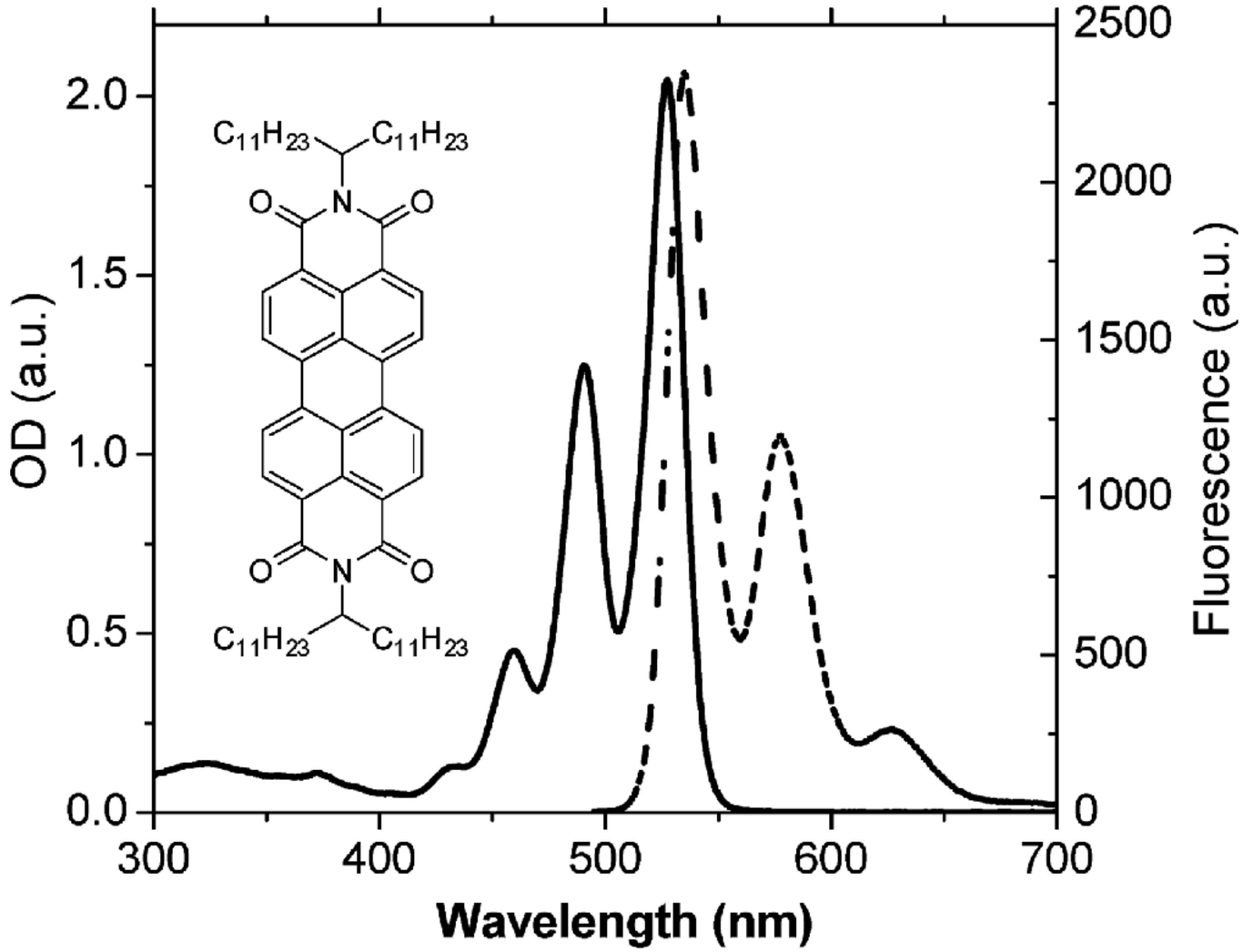


J. Org. Chem. 2011, 76, 8, 2386–2407

# Perylene bisimides

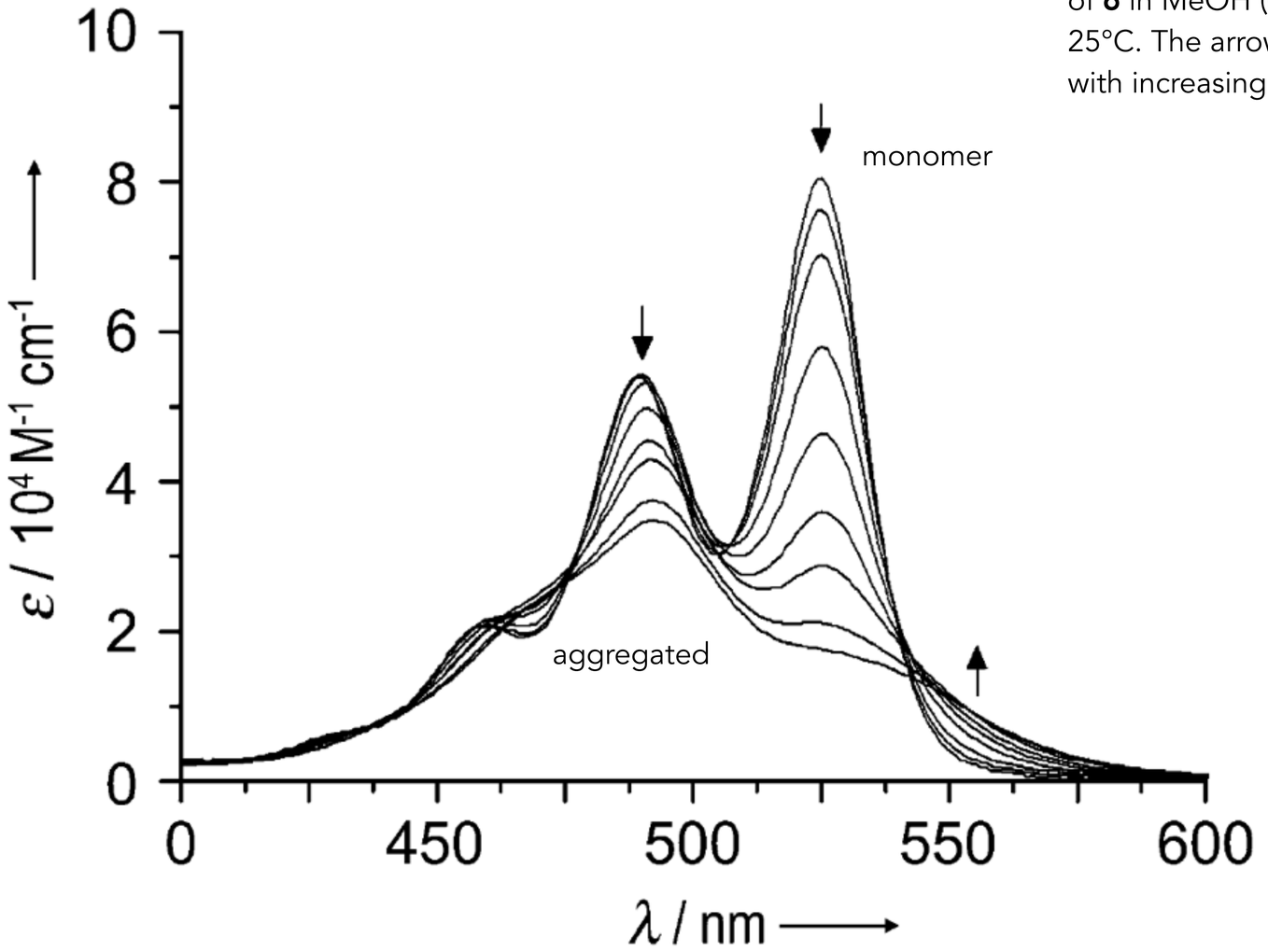


Concentration-dependent UV/Vis spectra of **6** in MeOH (6.1x10-7 M to 2.5x10-4 M) at 25°C. The arrows indicate the spectral changes with increasing concentration.

Frank Würthner and coll.

**Angewandte Chemie International Edition**
Volume 51, Issue 26, pages 6328-6348, 9 MAY 2012 DOI: 10.1002/anie.201108690
http://onlinelibrary.wiley.com/doi/10.1002/anie.201108690/full#fig4

# Artificial Quantasomes: Perylene Bis-imides and Polyoxometalates supramolecular complexes

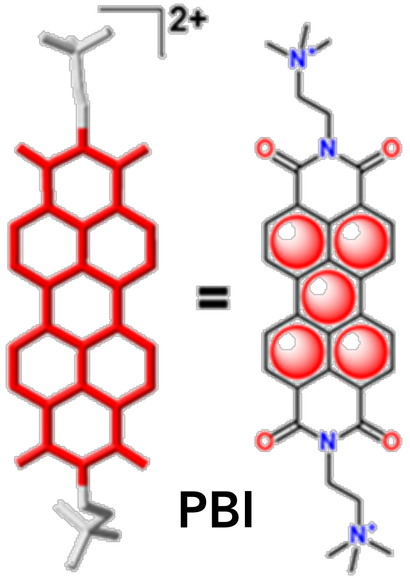


25 – 100 µM

$H_2O$, pH 7

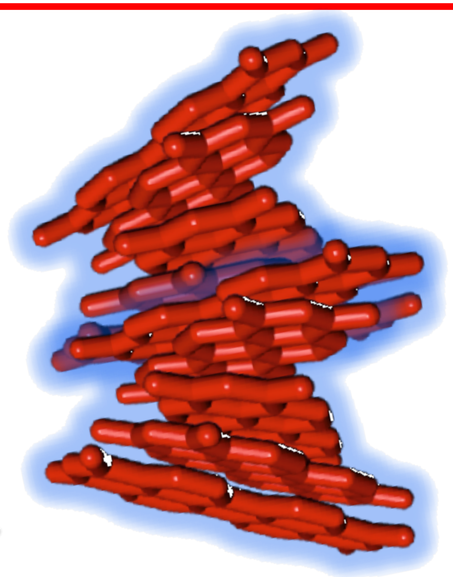

$Ru_4POM$

$H_2O$, pH 7

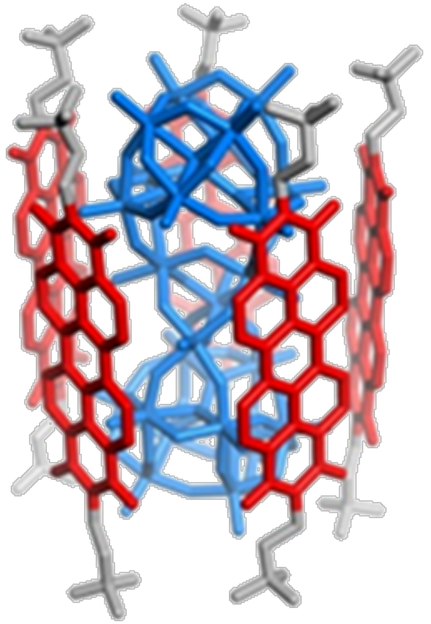

$[PBI]_5Ru_4POM$

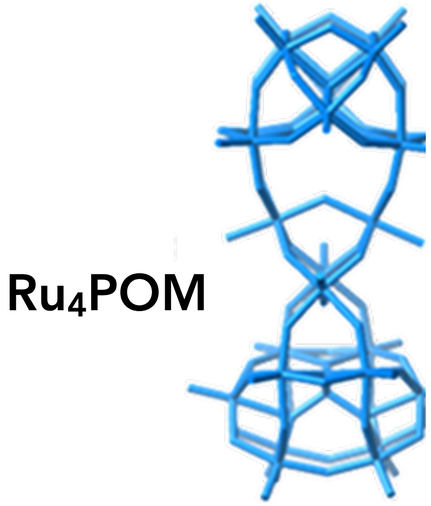

$Ru_4POM$

$10^-$

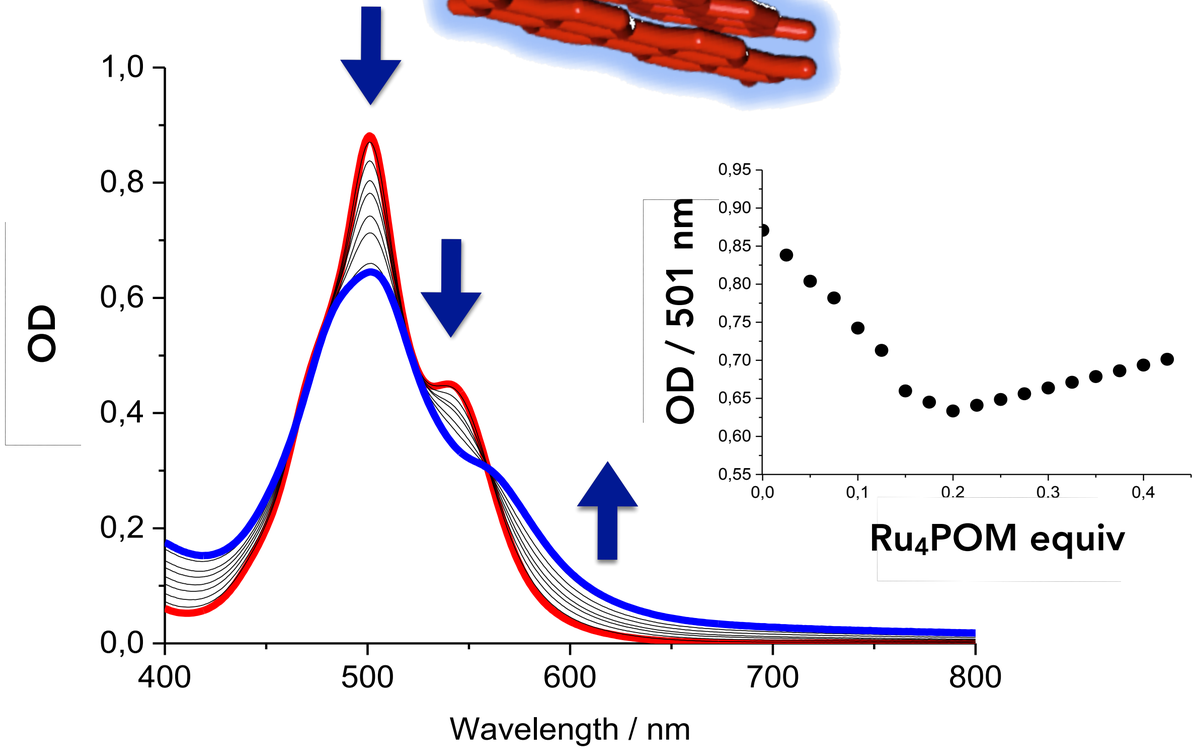





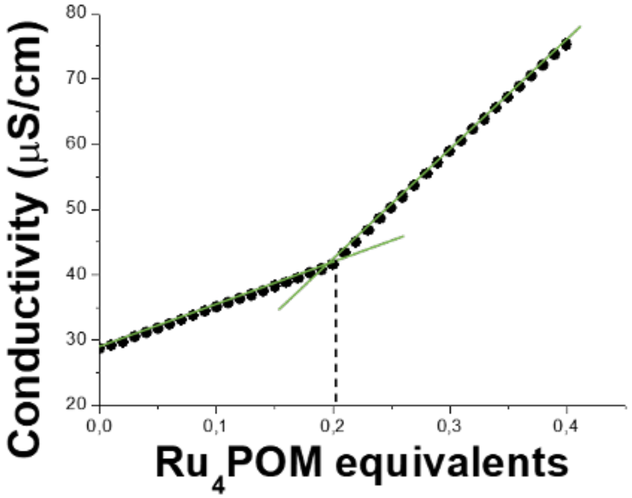

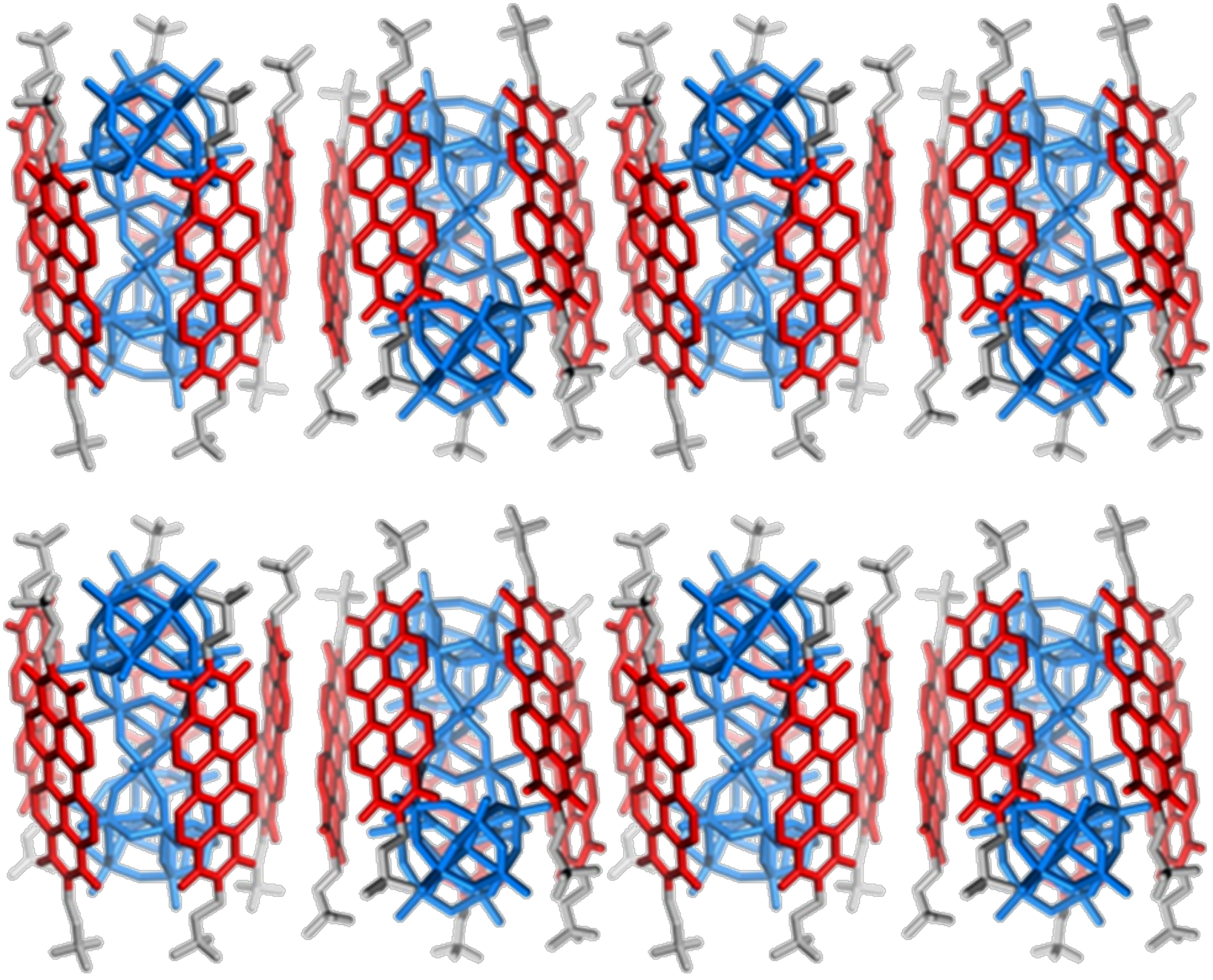

# Self Assembly of Artificial Quantasomes: formation of 2D-paracrystalline domains

2D hierarchical assembly

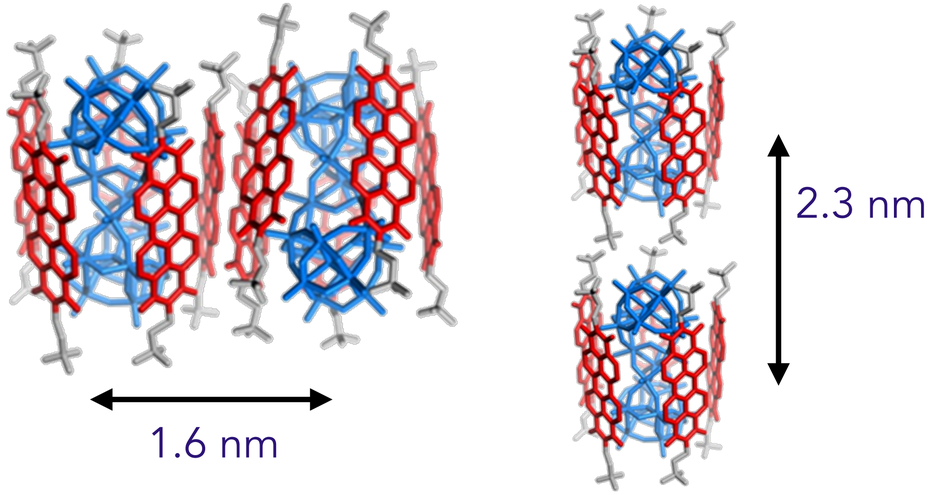


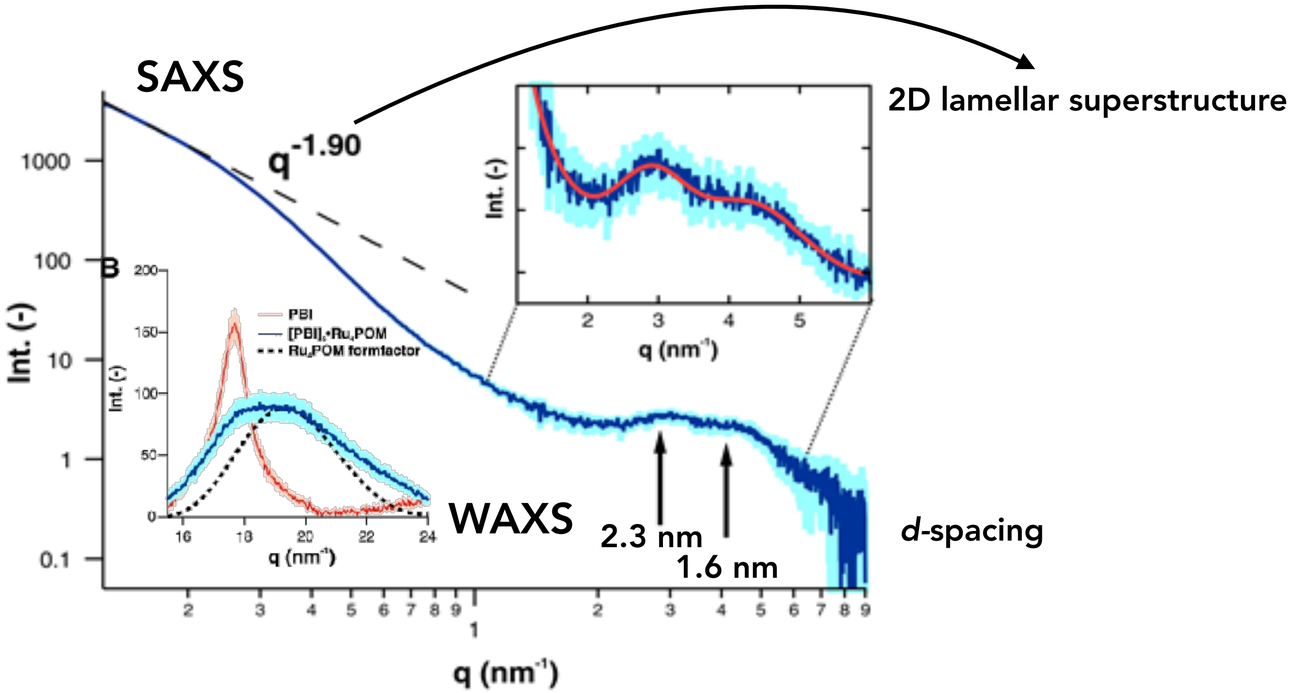


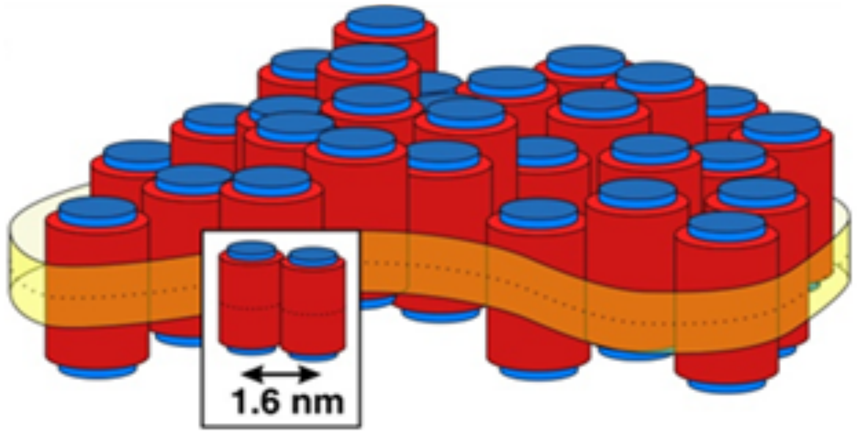


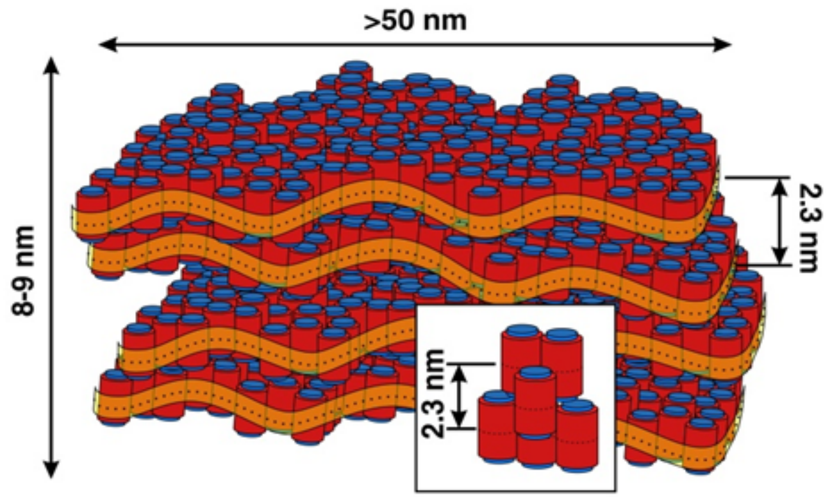


*with Max Burian and Heinz Amenitsch (Elettra Synchrotron)*

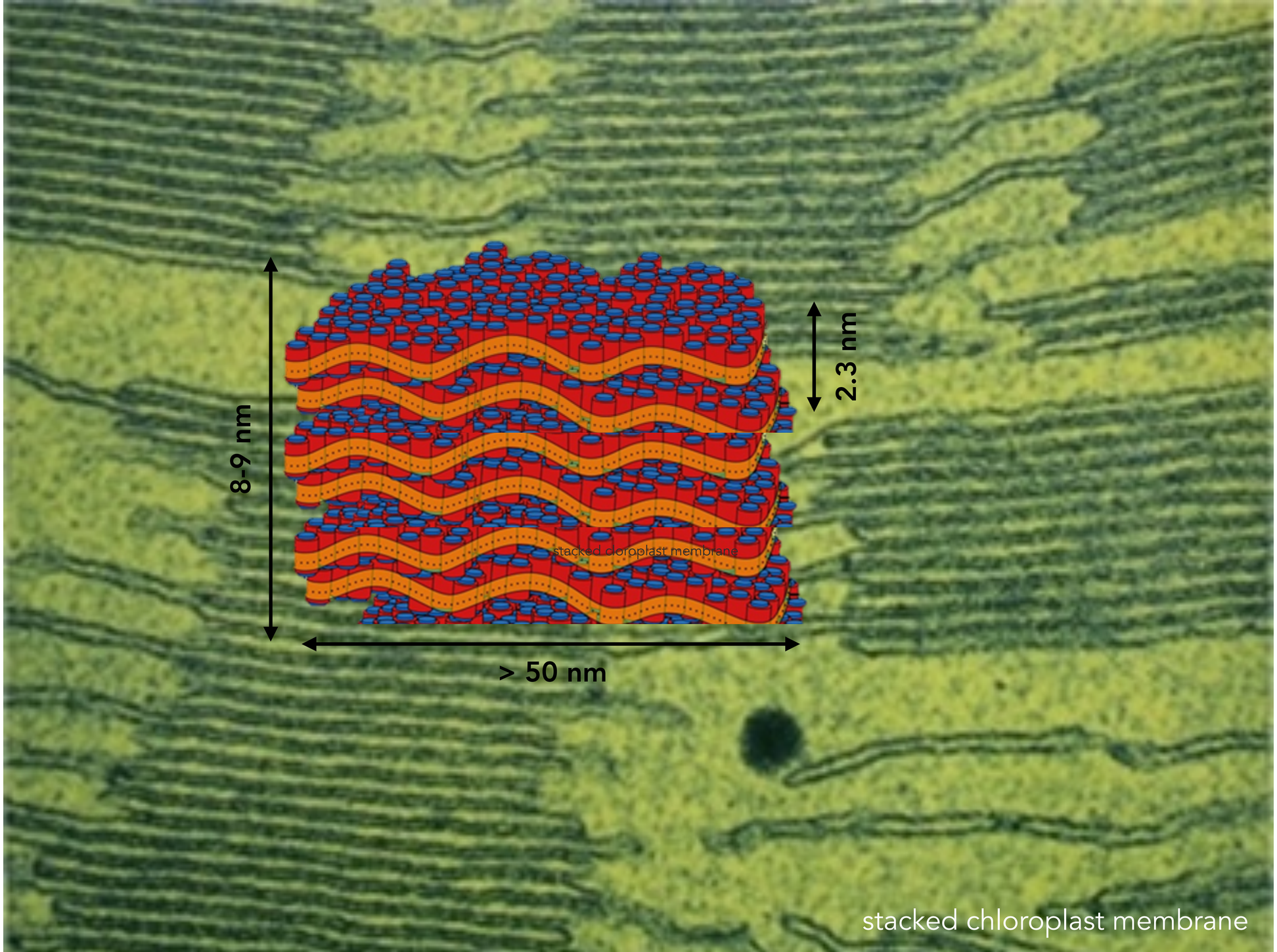


stacked chloroplast membrane

# Photo-catalytic water oxidation by $\{[PBI]_5Ru_4POM\}_n$:

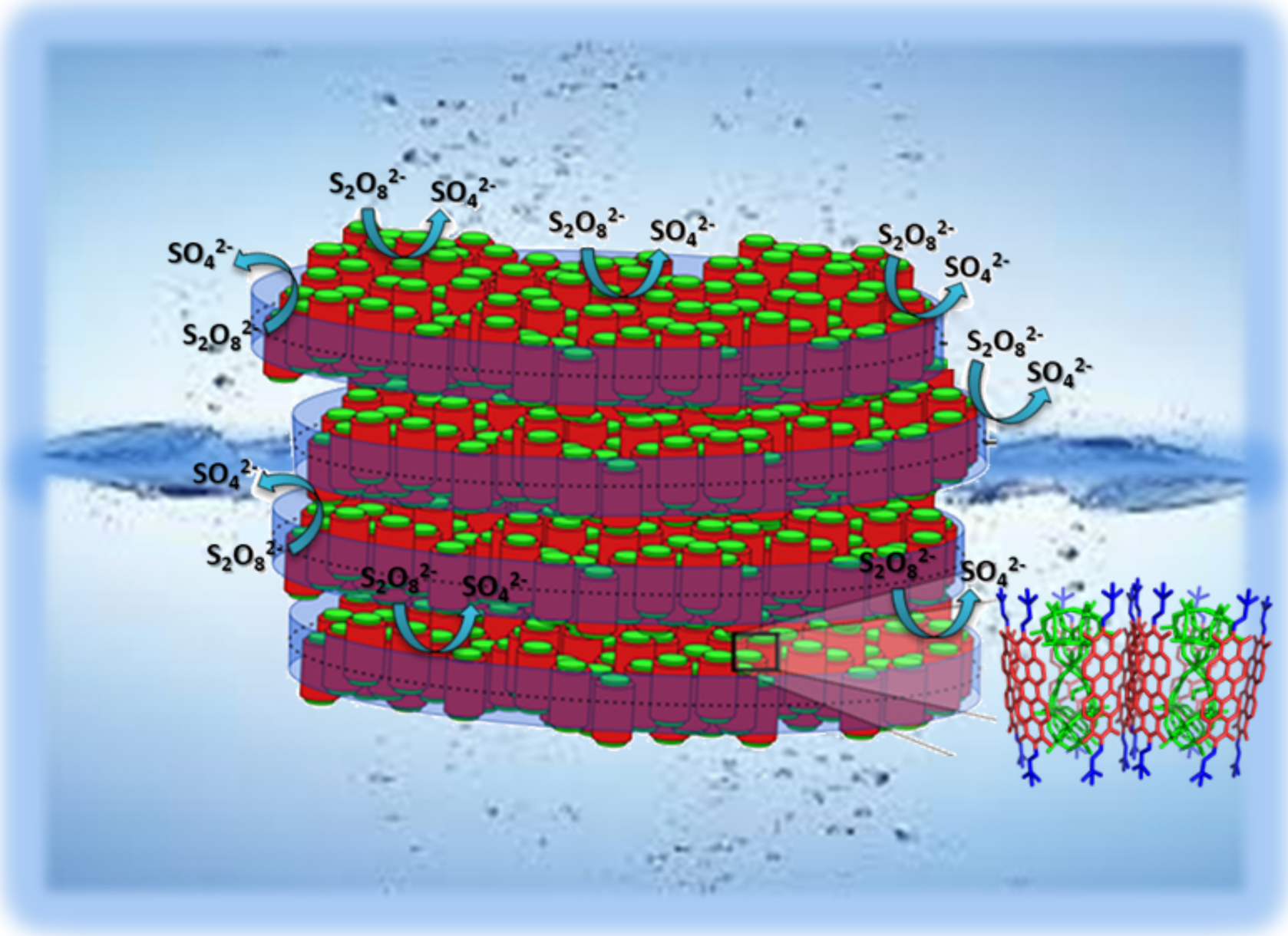


*Nature Chem.* 2019

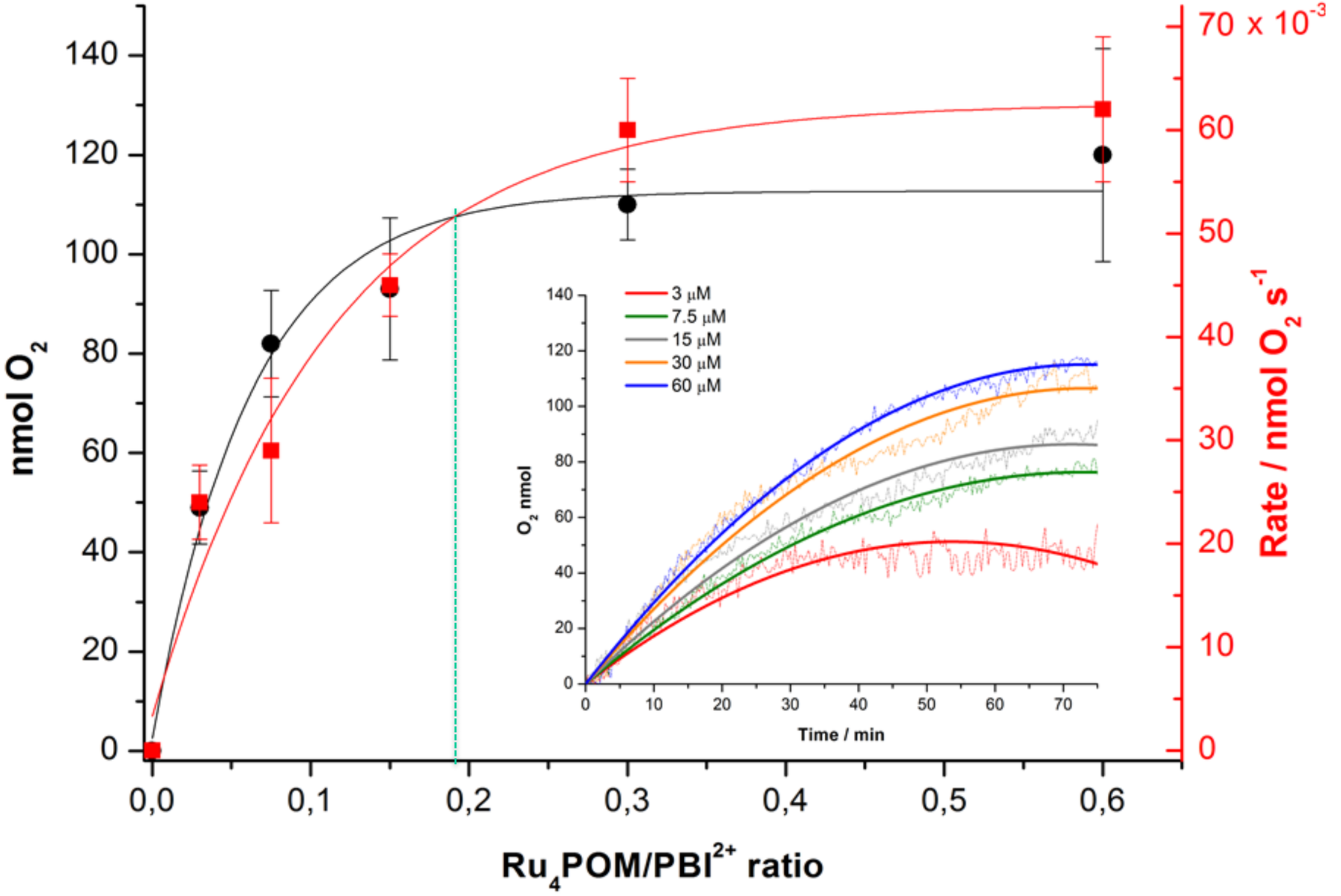


*Nature Chem.* 2019

## *nano*$WO_3$I{[PBI]$_5$$Ru_4$POM}$_n$ photoanodes

faradaic yield > 97 % , **APCE% = 1.3**

(λ> 450 nm, 0.91 V applied bias vs RHE)

**Absorbed Photon-to-Current Efficiency**
**% absorbed photons converted to current (oxygen)**

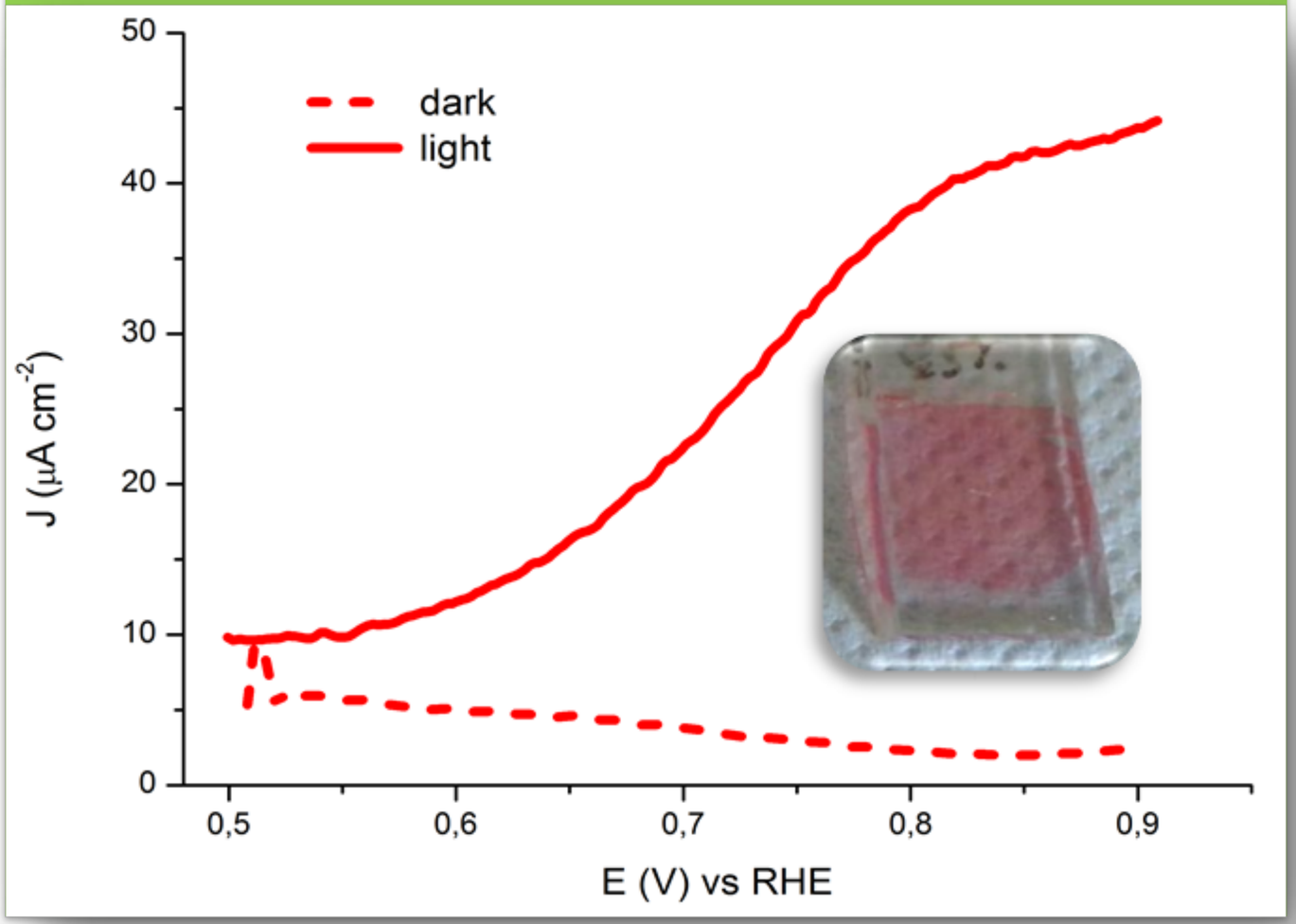


*with Serena Berardi, Stefano Caramori, Alberto Bignozzi (University of Ferrara)*

# $nanoWO_3$ $l[(PBI)_5 \cdot Ru_4POM]_n$ photoanodes

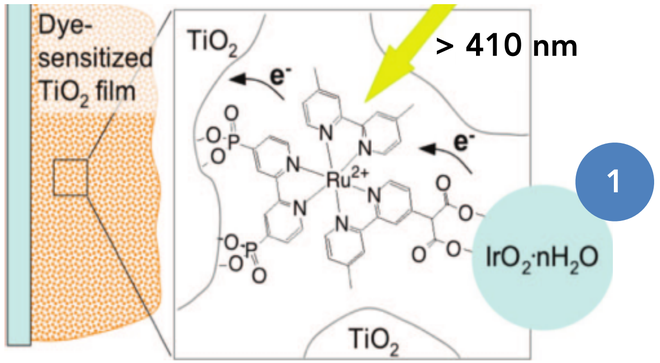


[1] Mallouk, *J. Am. Chem. Soc.* 2009, **131**, 926

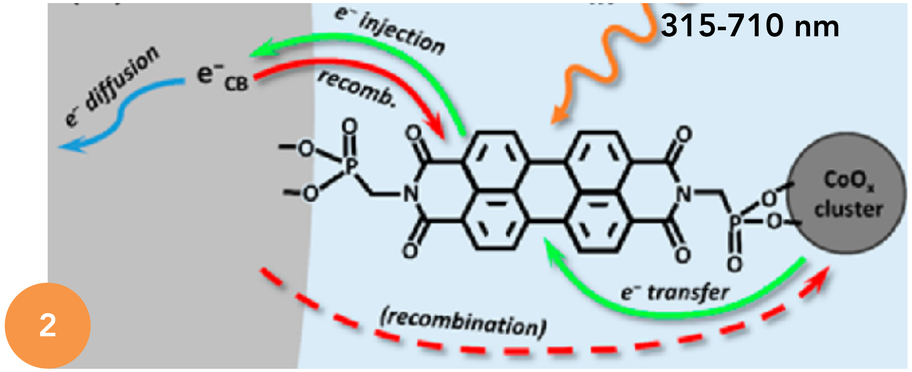


[2] Finke, *ACS Appl. Mater. Interfaces* 2014, **6**, 13367

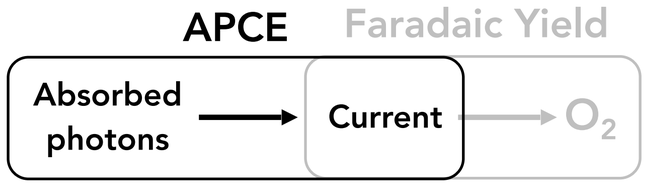


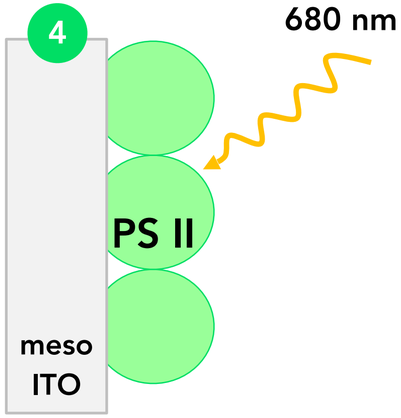


[4] Reisner, *Faraday Discuss.* 2014, **176**, 199-211

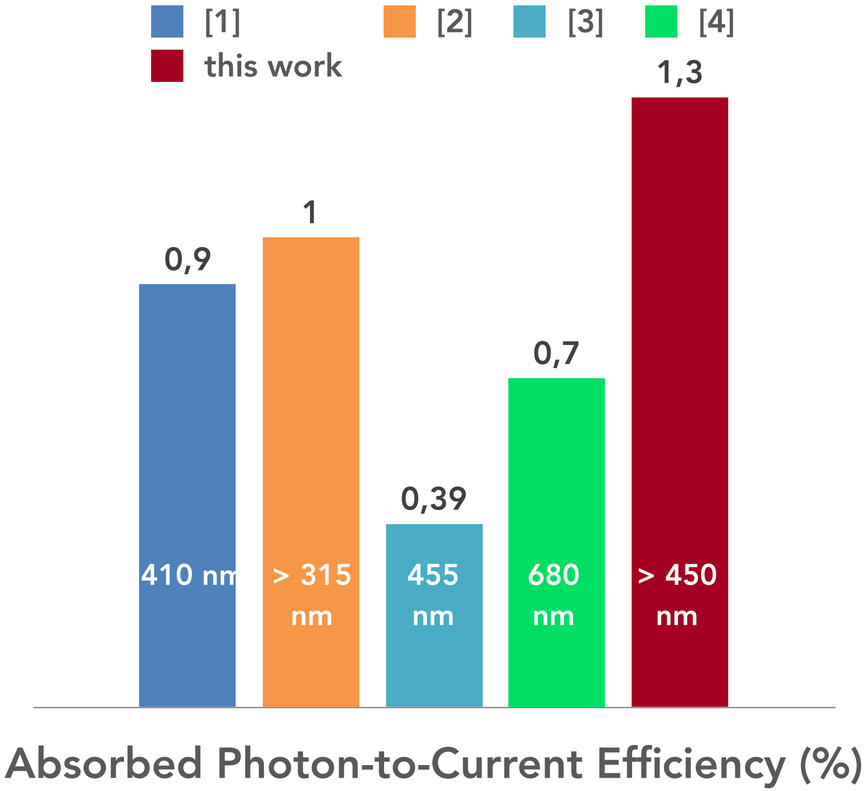


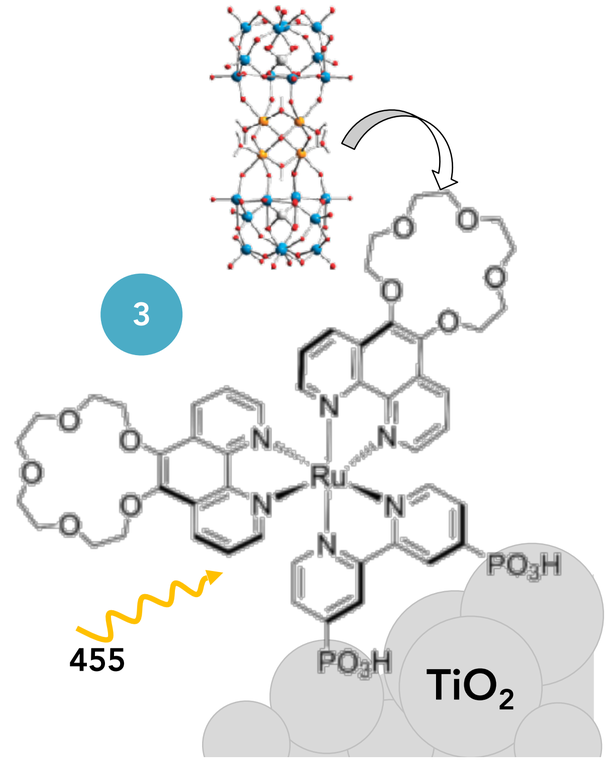


[3] Hill, *Chem. Sci.* 2015, **6**, 5531

# *Improving Quantasomes*

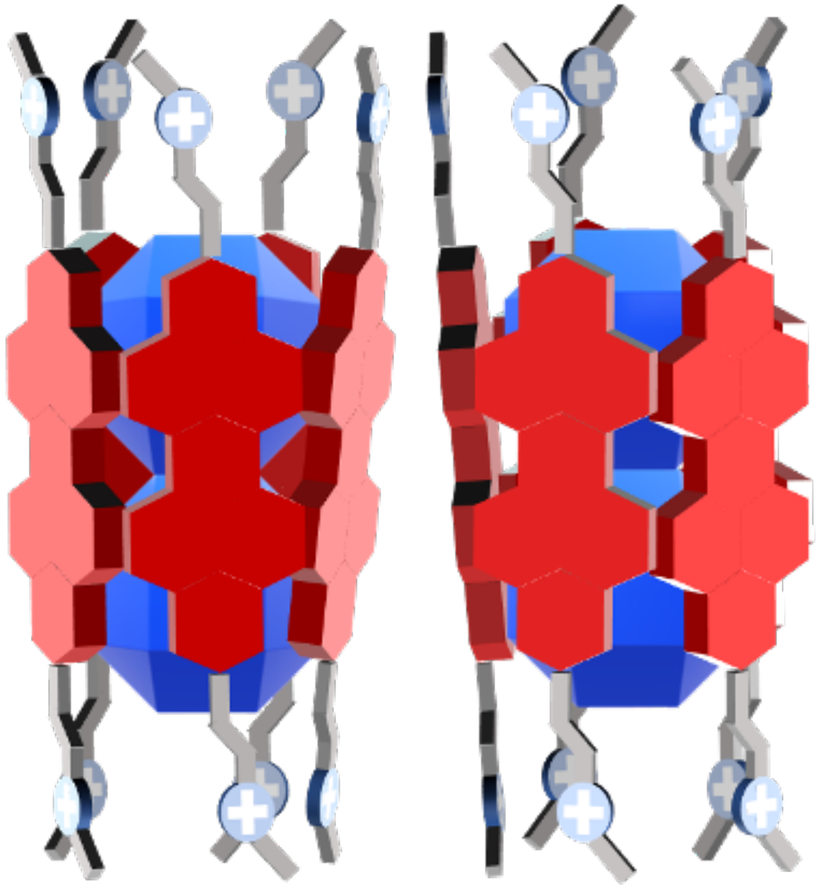

1) Improving water solubility
2) Improving water accessibility and transport
3) Improving light harvesting

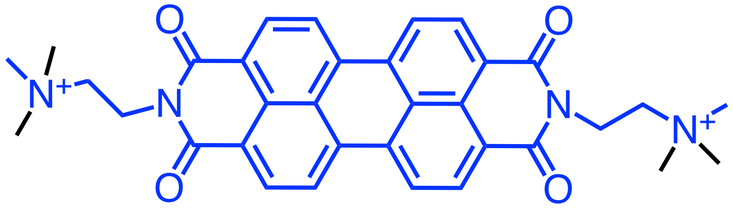


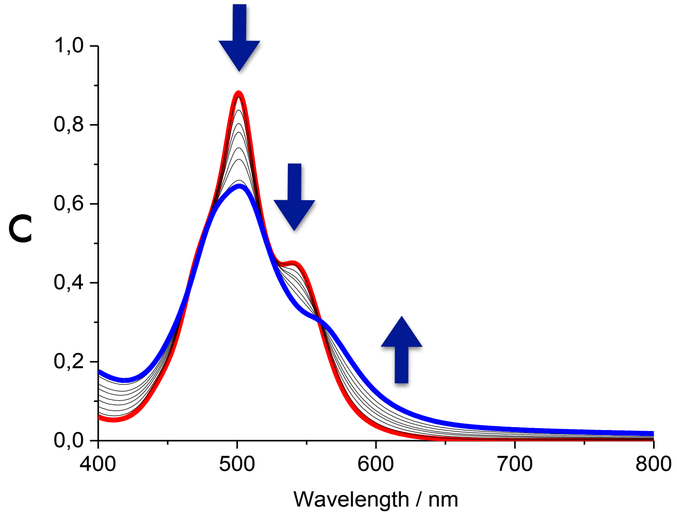

# $N_2$

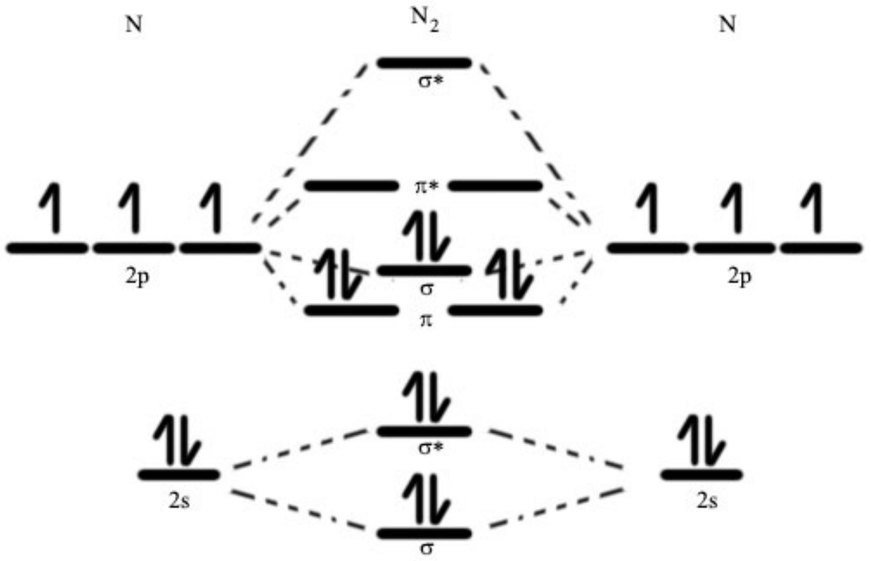
N
N2
N
σ*
π*
2p
σ
π
2p
σ*
2s
2s
σ

# $O_2$

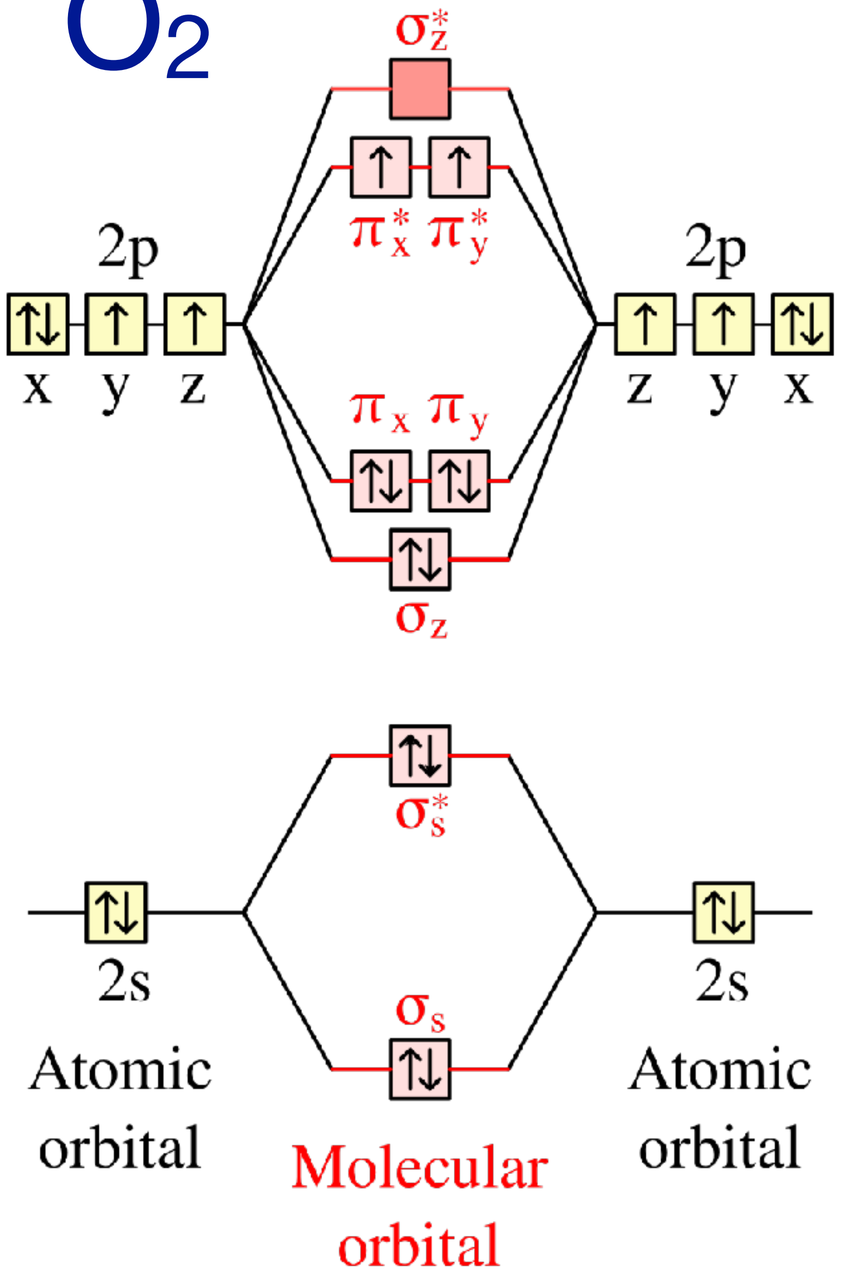
σz*
π*x π*y
2p
2p
x y z
z y x
πx πy
σz
σ*s
2s
2s
σs
Atomic orbital
Molecular orbital
Atomic orbital

# Role of the Electron Spin Polarization in Water Splitting (spin filtering)

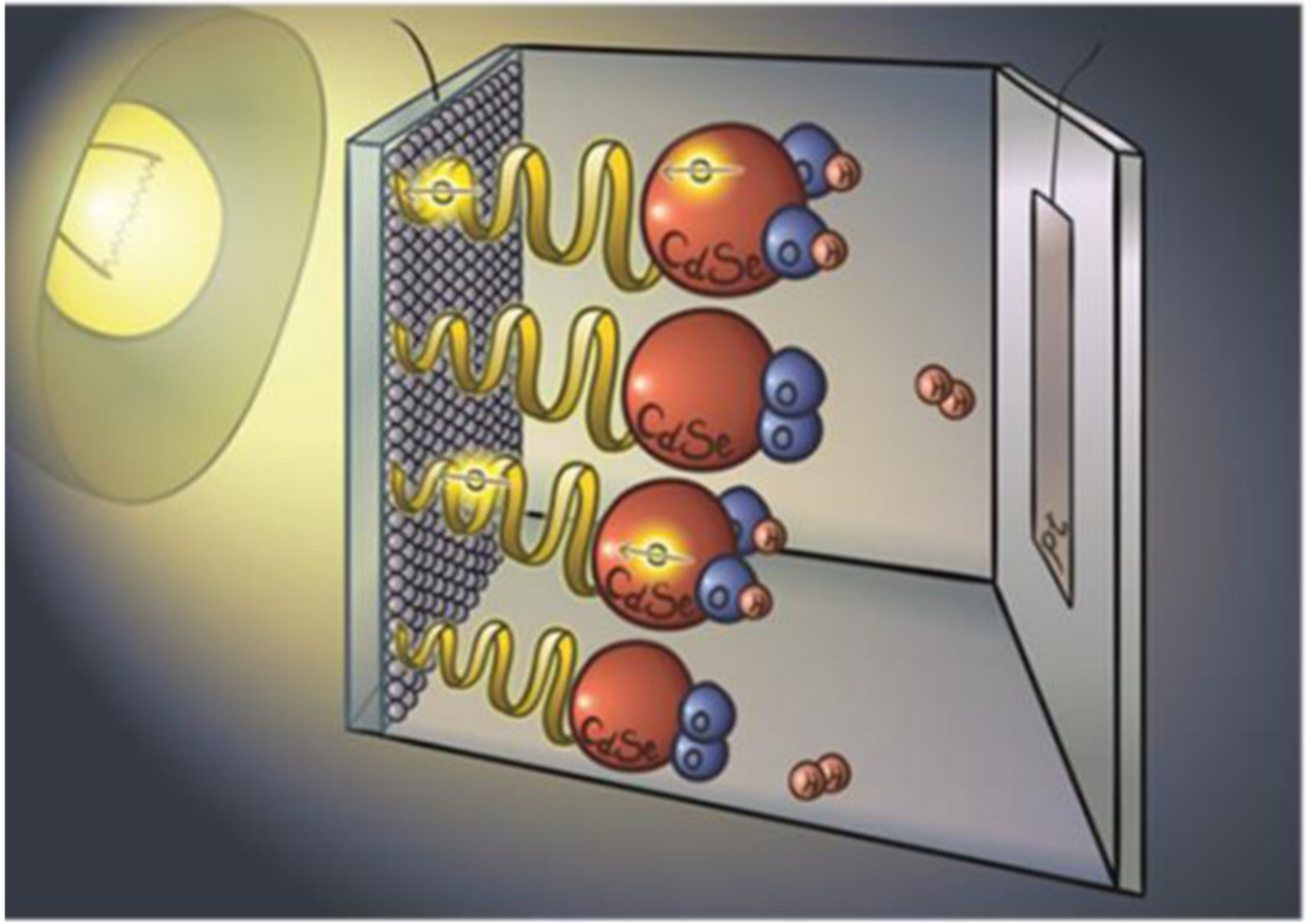


In an electrochemical cell, in which the photoanode is coated with chiral molecules, the overpotential required for hydrogen production drops remarkably, as compared with cells containing achiral molecules. The spin specificity of electrons transferred through chiral molecules is the origin of a more efficient oxidation process in which oxygen is formed in its triplet ground state.

J. Phys. Chem. Lett. 2015, 6, 24, 4916–4922

# Chirality Induced Spin Selectivity (CISS)

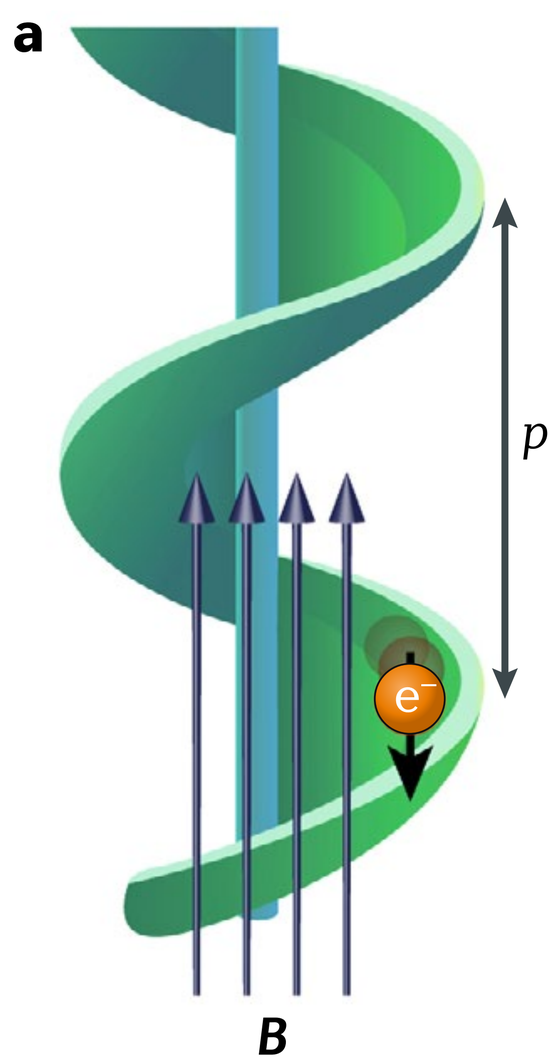


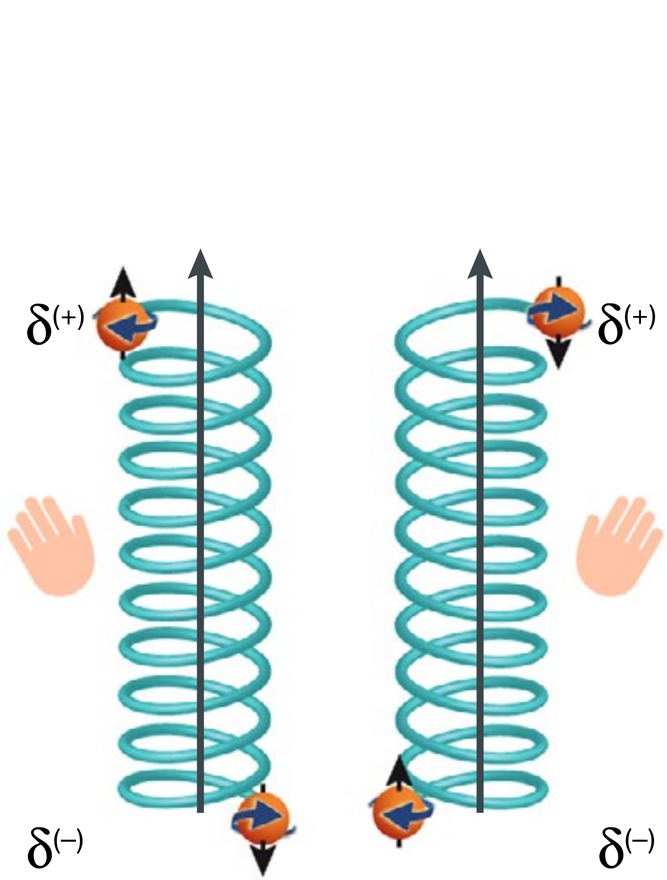


Ron Naaman et al.

# Control of Electrons' Spin Eliminates Hydrogen Peroxide Formation During Water Splitting

Wilbert Mtangi, Francesco Tassinari, Kiran Vankayala, Andreas Vargas Jentzsch, Beatrice Adelizzi, Anja R. A. Palmans, Claudio Fontanesi, E. W. Meijer,* and Ron Naaman*

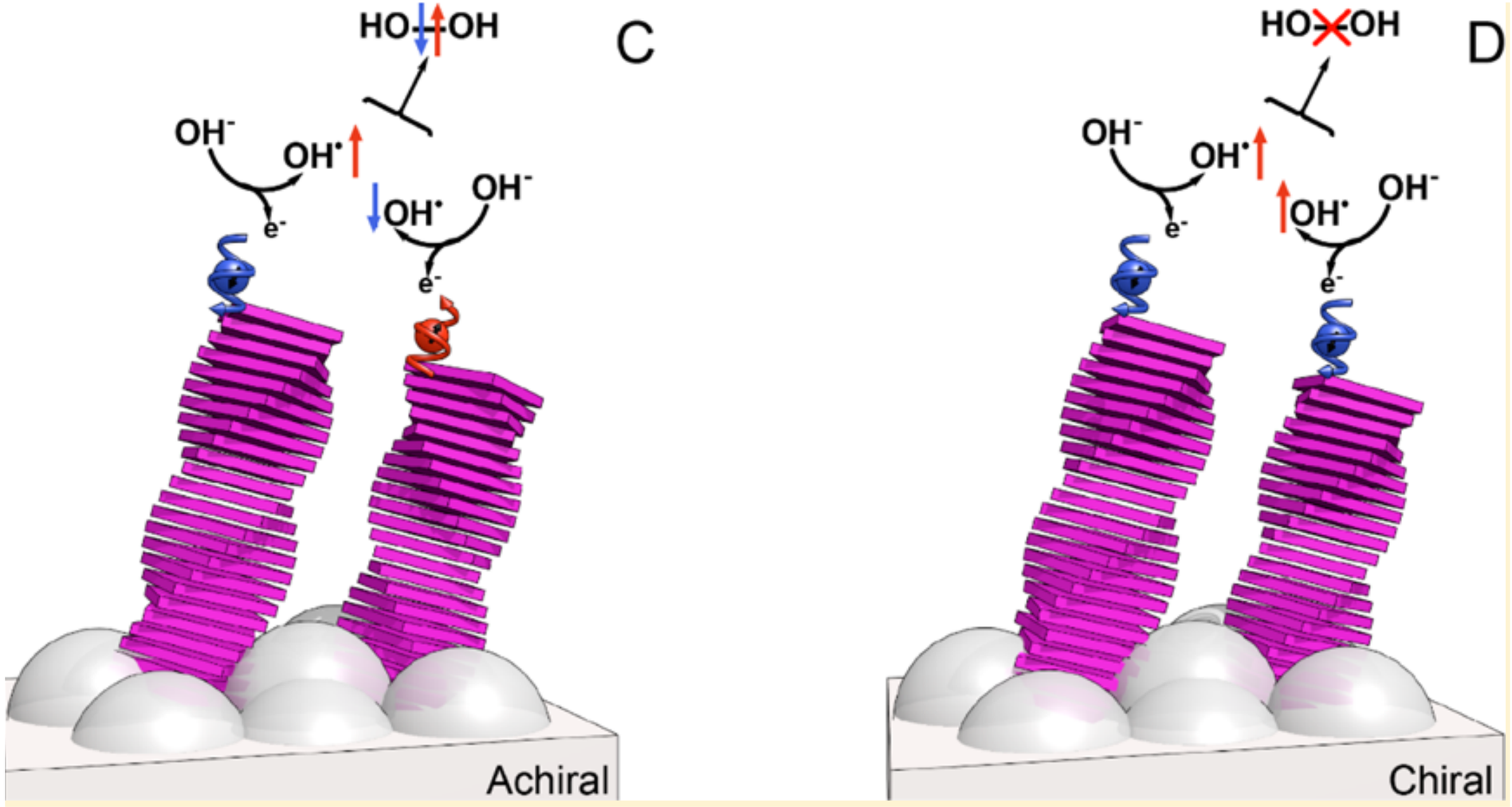


J. Am. Chem. Soc. 2017, 139, 2794–2798

# *The catalytic system (artificial quantasome)*

The catalyst

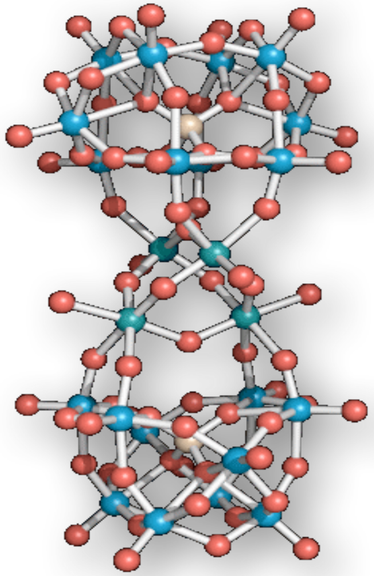

The antenna
(photosensitizer)

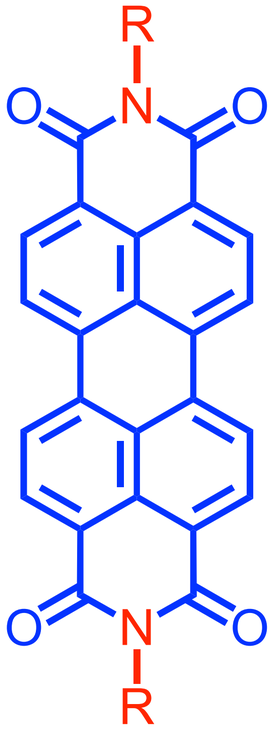


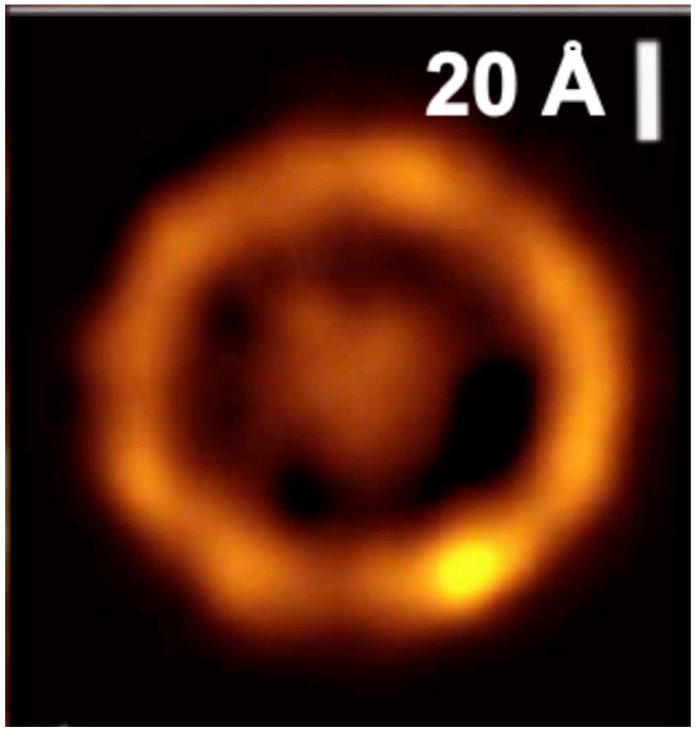

# PDI Synthesis

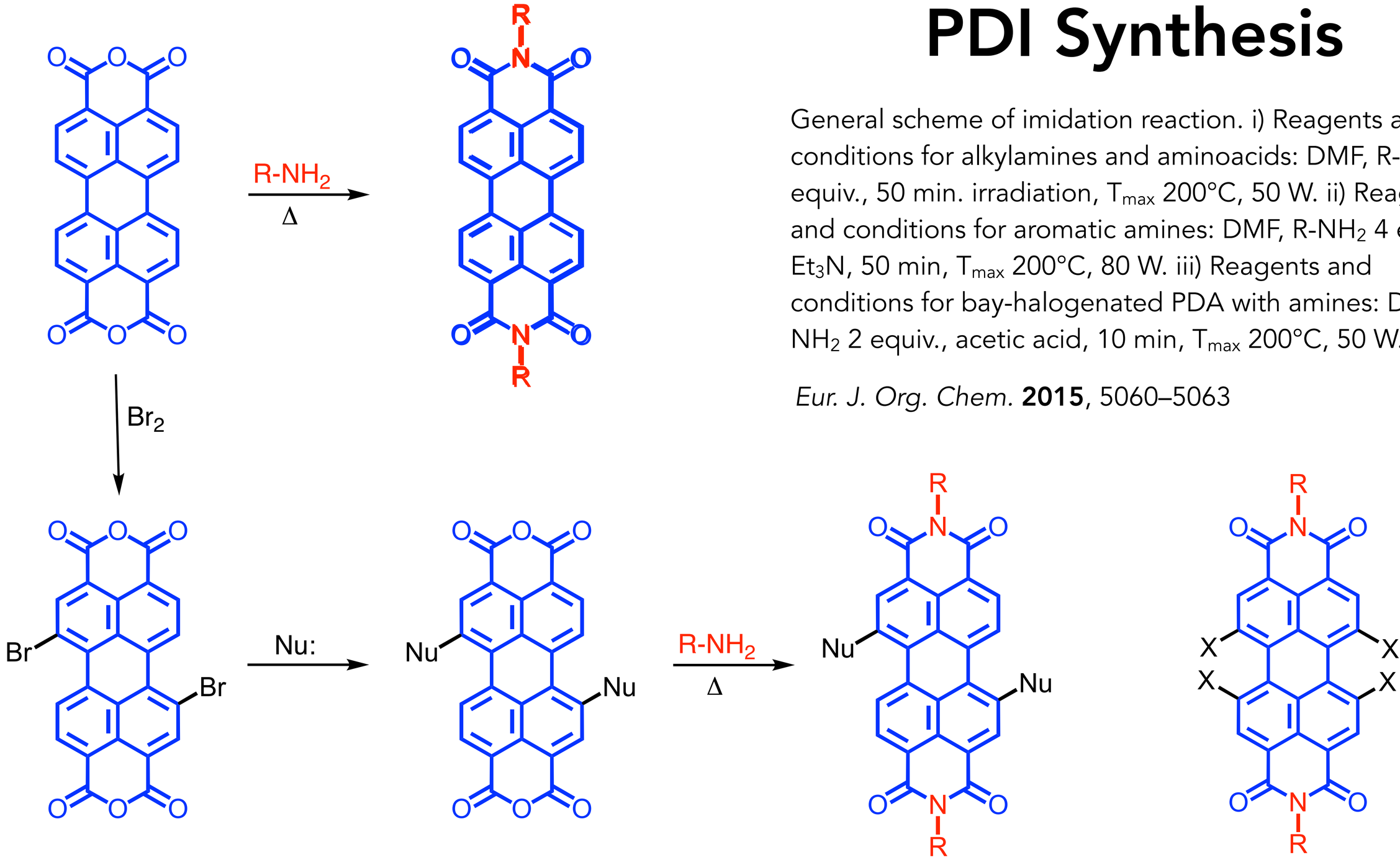


General scheme of imidation reaction. i) Reagents and conditions for alkylamines and aminoacids: DMF, R-$NH_2$ 2 equiv., 50 min. irradiation, $T_{max}$ 200°C, 50 W. ii) Reagents and conditions for aromatic amines: DMF, R-$NH_2$ 4 equiv., $Et_3N$, 50 min, $T_{max}$ 200°C, 80 W. iii) Reagents and conditions for bay-halogenated PDA with amines: DMF, R-$NH_2$ 2 equiv., acetic acid, 10 min, $T_{max}$ 200°C, 50 W.

*Eur. J. Org. Chem.* **2015**, 5060–5063

# Synthesis of Brominated PDI

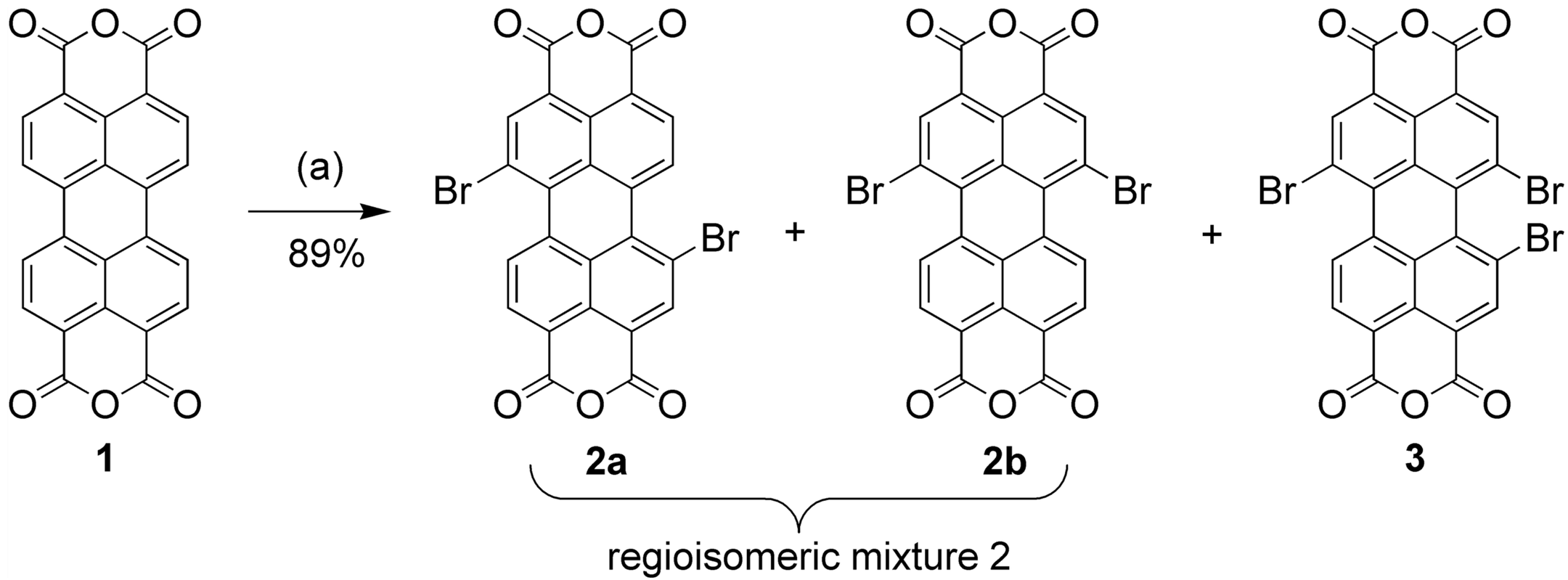


(a) bromine, I2/$H_2SO_4$, 85 °C, 24 h

*Eur. J. Org. Chem.* **2015**, 3296-3302

# Chirality of PDIs

***i Twisted planes***

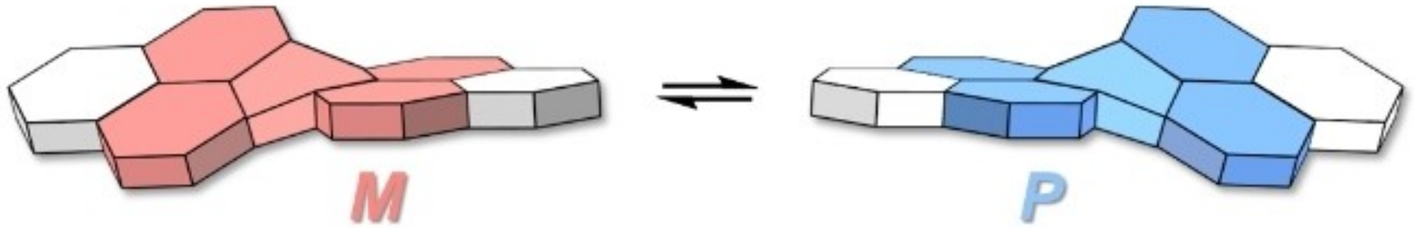


***ii Chiral substituents***

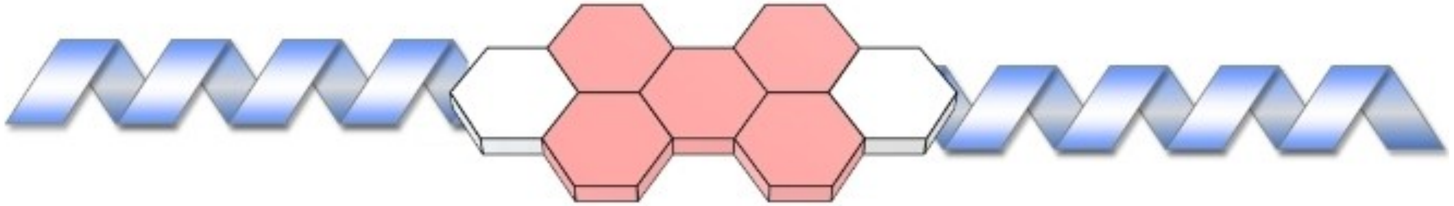

***iii Chiral guests***

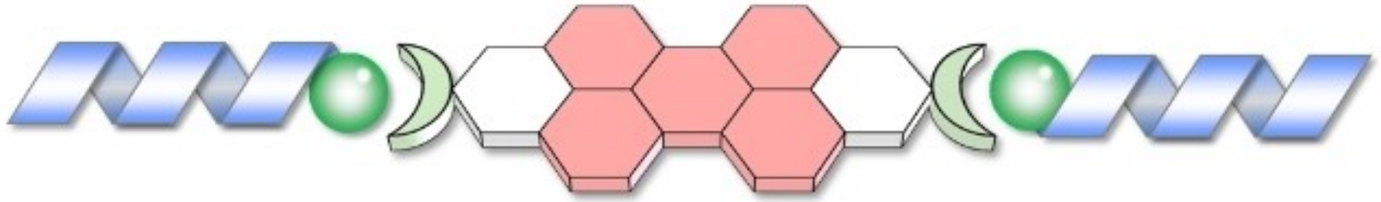

*Angew. Chem. Int. Ed.* **2022**, *61*, e202202532

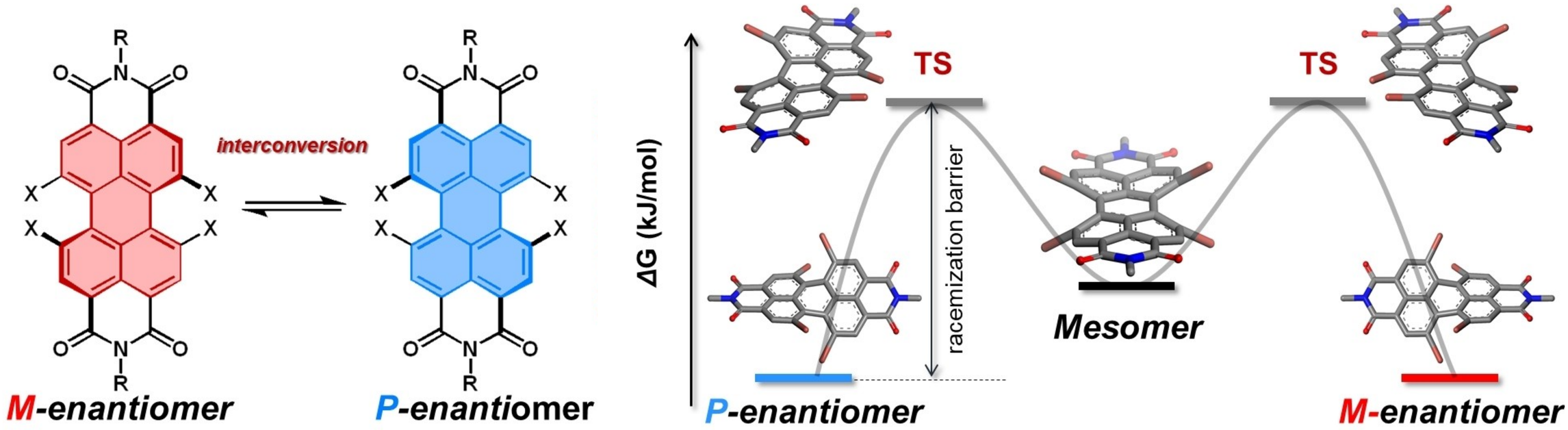


*Angew. Chem. Int. Ed.* **2022**, *61*, e202202532

***Bay-linked***

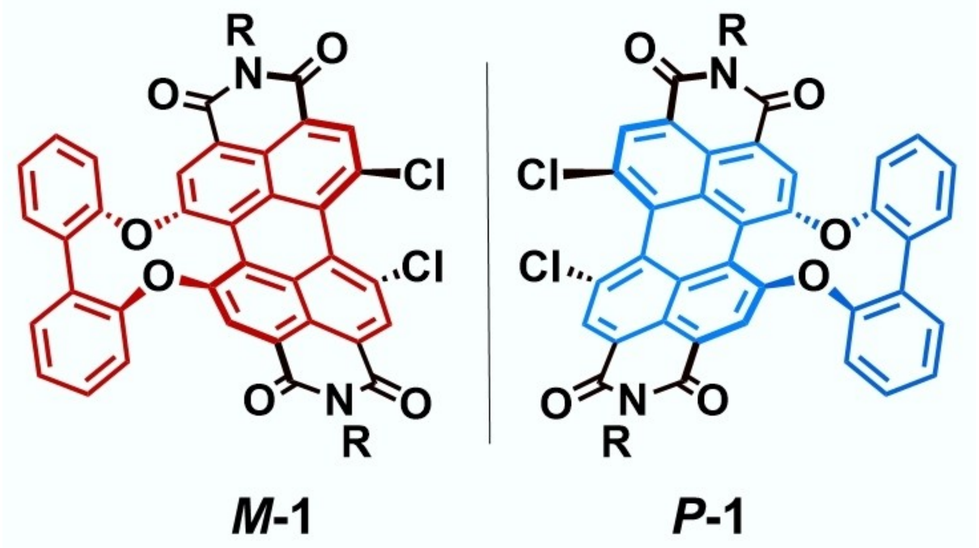


$\Delta G$ = 98.5 kJ mol

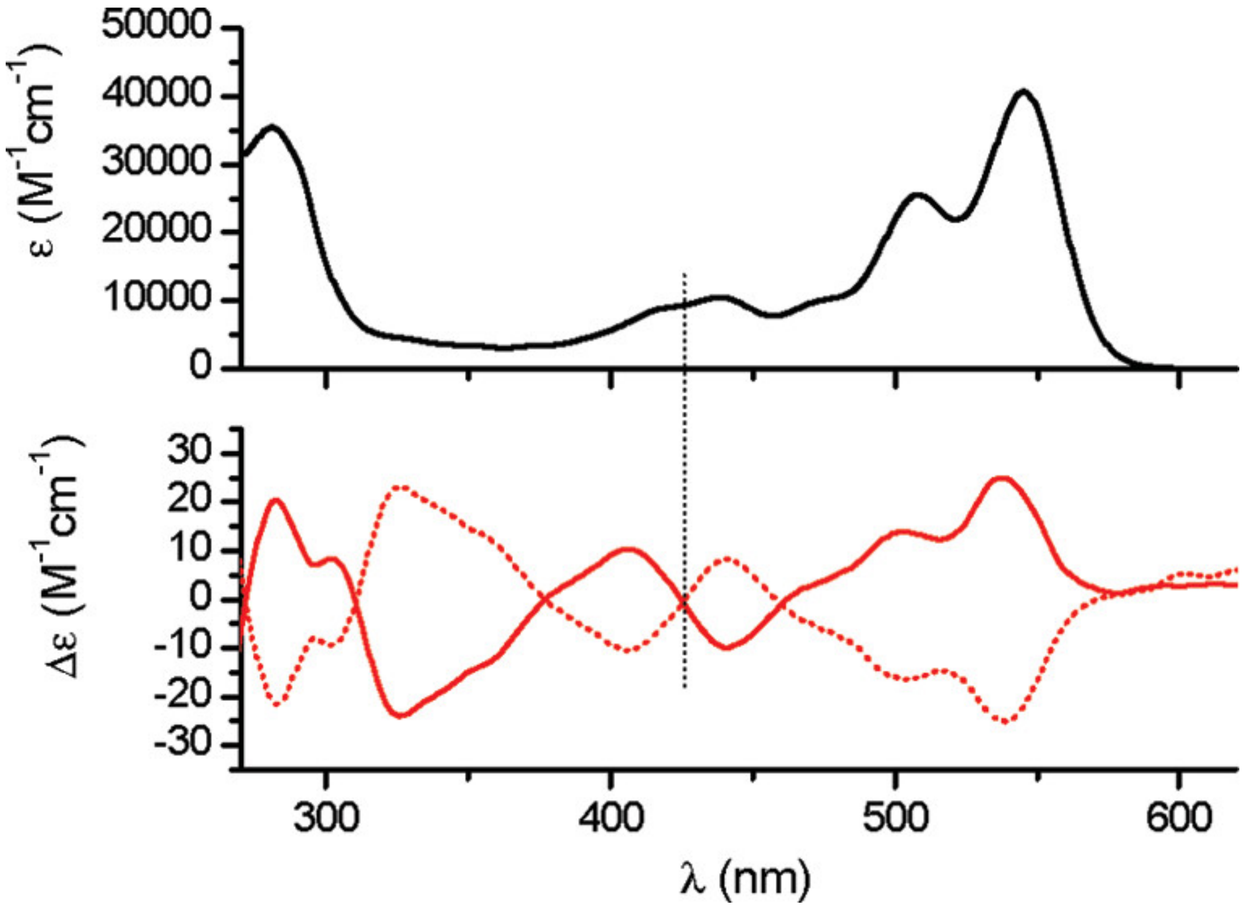


Org. Lett. 2010, 12, 14, 3204–3207

**Laterally-linked**

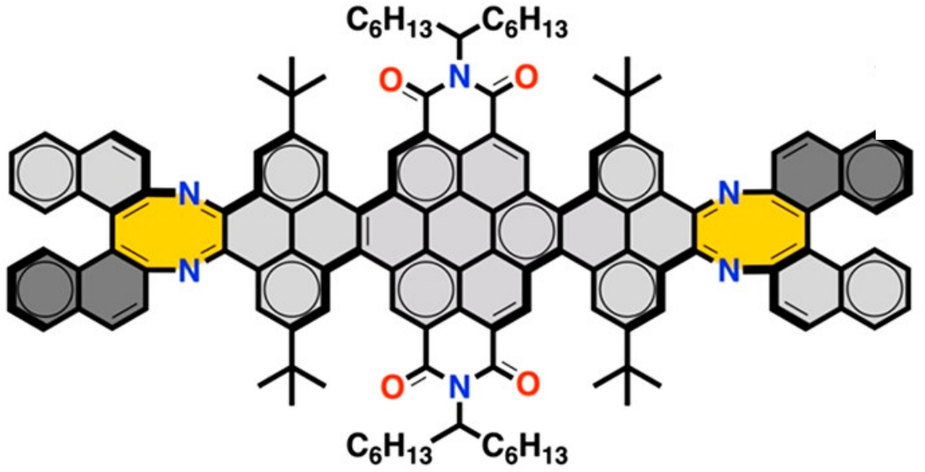


III

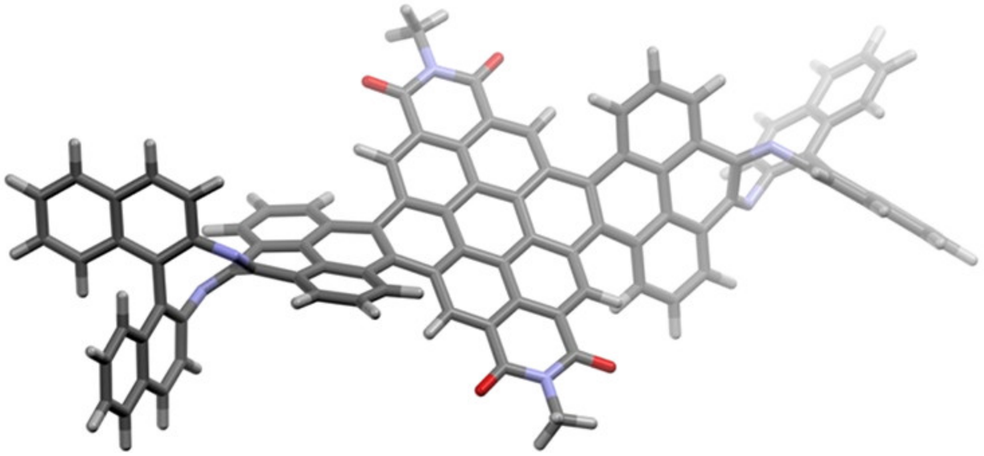

**Induction of Single-Handed Helicity**

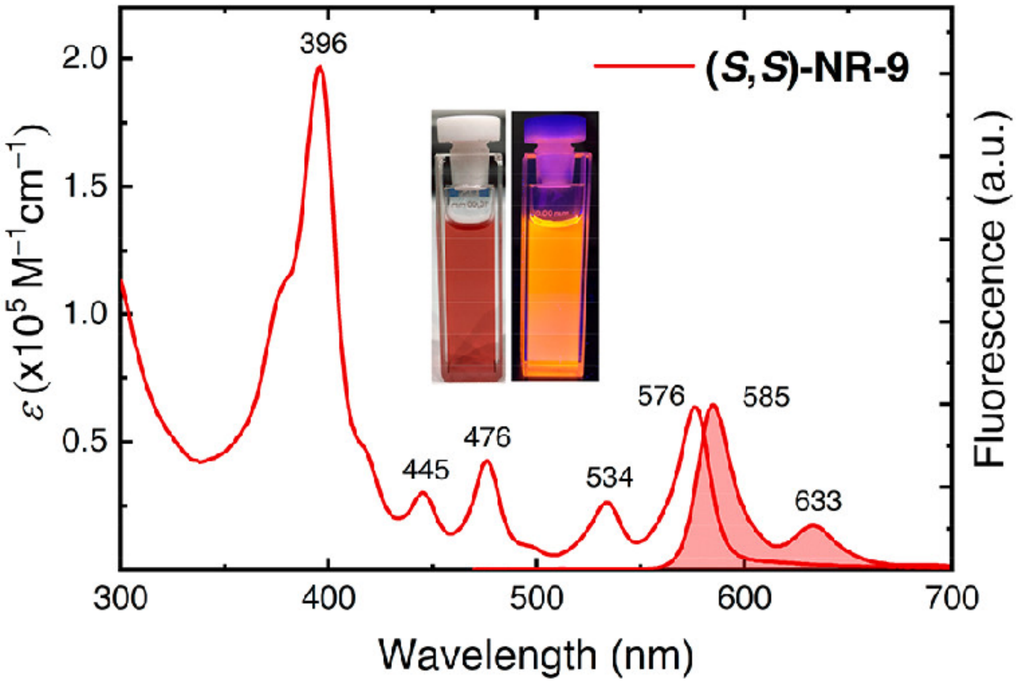


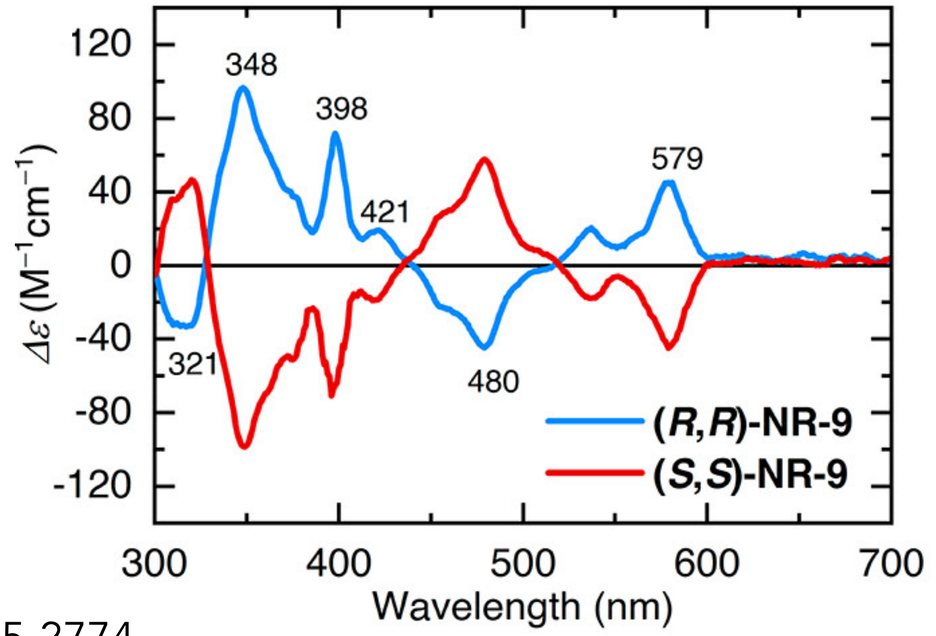


J. Am. Chem. Soc. 2022, 144, 6, 2765-2774

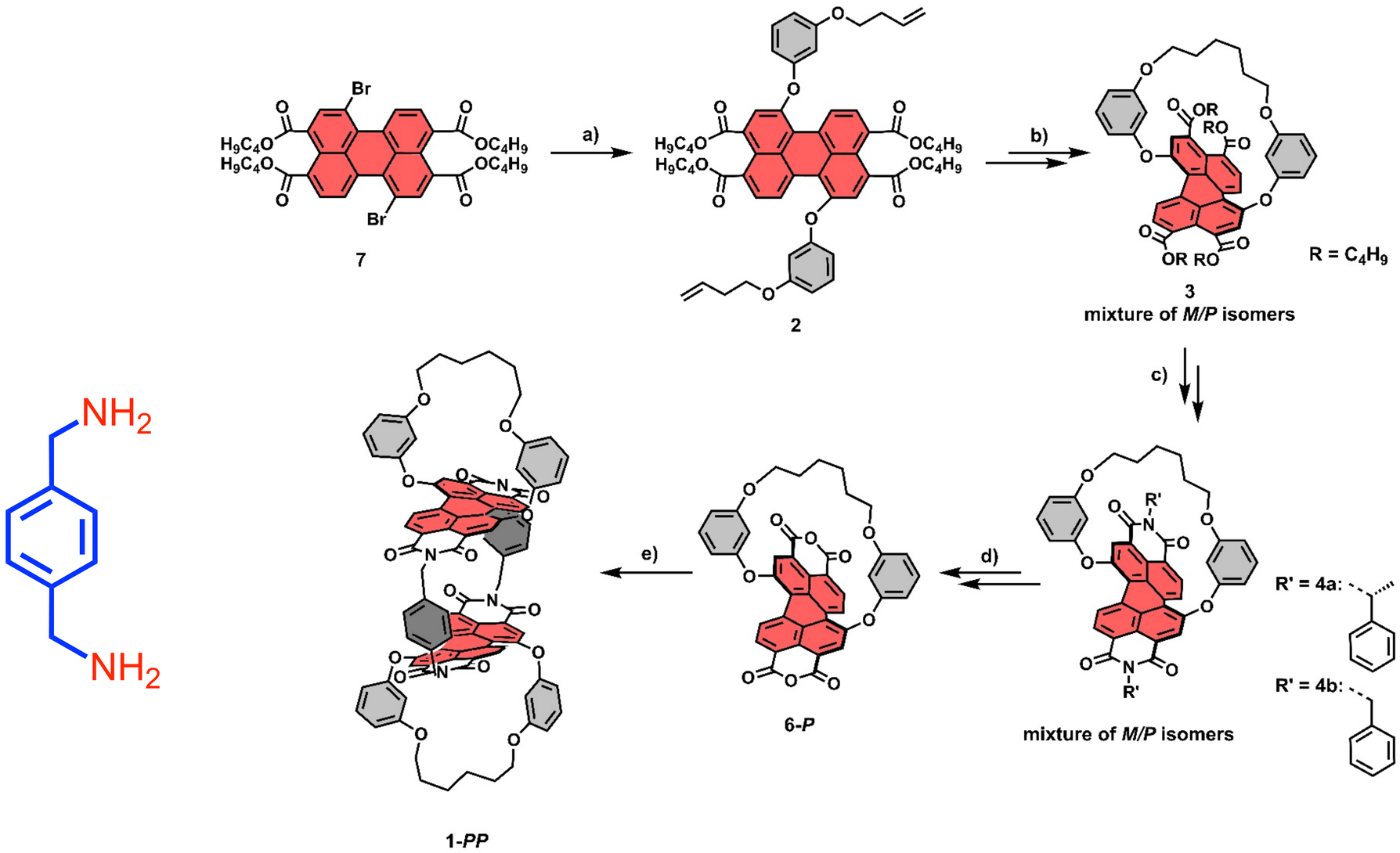


Synthetic route to PBI cyclophane **1-*PP*** (route to **1-*MM*** analogous). In addition, the chemical structures of PBI dye **4b** is shown. Reaction conditions: a) 3-(but-3-en-1-yloxy)phenol, Cs2CO3, DMF, 100 °C, 7.5 h, 49%; b) 1. Grubbs II catalyst, DCM, reflux, 2 h, 82%; 2. H2, Pd/C, EtOAc/MeOH (10:1), 2.5 h, 97%; c). 1. *p*-TsOH · H2O, toluene, 140 °C, 17 h, quantitative, 2. **4a**: *R*-1-phenylethylamine, quinoline, Zn(OAc)2, 140 °C, 5 h, 90% (diastereomeric mixture), d) 1. Chiral HPLC resolution of **4a**; 2. KOH, *tert*-butanol, 90 °C, 2 h, 72–90%; e) *para*-xylylenediamine, imidazole, toluene, 120 °C, 16 h, 17%. Würthner, F. et al. *Angew. Chem., Int. Ed.* 2021, *60*, 15323–15327.

Deracemization of Carbohelicenes by a Chiral Perylene Bisimide Cyclophane Template Catalyst

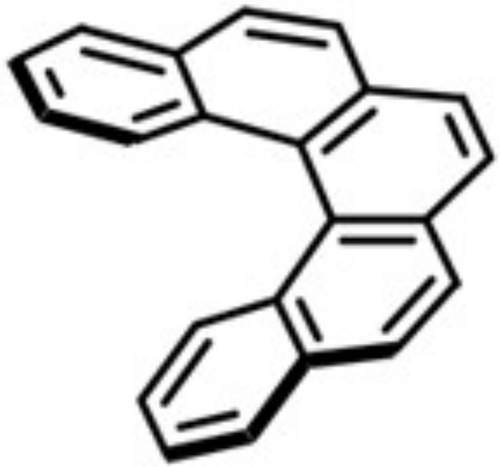

[5]helicene

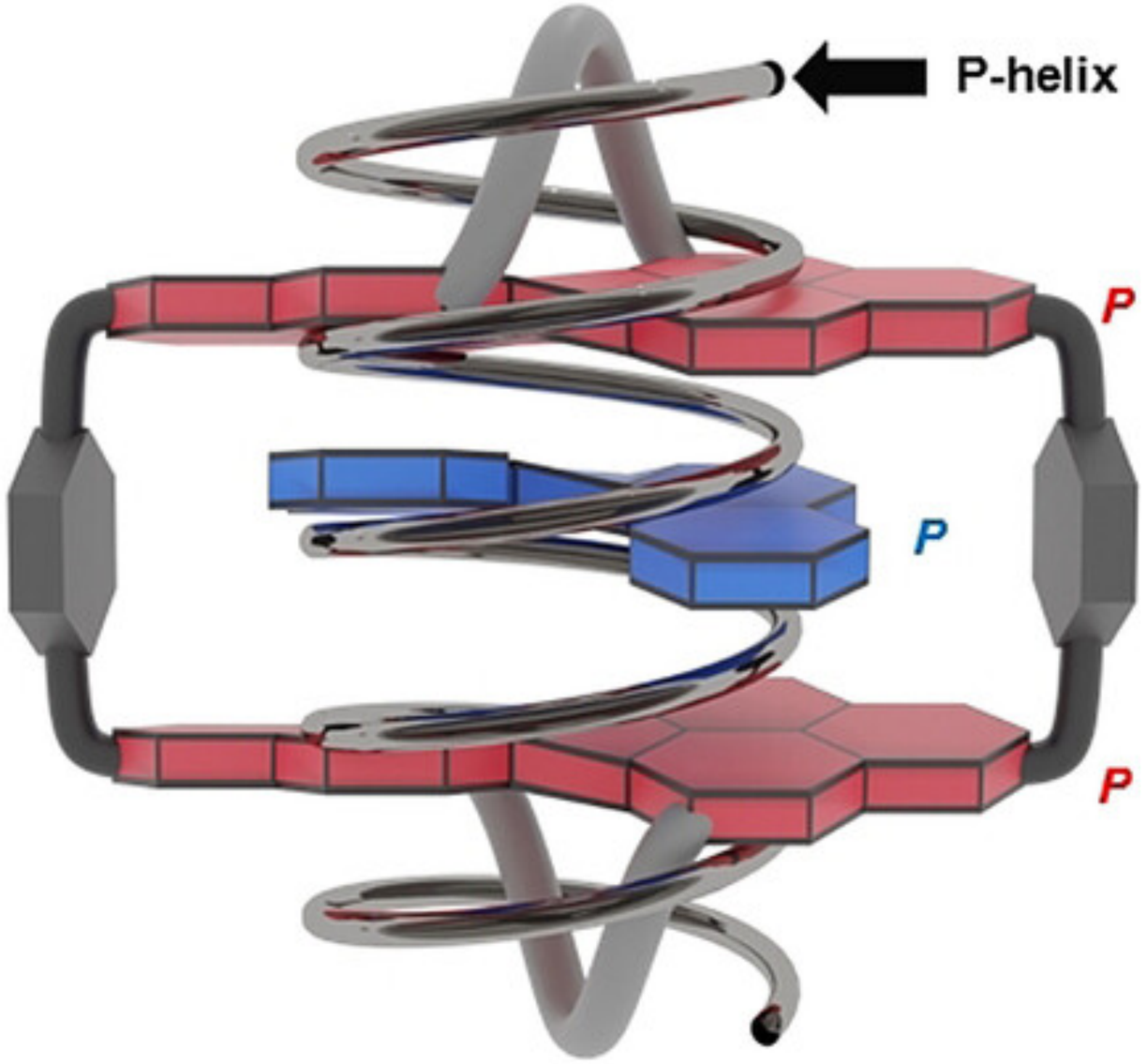


Würthner, F. et al. *Angew. Chem., Int. Ed.* 2021, *60*, 15323–15327.

*P* isomer

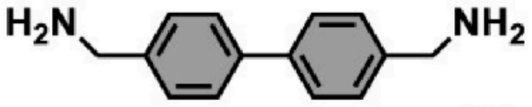

imidazole, toluene

120 °C, 16 h, 12%

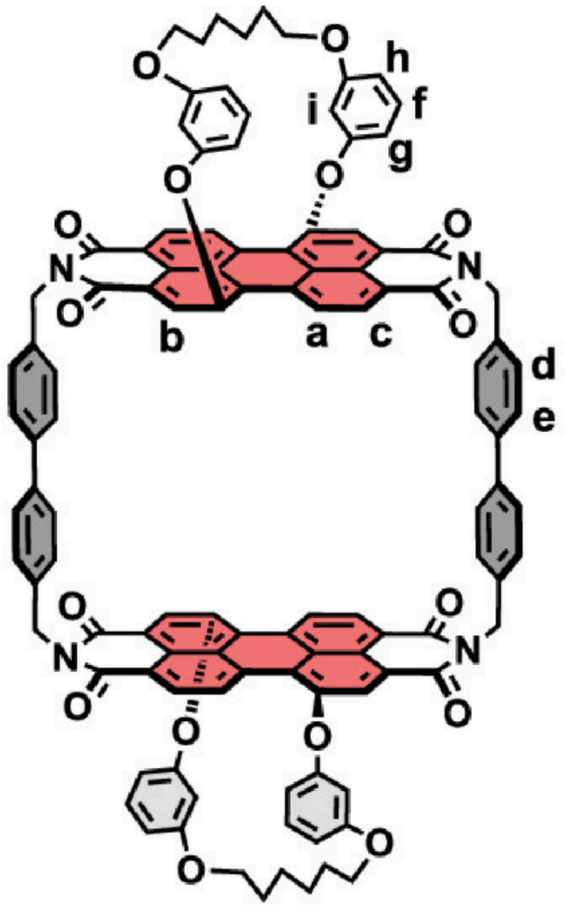

cyc-*PP*

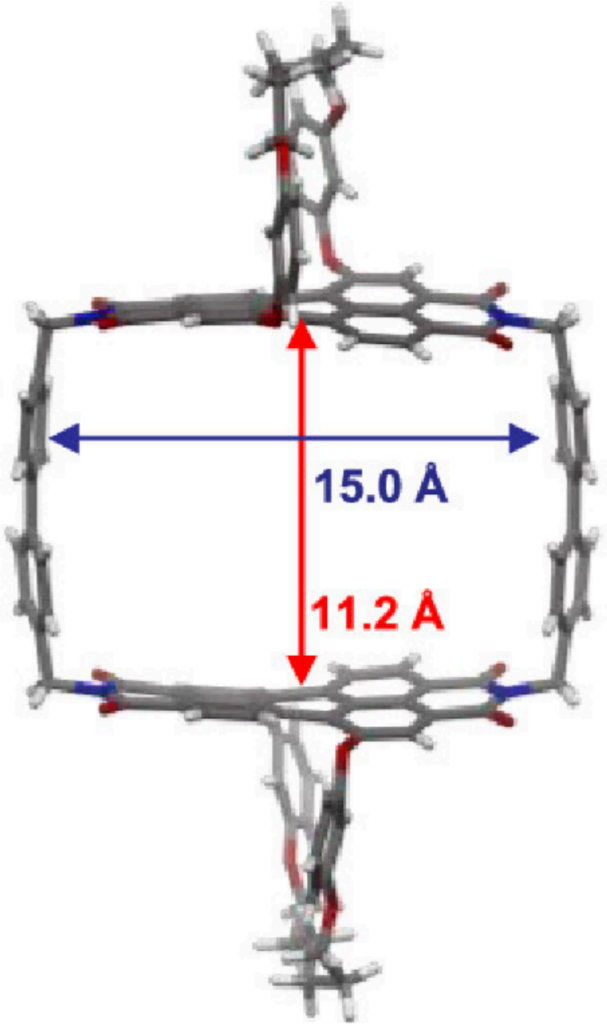


F. Würthner et al. JACS asap July 2024, https://doi.org/10.1021/jacs.4c08073

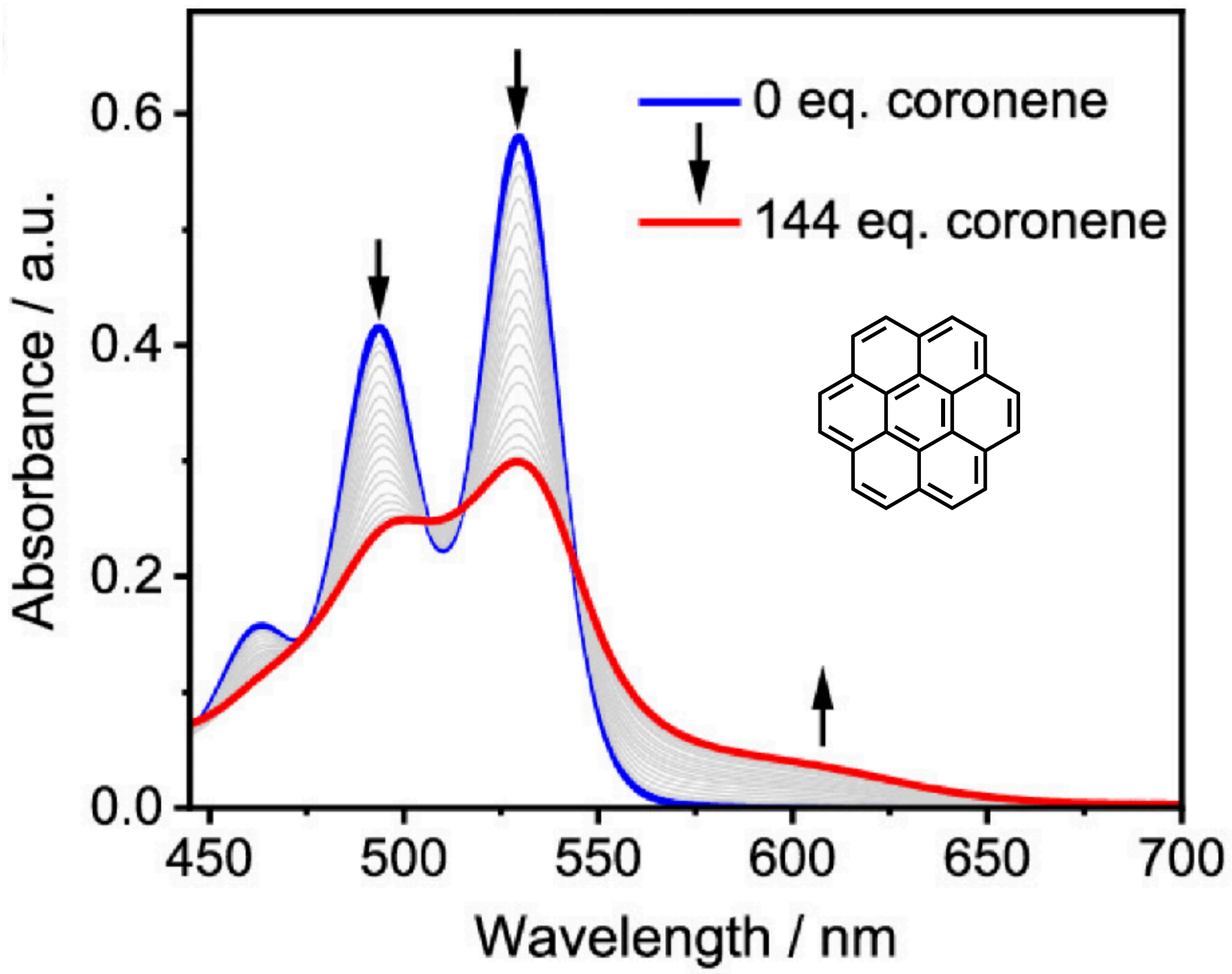


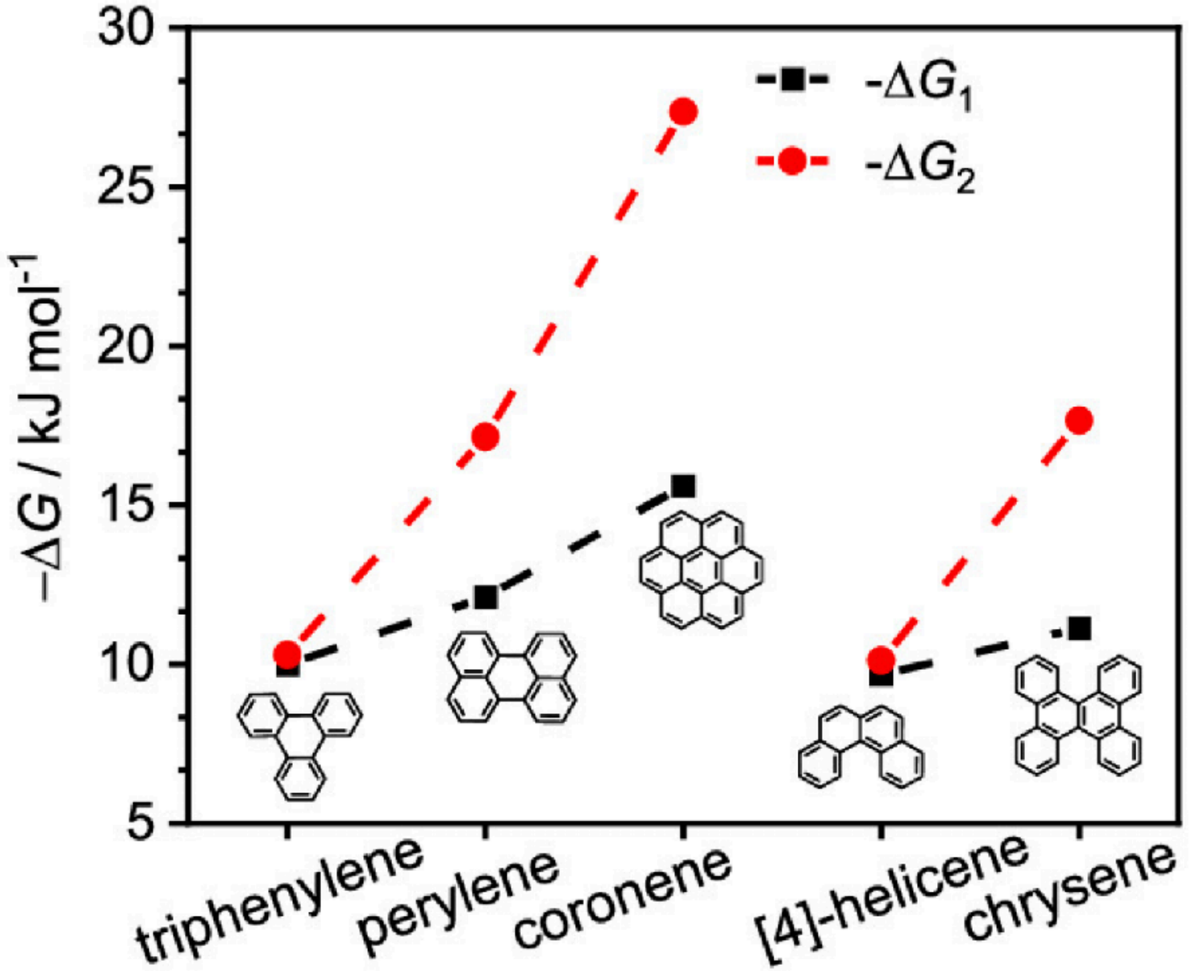


F. Würthner et al. JACS asap July 2024, https://doi.org/10.1021/jacs.4c08073

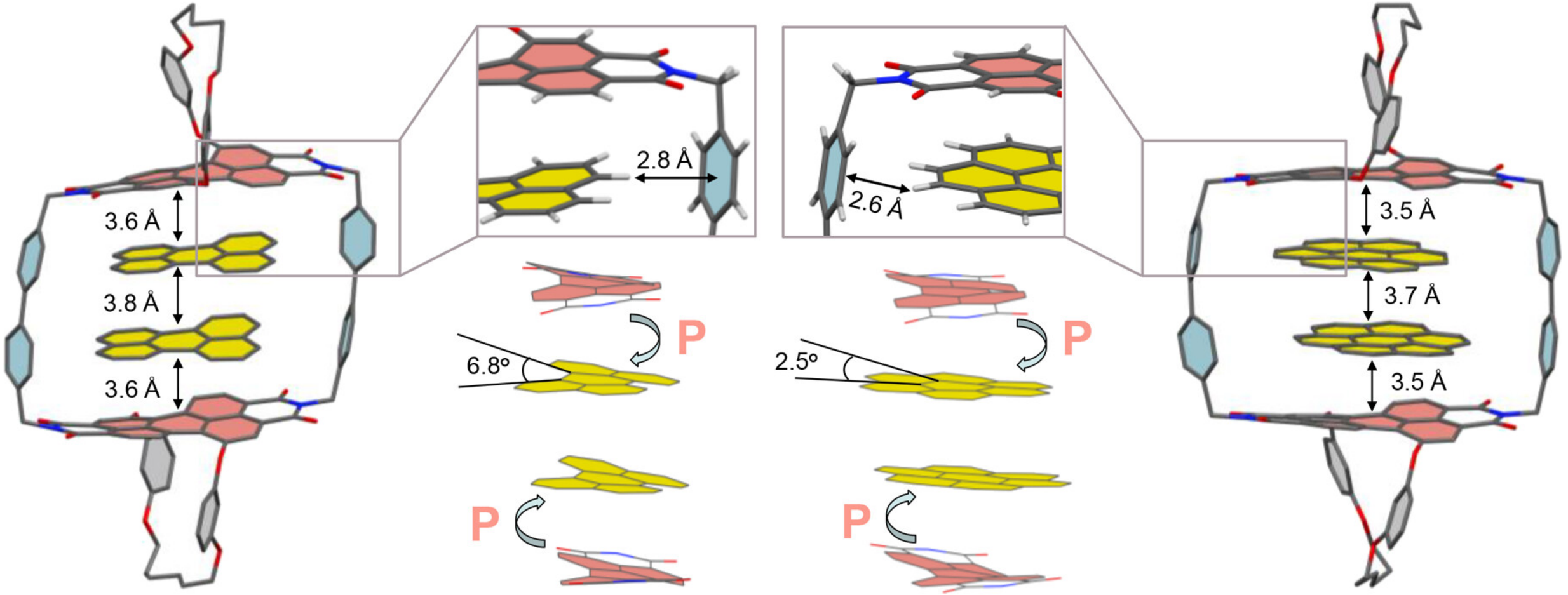


F. Würthner et al. JACS asap July 2024, https://doi.org/10.1021/jacs.4c08073

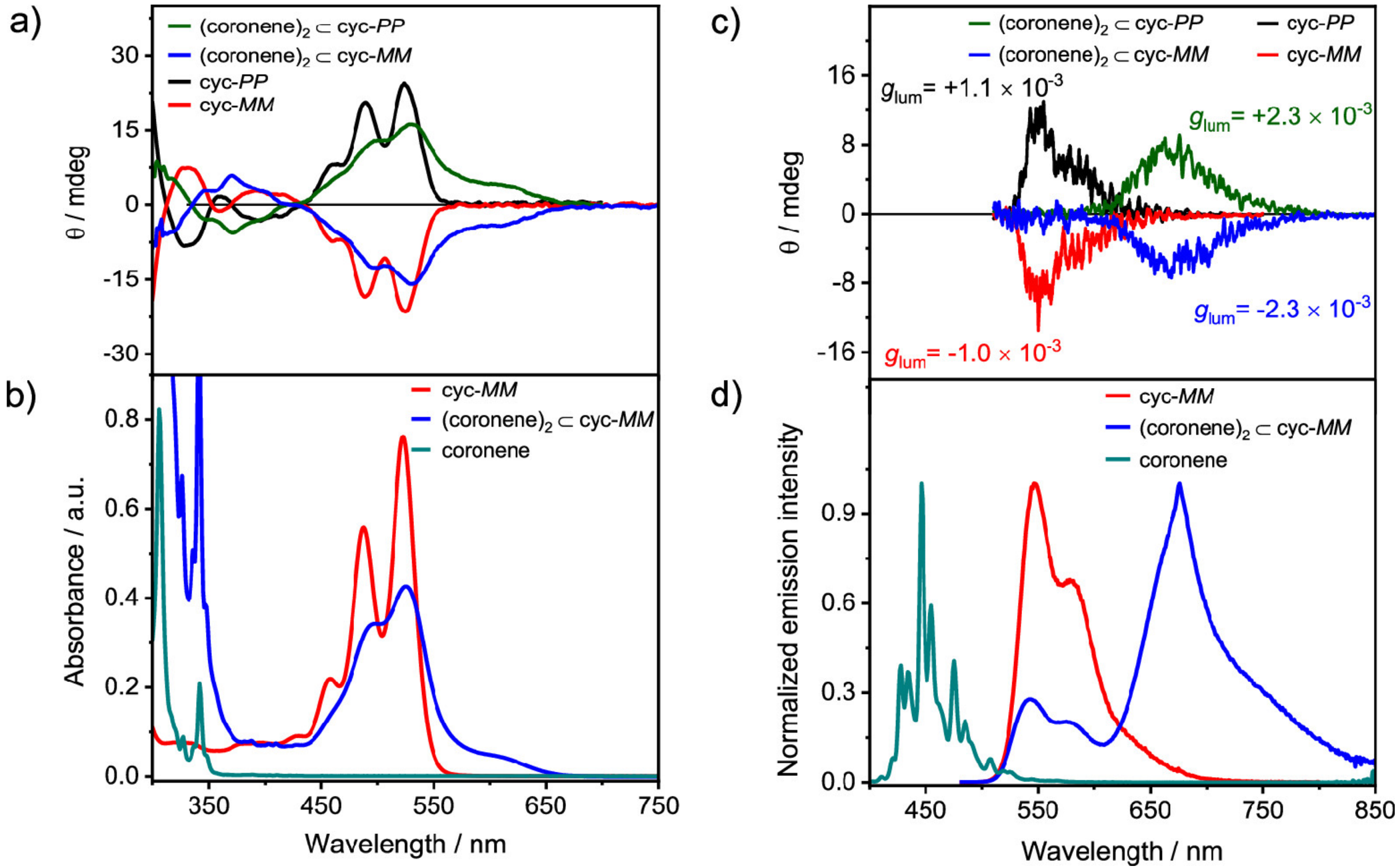


F. Würthner et al. JACS asap July 2024, https://doi.org/10.1021/jacs.4c08073

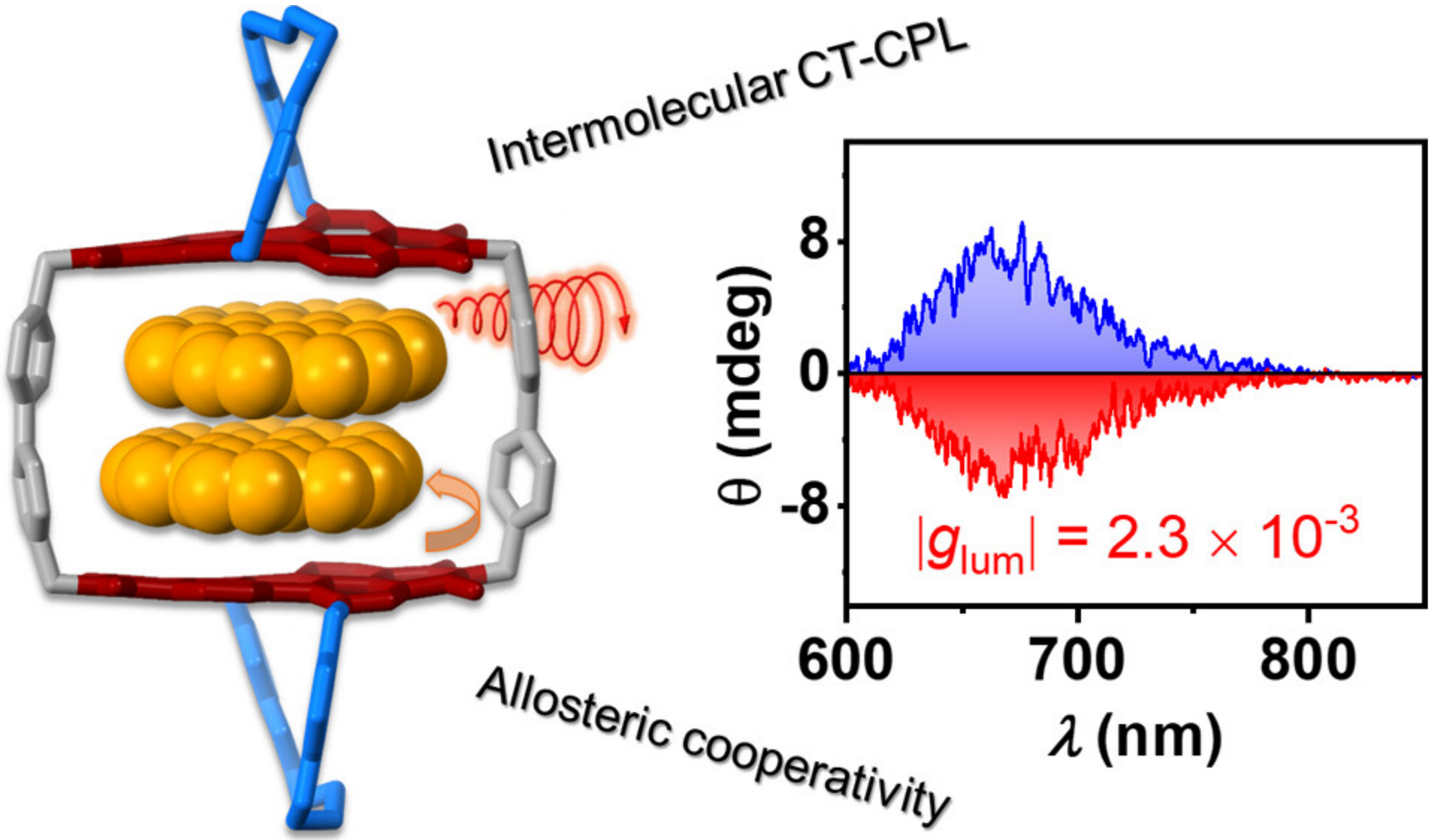


F. Würthner et al. JACS asap July 2024, https://doi.org/10.1021/jacs.4c08073

# Chiral Substituents on Imidic Nitrogen in PDI

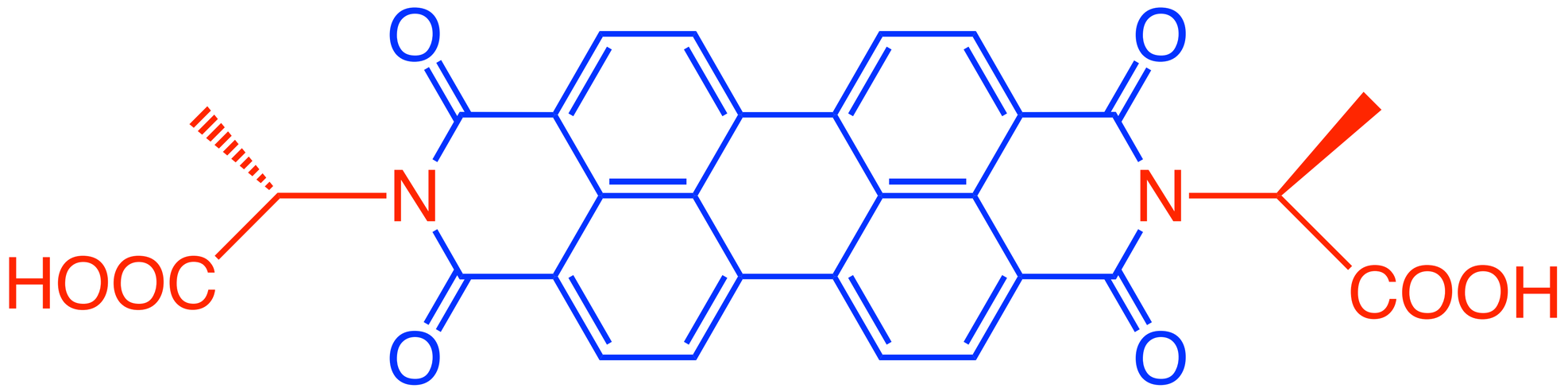

# Helical arrangements of planar PDIs with chiral substituents.

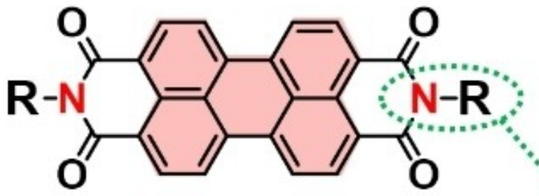


Chirality transfer and amplification

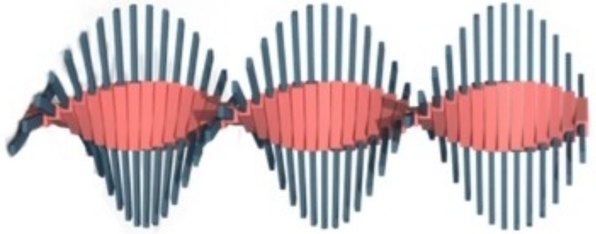

Helical arrangements

*Resources of chiral substituents*

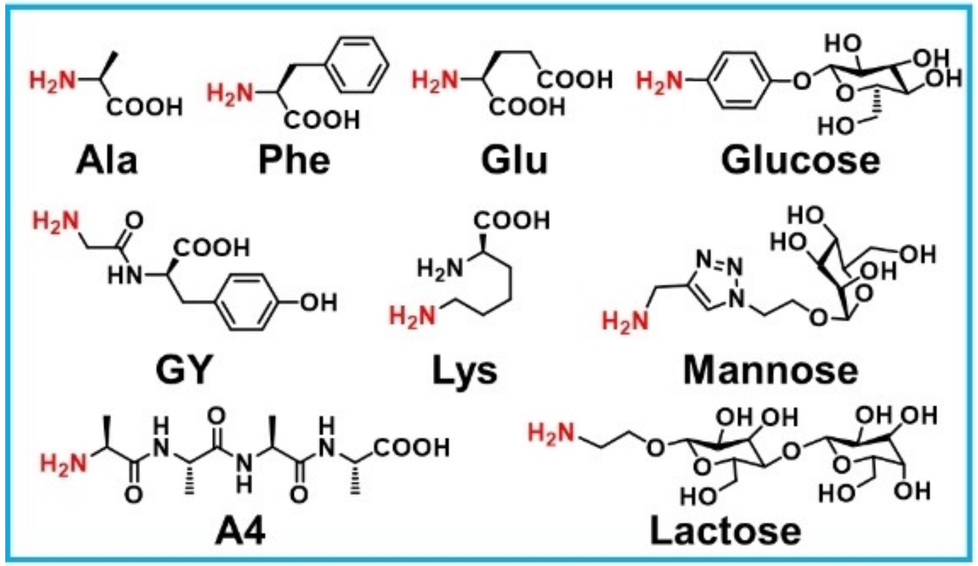


*Natural chiral pool*

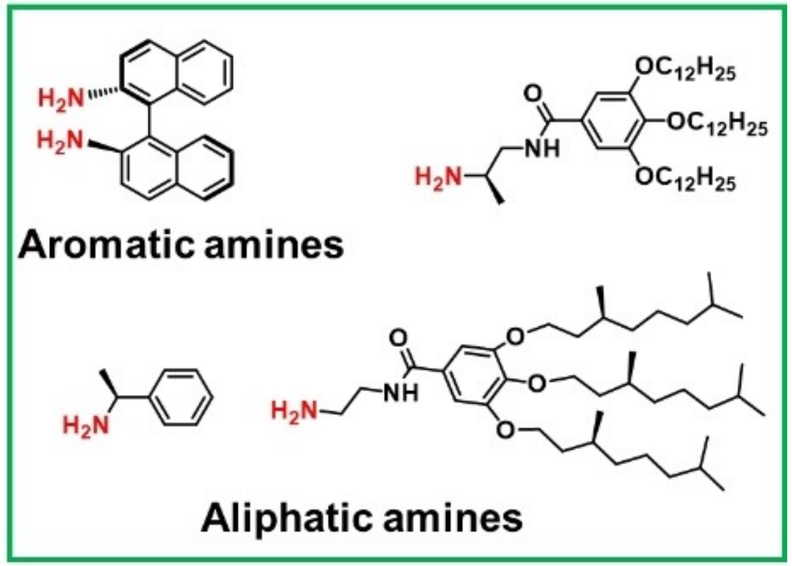


*Artificial chiral pool*

*Angew. Chem. Int. Ed.* **2022**, *61*, e202202532

# Chiral Substituents on Imidic Nitrogen in PDI

*Adv. Mater.* **2017**, *29*,1605828

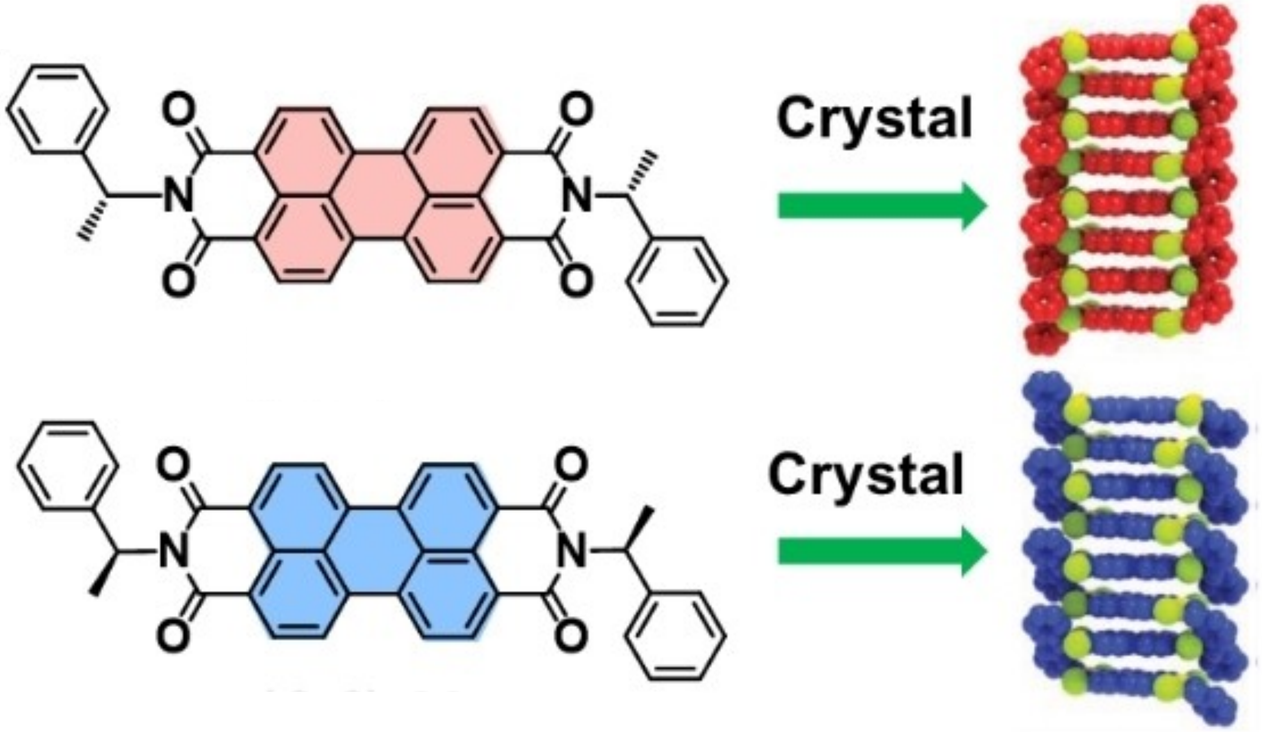


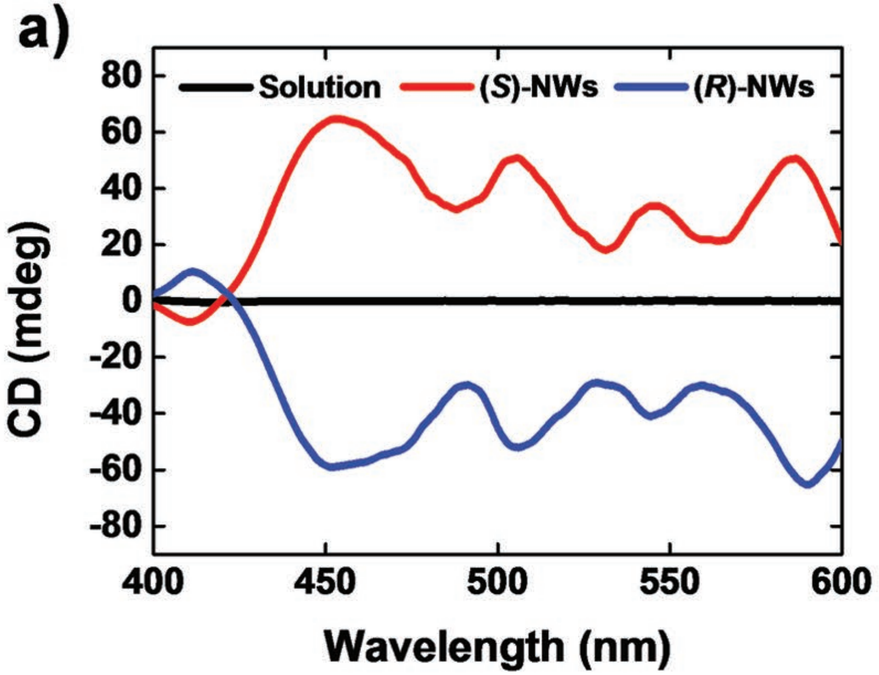


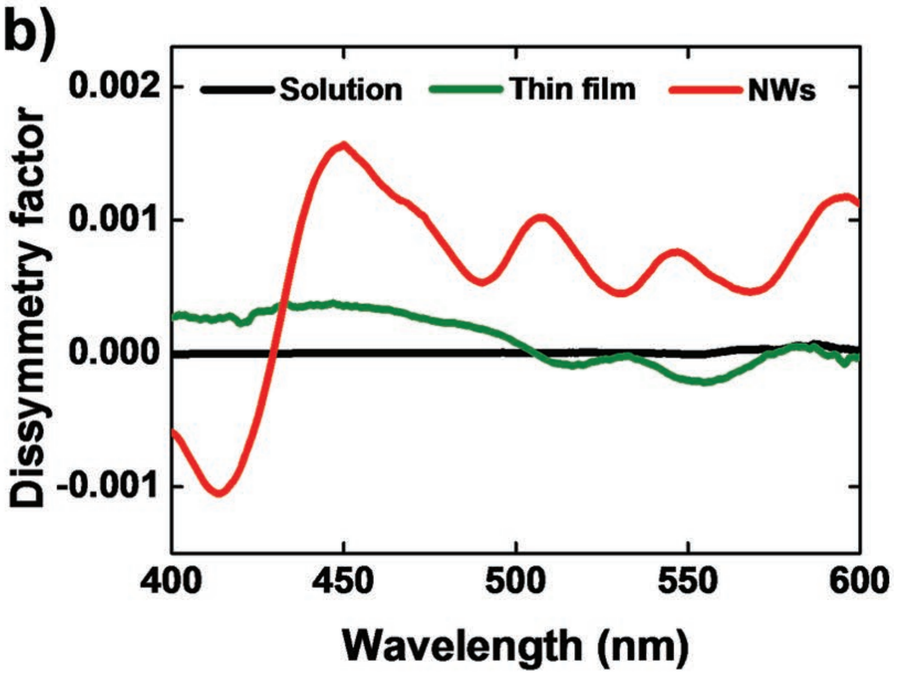

# CPL Sensing

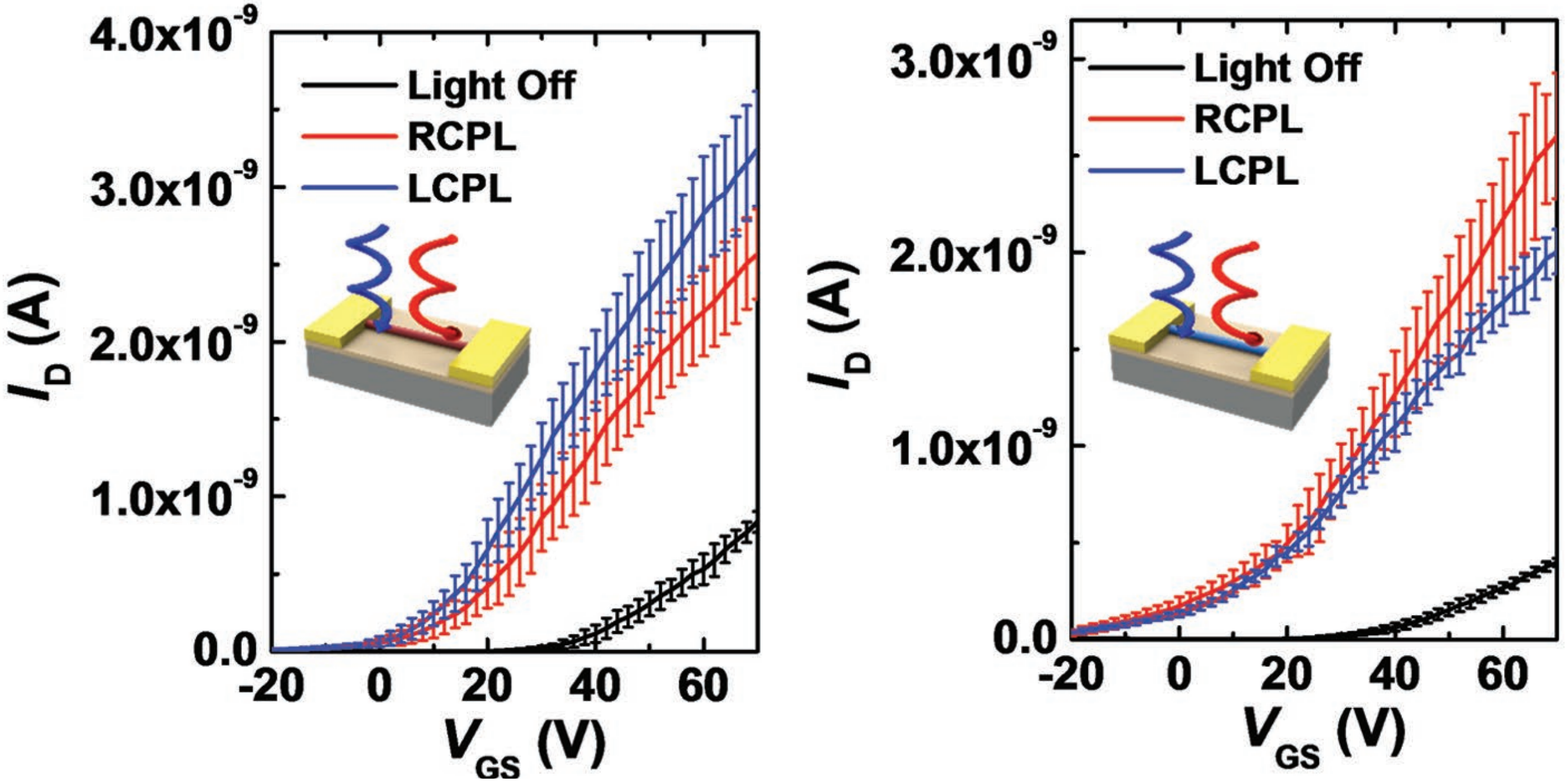


Organic Photo Transistors based on left (*S*)-CPDI NWs, right (*R*)-CPDI-Ph NWs

*Adv. Mater.* **2017**, *29,1605828*

# Supramolecular Arrangements

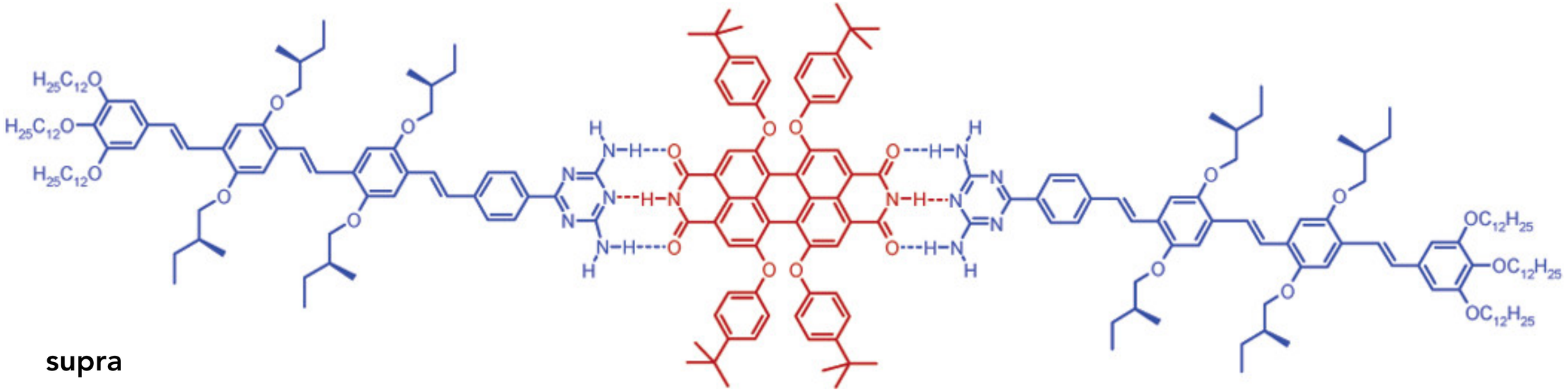

**supra**

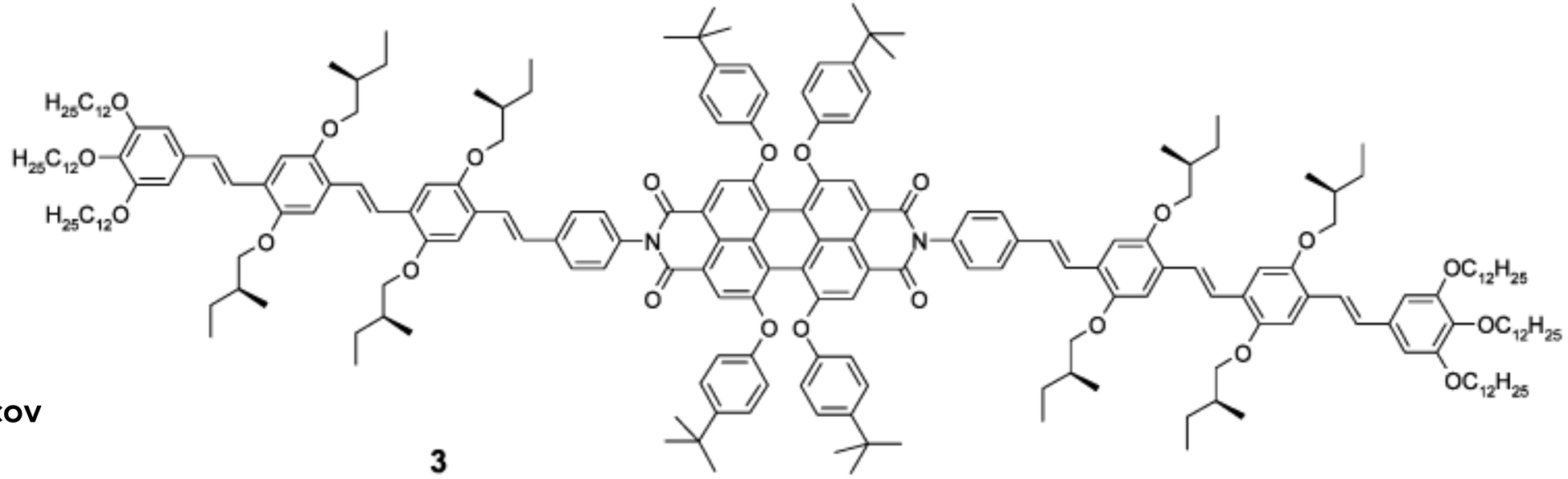

**cov**

**3**

**J. AM. CHEM. SOC. 2004**, 126, 10611-10618

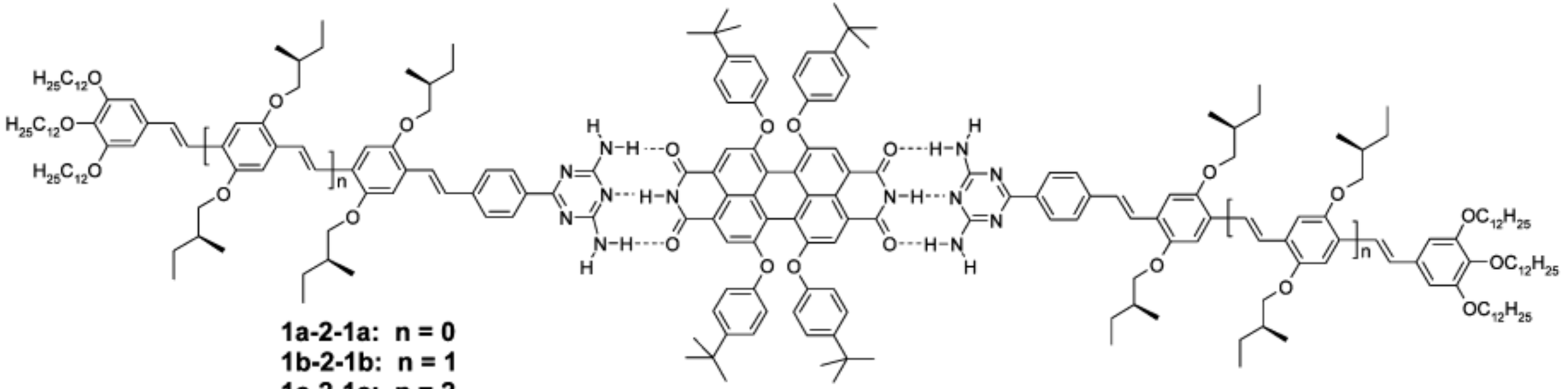

**1a-2-1a: n = 0**
**1b-2-1b: n = 1**
**1c-2-1c: n = 2**

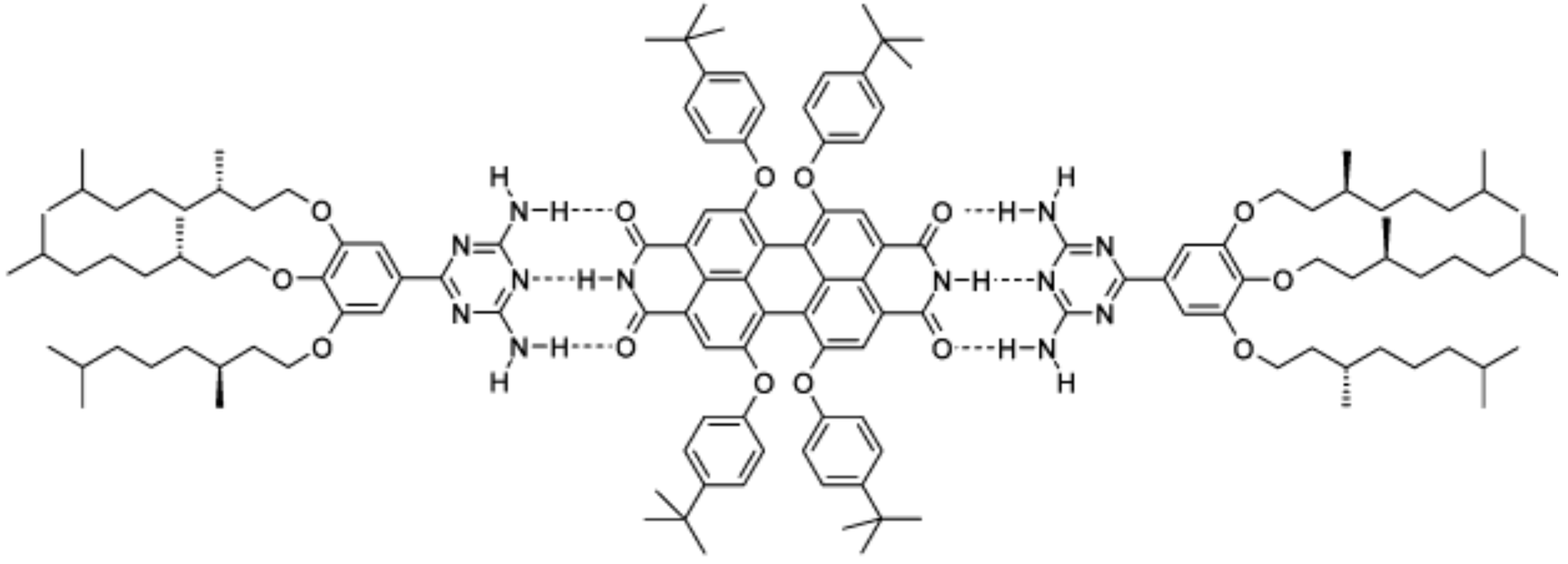

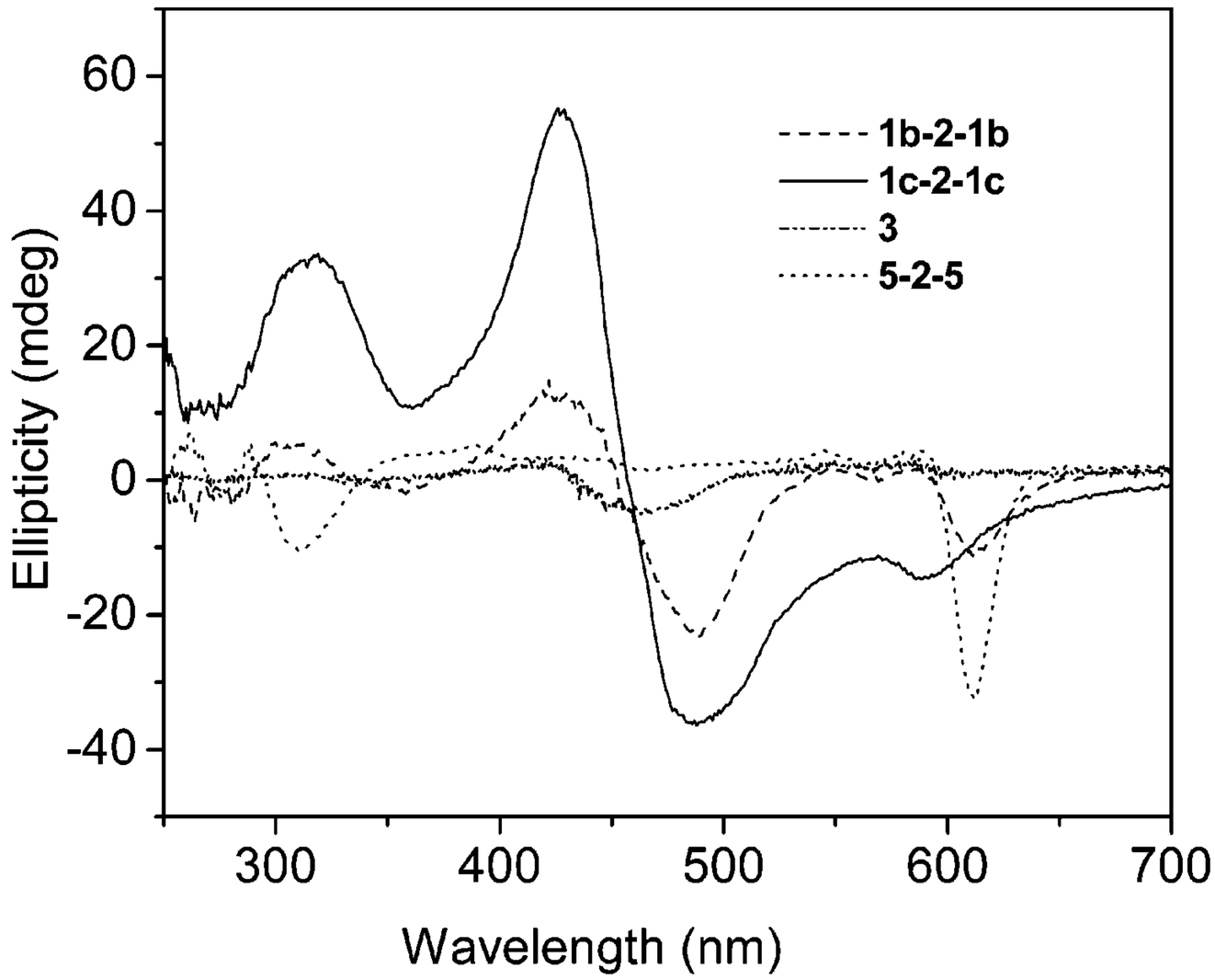


CD spectra of **1b**-**2**-**1b**,**1c**-**2**-**1c**, and **5**-**2**-**5** at concentration of 4 × 10-5 mol L-1 and **3** at concentration of 1 × 10-4 mol L-1 in MCH at 20 °C.

# Variable Temperature CD

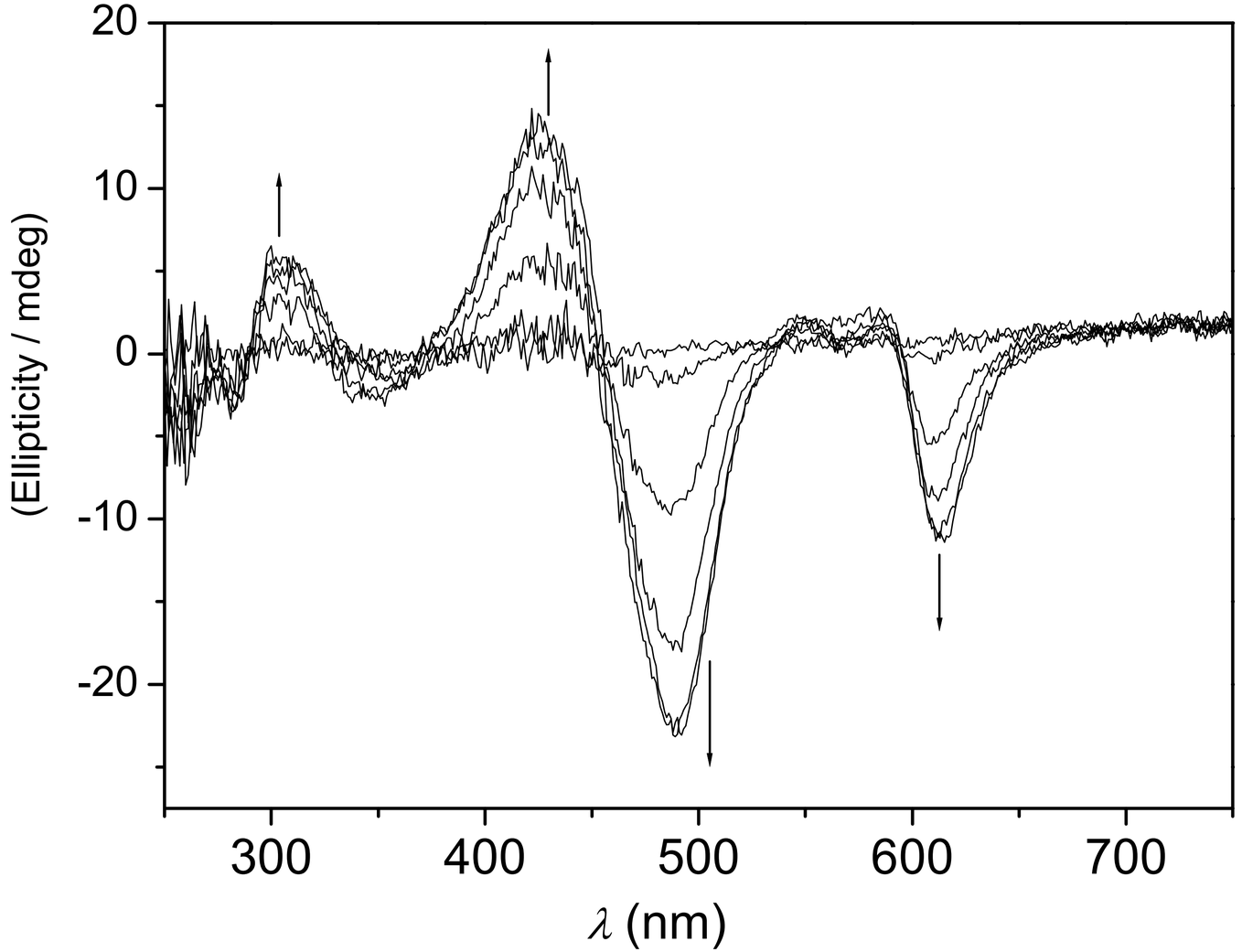


The signal change from positive to negative with increasing $\lambda$ indicates a left-handed helical arrangement of the transition dipoles, which are polarized along the long axis of the OPVs. Temperature-dependent CD spectra of the **supra** complex (c = $3.7 \times 10^{-5}$ mol $L^{-1}$) in MCH from 10 °C to 60 °C. Arrows indicate the changes upon cooling. The negative CD signal of the PERY band can be related to the preferential formation of *M* enantiomers caused by the left- handed helical stacking of the **1**-**2**-**1** complex

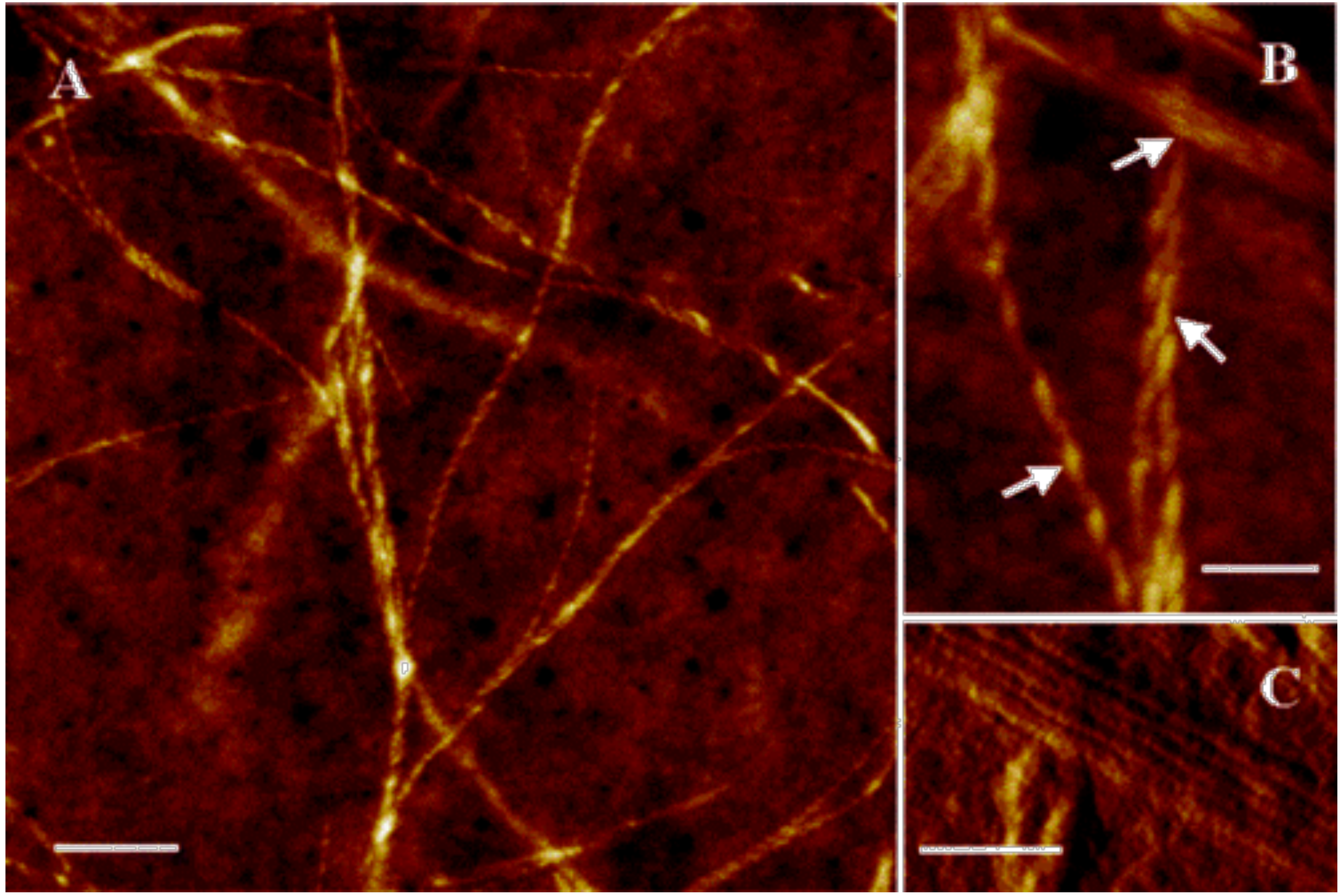


Tapping mode AFM topographic images of the **supra** complex after spin-coating from MCH (scale bar 500 nm) on a glass// PEDOT:PSS slide

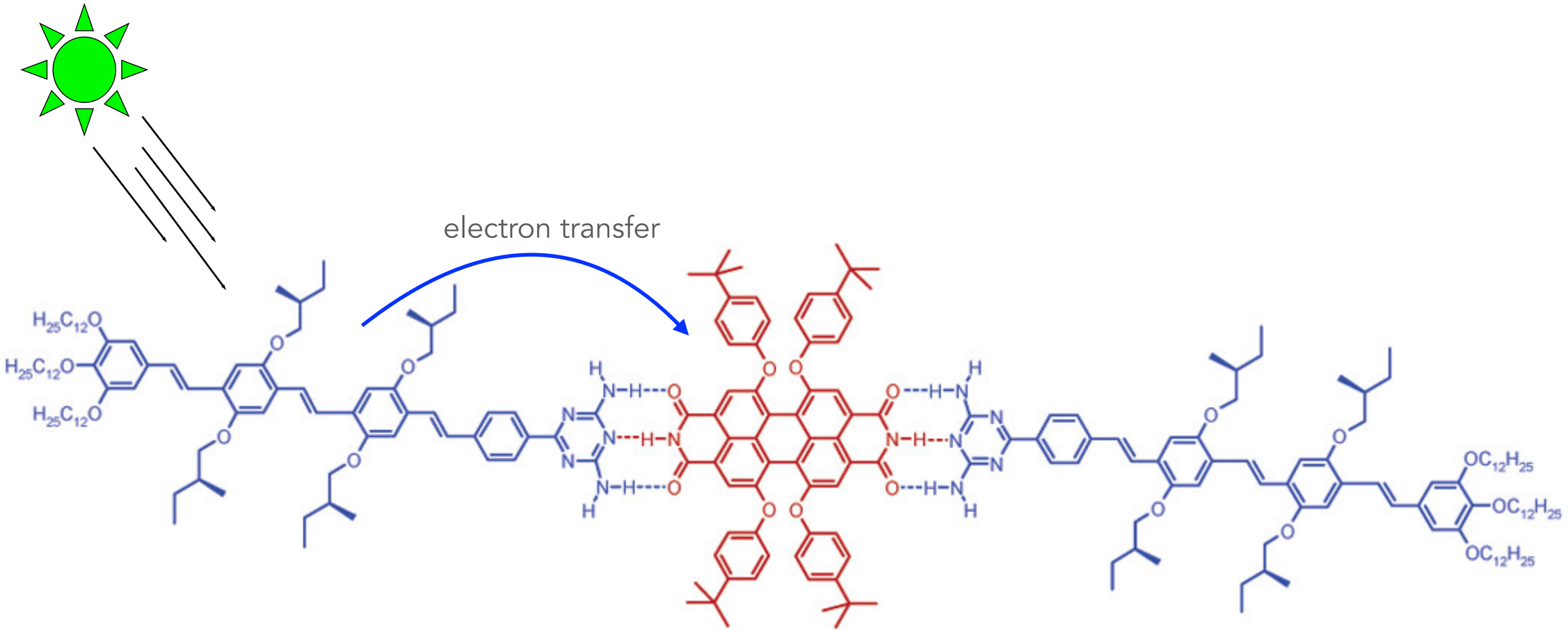


**J. AM. CHEM. SOC. 2004**, 126, 10611-10618

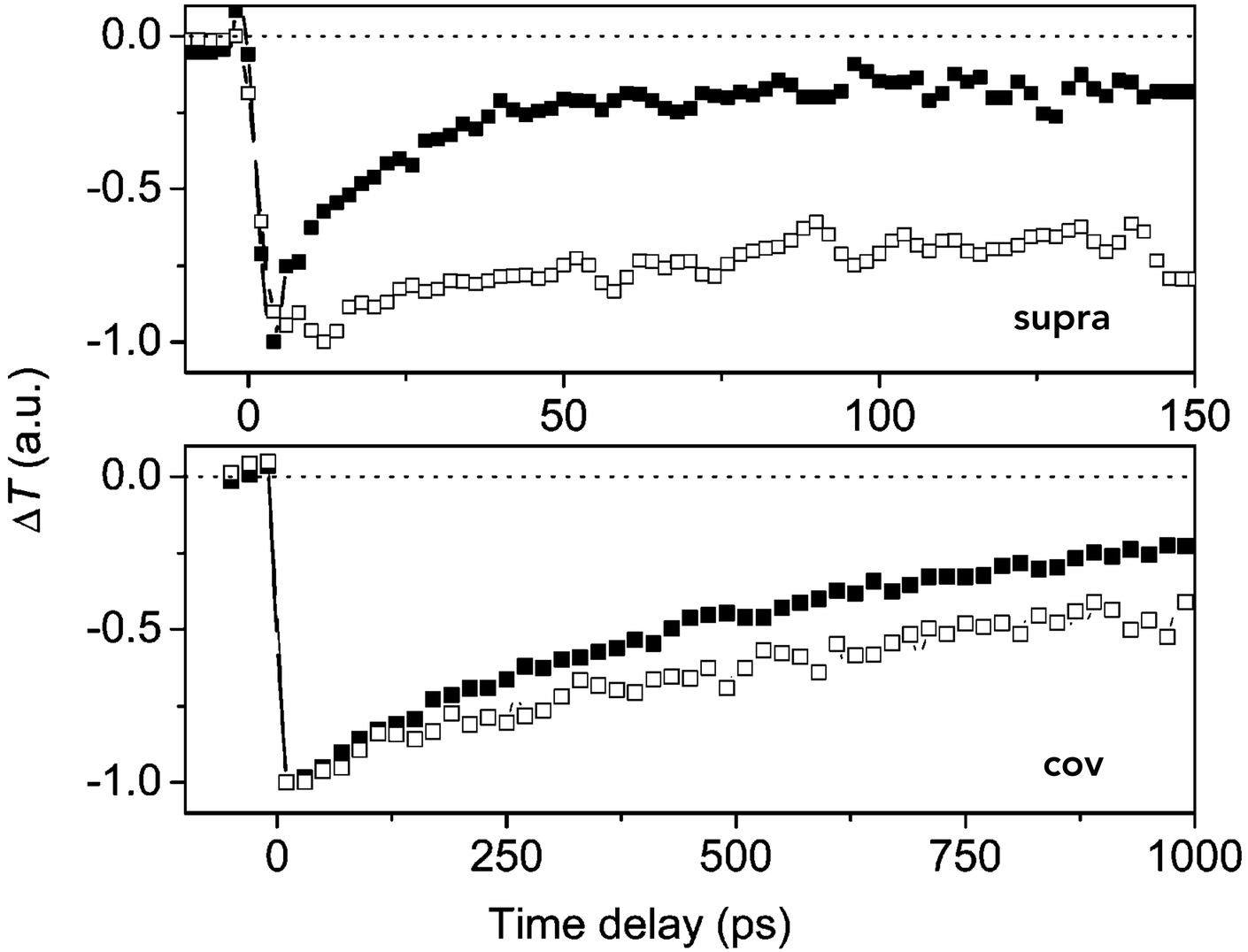


Differential transmission dynamics of **supra** (top) and **cov** (bottom) at 20 °C (■) and 80 °C (□) recorded at 1450 nm (low-energy absorption of OPV radical cations) after excitation at 455 nm. Both samples are $5\times10^{-5}$ mol $L^{-1}$ in MCH.

$k_{CS} > 10^{12}\ s^{-1}$

$k_{CR} = 6.3 \times 10^{10}\ s^{-1}$ (corresponding to a time constant of 16 ps) for **supra**

$k_{CR} = 2.0 \times 10^{9}\ s^{-1}$ (time constant of 500 ps) for **cov**

Temperature changes for **supra**: 16 ps at 20 °C to more than 200 ps at 80 °C

# *The catalytic system (artificial quantasome)*

The catalyst

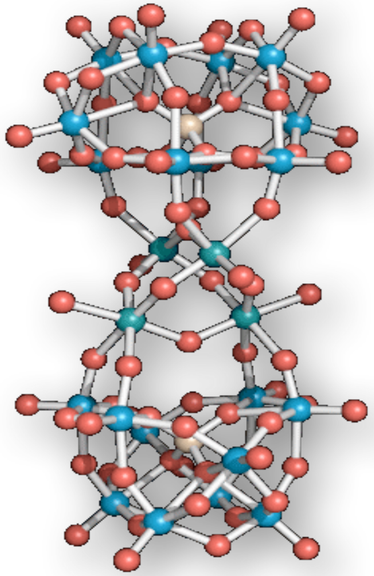

The antenna
(photosensitizer)